Shoot Apical Meristem Architecture in Maize: Diversity, Genetic Control, and its Relationship to Adult Plant Morphology

A Dissertation
SUBMITTED TO THE FACULTY OF
UNIVERSITY OF MINNESOTA
BY

Addie M. Thompson

IN PARTIAL FULFILLMENT OF THE REQUIREMENTS
FOR THE DEGREE OF
DOCTOR OF PHILOSOPHY

Gary J. Muehlbauer

July 2014

Acknowledgements

I would like to thank my advisor, Dr. Gary Muehlbauer, for all his guidance throughout my graduate career. His patience and support were so greatly appreciated. He helped to form my critical thought processes, approach to research, worth ethic, and writing abilities - skills that will forever stay with me and shape who I become as a scientist.

The members of my committee deserve high praise for their patience and willingness to work with me through this process. Dr. Nathan Springer shared his field space, generously provided seeds, sorted through many poor drafts of manuscripts, and provided honest and lively scientific discussion. Dr. Rex Bernardo was always available to help talk and think through any questions that arose for me (whether simple or overly-complex), with immeasurable patience and support. Dr. Robert Stupar and Dr. Ruth Shaw provided helpful conversations and comments throughout my time in graduate school.

Through the NSF SAM project I had the privilege of working with renowned scientists across the country, especially Dr. Jianming Yu, Dr. Patrick Schnable, Dr. Michael Scanlon, and Dr. Marja Timmermans, as well as numerous graduate students and post-docs. I appreciated their continuous input and feedback on my project, and particularly enjoyed participating in discussions and socializing at group meetings.

This collaboration also helped introduce me to and integrate me into the maize genetics research community. I am grateful for the lively conversations and friendships I would not have otherwise encountered, particularly James Schnable, who provided input, feedback, and support from an outside perspective.

I am also indebted to my lab mates and fellow graduate students, particularly James Crants for his painstaking labor on meristem sectioning and measuring, Shane Heinen and Catherine Springer for taking care of lab logistics, and everyone who helped dissect meristems for hours on end. I could not have done many of my experiments without all of the tireless efforts of dissection volunteers, or the fulfillment by Pete Hermanson of repeated seed requests. Many thanks also to Liana Nice, Stephanie Gardiner, Brian Seda, Michael Kantar, and other current/former APS students who helped by reading my work, discussing my science and life, and keeping me sane and social.

Last but not least, I owe a debt of gratitude to my family: my parents, John and Verlaine Hall, and sister, Amanda Hall, who were my first and most important teachers. They continue to inspire me and provide endless encouragement and support. Finally, to my husband Ryan Thompson and son Owen -- you are my lifeline. We make an amazing team, and I could not have made it this far without your patience, flexibility, honesty, humor, and unconditional support and love. Thank you.

Abstract

The maize shoot apical meristem (SAM) contains a pool of undifferentiated stem cells that produce all above-ground plant organs. Previous studies of the SAM have focused mainly on analysis of mutants conferring visible phenotypes. Though these approaches indicated the effect of genotype on SAM size, this represents the first work to characterize natural diversity in SAM architecture and its genetic control, as well as its relationship to adult plant traits.

A time course of SAM growth throughout vegetative development was conducted to assess growth over time, resulting in the description of three phases of growth: initial proliferation, slower growth, and rapid expansion before transition. The results also indicated that 14 days after planting was the most appropriate time point for subsequent measurements.

Quantitative trait loci for meristem traits (height, width, midpoint width, arc length, L1 arc cell number, plastochron internode, height:width ratio, volume, cell size) were mapped in the intermated B73 x Mo17 recombinant inbred line population. Distinct control of height- and width-related traits via several small-effect loci, as well as a lack of overlap with known meristem genes, was detected. One locus was validated using near-isogenic lines. Candidate genes were identified by correlating expression in the shoot apex with meristem traits across the population.

To assess natural diversity and the impact of heterosis on maize SAM architecture, a set of 27 diverse inbreds and several of their F1 crosses were examined. This revealed that B73 and P39 were among the tallest outliers for SAM height and

CML277 was the shortest. Heterosis was observed for meristem traits in several crosses of diverse inbreds to Mo17; some showed dominant effects. Only P39 exhibited heterosis with B73, demonstrating unique alleles contributing to the extreme heights observed in these inbreds.

Recombinant inbred populations derived from crosses of P39 and CML277 inbreds to B73 were also used for mapping. Here, a few large-effect loci were identified that affected many meristem traits; most overlapped with known SAM-related genes. Genetic control was shown to be population-dependent. Architecture traits in the meristem were correlated with several adult plant traits, including flowering time, indicating potential shared regulatory mechanisms.

Table of Contents

List of Tables

List of Figures

Chapter Two

Chapter Three

Chapter 1

Literature Review

Shoot Apical Meristem Function

SAM Initiation and Maintenance

The shoot apical meristem, or SAM, is an undifferentiated group of stem cells that divide to develop all of a plant's shoot-derived organs (Wang and Li 2008). Maize SAMs are formed at the base of the cotyledon during embryogenesis, where leaf production starts and is arrested at seed maturity, resuming at germination. Upon receiving the signals later in development to switch from leaf production to floral production, the vegetative meristem transitions to an inflorescence meristem. The terminal apical meristem forms the tassel, while the adult axillary meristems form ears.

Meristems are composed of several discrete areas of cells. The outermost layer of cells, called the L1, divides anticlinally, in a plane parallel to the meristem surface. In maize, the inner L2 layer of cells divides in multiple directions and is less discrete (Poethig *et al.* 1986). As the plant grows, the SAM continues to divide at a regular rate. The region of small cells around the low outer portion of the meristem is referred to as the peripheral zone (PZ). Leaves form by branching off from the PZ on the sides of the meristem, where a relatively high rate of cell division occurs. The larger cells of the central zone (CZ) are located at the middle top portion of the meristem, and are responsible for maintaining meristematic cells and replenishing cells used to form leaf or stem tissue. Below the CZ is the rib zone (RZ), which contains files of cells that form the stem. The meristem produces leaves along its flank while preserving enough meristematic cells to retain function by maintaining a low rate of cell division in the CZ of the SAM (Scanlon 2000). Organogenesis begins slightly before meristem

maintenance, according to transcript profiling and mutant analysis (Takacs *et al.* 2012; Vollbrecht *et al.* 2000). As a result of the tight balance maintained between leaf initiation in the PZ and meristem maintenance in the CZ, the overarching structure of the meristem remains relatively constant throughout vegetative development.

The *Arabidopsis thaliana* SAM differs from that of maize in three ways. First, *Arabidopsis* meristems maintain radial symmetry throughout development, while the maize vegetative meristem is distichous, producing only one leaf per node on alternating sides of the stem. Upon transition, the maize inflorescence meristem takes on radial symmetry. Second, as compared to the two layers of the maize meristem, the *Arabidopsis* meristem has two outer layers (L1 and L2) that divide in a regular parallel fashion, with a third layer (L3) that divides less regularly. Finally, the maize meristem is much larger and proportionately taller than that of *Arabidopsis* (Barton 2010).

Leaf development

There are three stages of leaf development. The first is organogenesis, where a small group of 100-200 cells at the base of one side of the meristem are recruited as founder cells for the developing leaf (Poethig 1984; Sinha 1999). Here, the group of cells in the L2 begin dividing perpendicular to the surface of the meristem, forming a bulge of cells on the side of the SAM (Barton 2010). In the second stage of development, cells are recruited from the L1 and other areas surrounding the founder cells (Barton 2010), and the domains of the leaf start to be defined. The final stage is that of cell and tissue

differentiation of the leaf primordium (Sinha 1999). The L1 layer gives rise to the epidermis, while the L2 creates the inner tissues of leaves and stems (Poethig *et al.* 1986).

The number of founder cells allocated to form the new leaf is tightly regulated (Kerstetter *et al.* 1997). When this regulation is perturbed, plant morphology is disrupted. Maize *narrow sheath* mutants develop narrow leaves, caused by a smaller number of founder cells (Scanlon *et al.*, 1996). In contrast, an increased number of founder cells quickly depletes the meristem, as seen in the Arabidopsis *forever young* mutant (Callos *et al.* 1994).

About five leaves begin to develop in the maize embryo between fertilization and seed maturation, and leaf production and growth resumes upon germination. Leaves are formed from the SAM as cells differentiate and begin to branch off from the PZ (Scanlon 2000). These leaf primordia are initiated at regular intervals; the time between initiation is measured in plastochrons (P) (Jackson *et al.* 1994). The P1 leaf is the closest and youngest lateral protrusion from the meristem, P2 the second, and so forth. Leaf initiation in the SAM is part of a repeating unit called a phytomer, consisting of a leaf, node, internode, and axillary bud (Galinat 1959). In maize, clonal sector analysis of founder cells has been shown to mark the resultant phytomer (Poethig and Syzmkowiak 1995). This approach can also be utilized to assay gene function, as with *narrow sheath1* and *narrowsheath2* (Scanlon 2000).

The transition from juvenile to adult vegetative phase in maize is marked by several characteristic phenotypic changes. Adult leaves are shorter, wider, and thicker than juvenile leaves, with a thicker cuticle and trichomes on the adaxial surface. In

addition, adult leaves have only cuticular wax, while juvenile cells have epicuticular wax. Mutations in maize *Glossy15*, a gene controlling phase change in the epidermis, lead to abnormally early expression of these adult features (Moose and Sisco 1994). Cell wall composition and staining properties of the cells in the two stages also differ. Axillary buds and adventitious roots formed at juvenile nodes may produce tillers; adult nodes do not form adventitious roots, and axillary buds are either suppressed or form ear primordia (Scanlon 2000).

Genetic Control of SAM function

A negative feedback loop containing three *CLAVATA (CLV)* genes and the *WUSHEL (WUS)* gene are the primary SAM activity regulators in *Arabidopsis thaliana* (Wang and Li 2008, Schoof *et al.* 2000). The three *CLV* genes are responsible for maintaining the balance between PZ and CZ cells in the SAM (Kayes and Clark 1998; Clark *et al.* 1993, 1995). *WUS* is expressed in the cells of the organizing center (Baurle and Laux 2005), acting as a transcription factor (Laux *et al.* 1996, Mayer *et al.* 1998) as well as an integrator of information from various regulatory pathways in the SAM (Wang and Li 2008). In maize, *faciated ear2 (fea2)* (Taguchi-Shiobara *et al.* 2001) and *compact plant2 (ct2)* (Bommert *et al.* 2013) are mutants in this pathway that affect vegetative SAM size. Although *thick tassel dwarf (td1)* (Taguchi-Shiobara *et al.* 2001) is similar in function to CLV1 in inflorescence and floral meristems, its function in the vegetative SAM is more similar to BAM genes (DeYoung *et al.* 2006; Lunde and Hake 2009).

Maize *Knotted-1*, or *Kn-1*, is the founding member of the *Knotted-1-like homeobox (KNOX)* gene family (Hake *et al.* 1989; Vollbrecht *et al.* 1991). Maize plants without functional *Kn1* display a decrease in meristem size due to an inability to maintain the SAM (Kerstetter *et al.* 1997), with penetrance dependent on genetic background (Vollbrecht *et al.* 2000). The Arabidopsis ortholog of *Kn1*, *SHOOTMERISTEMLESS (STM)* (Long *et al.* 1996; Uchida 2007), maintains the function of SAM maintenance by down-regulating *CLV* (Clark *et al.* 1996); mutants in this gene also result in a meristem termination phenotype (Long *et al.* 1996).

Both *Kn-1* and *KNOX* genes are expressed in the main part of the SAM but not in leaf primordia (Smith *et al.* 1992; Jackson *et al.* 1994). KNOX expression marks SAM formation in the embryo (Hake *at el.* 1995), and functions to maintain the SAM by keeping stem cells in an undifferentiated state. It is subsequently down-regulated in initiating leaves and leaf cells (Smith *et al.* 1992, Jackson *et al.* 1994), starting just before the founder cells become histologically distinct from surrounding cells (Barton 2010). Dominant *Knox* mutants display ectopic expression of KNOX protein in the leaf, causing cell identity to change in leaf tissue, leading to blade-to-sheath transformation. Examples of this are found in the dominant *Knox* mutants of maize, which include *Liguleless3* (Muehlbauer *et al.* 1999), *Rough sheath1 (Rs1, knotted2)* (Schneeberger *et al.* 1995), *Gnarley1 (Gn1, KNOX4)* (Foster et al. 1999), and *Liguleless4* (Bauer *et al.* 2004).

Another category of genes that affect the SAM are those that regulate *KNOX* expression. An example of this is *rough sheath2 (rs2)*, which encodes a Myb-domain that regulates *KNOX* epigenetically (Timmermans *et al.* 1999). Recessive mutations in

rs2 cause ectopic expression of *KNOX*, with phenotypes that are dependent on genetic background and environment (Schneeberger *et al.* 1998). *Rs2* is similar to the *Antirrhinum* gene *PHANTASTICA* (Tsiantis *et al.* 1999). *Semaphore1* (*sem1)* is another negative regulator of KNOX genes *Rs1* and *Gn1*, with recessive mutations causing ectopic expression of KNOX in the leaf and endosperm (Scanlon 2002). This affects development of the embryo and endosperm, as well as formation of lateral roots and pollen. *Sem1* mutants also have reduced polar auxin transport in their shoots (Scanlon 2002).

In the SAM, KNOX proteins control the ratios of plant hormones (Kyozuka 2007), the regulation and patterning of which is vital to meristem function (reviews in Hay *et al.* 2004 and Vanstraelen and Benková 2012). Two of the most important plant hormones are auxin and cytokinin, as their ratio regulates the balance between meristematic activities: auxin promotes organogenesis, while cytokinin promotes cell division and stem cell maintenance (Pernisová *et al.* 2009). Thus, without cytokinin, the SAM is lost (Yanai *et al.* 2005), but an insensitivity to cytokinin leads to larger meristems, as found in the maize *aberrant phyllotaxy1* (*abph1)* mutant (Jackson and Hake 1999; Giulini *et al.* 2004). Similarly, loss of auxin transport leads to the inability of the SAM to perform organogenesis (Reinhardt 2000; see Gallavotti 2013 and Forestan and Varotto 2012 for reviews). The ratio of cytokinin and auxin in plant development is also regulated by gibberellins and brassinosteroids (Vanstraelen and Benková 2012).

Small RNAs also affect the function and initiation of the SAM (Zhang *et al.* 2006; see Axtell 2013 for microRNA review). The movement of microRNA394 (miR394)

from the protoderm to the underlying cell layers helps to define the location of stem cells during formation of the SAM in *Arabidopsis* (Knauer *et al.* 2013). Another vital point of regulation is that of miR166 on the expression of class III homeodomain leucine zipper (HD-ZIPIII) transcription factors. Because of the importance of miRNA in meristematic function, mutants in this pathway lead to meristem defects. These mutants include *ago1* (Vaucheret *et al.* 2004), *ago10* (Liu *et al.* 2009), and *dcl1* (Schauer *et al.* 2002) in *Arabidopsis*. Maize mutants in this pathway are *leafbladeless* and *ragged seedling2*, which regulate the expression domain of miR166 and HD-ZIPIII transcription factors via *trans*-acting small interfering RNAs, and impact auxin response (Nogueira *et al.* 2007; Douglas *et al.* 2010). Rice *sho* mutants in this pathway show SAM morphology changes concomitant with differences in plastochron timing and phyllotaxy (Itoh *et al.* 2000; Nagasaki *et al.* 2007).

Another example of cross-talk between maize SAM regulatory pathways is in the interaction of cytokinin response with chromatin remodeling components (Efroni *et al.* 2013). Indeed, chromatin structure and remodeling regulators have been implicated in stem cell maintenance (Shen and Xu 2009; reviews in Wagner 2003, Kwon and Wagner 2007, Sang *et al.* 2009). Other downstream processes impacting the SAM include enzymatic variation in cell wall properties and changes in metabolic processes (Kierskowski *et al.* 2012; Peaucelle *et al.* 2011). An example is the maize thiamine auxotroph *bladekiller1-R* (*blk1-R*), which shows defects in SAM functionality leading to lack of stem cell maintenance as well as the inability to produce organs (Woodward *et al.* 2010). A list of SAM-related maize genes, including those described above, can be

found in Table 1. These genes have been cloned in maize, and have some effect on the growth of the shoot apical meristem.

Control of Maize Morphological Traits

QTL mapping

Quantitative trait locus, or QTL, mapping is a statistical method of identifying regions of the genome that control phenotypic traits. Associations between mapped markers and trait scores for a group of individuals are used to identify the QTL. In addition to utilizing different population types, there are several methods of QTL mapping, which vary in their consideration of markers (individually or in pairs, as intervals of the genome), treatment of traits (one at a time or together), and specific statistical formulations for calculating associations (Zeng 1994; Bauman 2008). In the end, the ability to detect any given QTL mainly depends on the magnitude of the QTL, the size and type of the population, the number of recombination events in the population, and the density of markers (Beavis 1998).

In maize, QTL analysis has been used to identify genomic regions for various morphological traits, including plant height (Beavis *et al.* 1991), inflorescence traits (Berke and Rocheford 1999; Upadyayula *et al.* 2006; Brown *et al.* 2011), node number, height, and days to anthesis (Vlăduţu *et al.* 1999), phase change (Salvi *et al.* 2002), root architecture (Zhu *et al.* 2005; Hochholdinger and Tuberosa 2009), flowering time (Salvi *et al.* 2007; Buckler *et al.* 2009), root angle (Omori and Mano 2007), and leaf shape (Tian *et al.* 2011) and number (Lauter *et al.* 2008). Most of these mapping studies have

focused on differentiated plant structures, though some work has been done on the maize embryo (Moore *et al.* 2013; Yang *et al.* 2012).

Some studies have successfully resolved the QTL region to a causative gene. One excellent example is the fine mapping and eventual cloning of *Vgt1* (*Vegetative to generative transition1*), a QTL contributing to node number, height, and maturity. Initially discovered by Vlăduţu *et al.* (1999), this QTL was found to play a role in the apical meristem's transition from vegetative to generative structures. In further work Salvi *et al.* (2002) used a set of near-isogenic lines (NILs) to further fine map the region. Fine mapping was accomplished by generating a mapping population by crossing a NIL containing the introgressed region of interest to its recurrent parent and identifying crossovers in the QTL region. Cloning of *Vgt1* showed that it encoded an APETALA2-like transcription factor controlled by a *cis*-acting regulatory element, located in a non-coding region 70 kb upstream of the *Vgt1* coding sequence (Salvi *et al.* 2007).

Maize genomics resources

Intermated B73 x Mo17 recombinant inbred line population (IBMRIL)

The intermated B73 by Mo17 recombinant inbred line, or IBMRIL, population was created by crossing B73 x Mo17, and the F1 progeny intermated five times. This was followed by a series of self-pollinations to form 302 RILs (Lee *et al.* 2002). A significant amount of resources are available for the recombinant inbreds. B73 is the current reference sequence for maize (Lawrence *et al.* 2008; Schnable *et al.* 2009) and sequencing of Mo17 is underway. A subset of the IBMRIL has also been mapped with

over 7500 SNP markers, using RNAseq expression data from shoot apices (Li *et al.* 2013). The combination of these genetic and expression datasets allow for computational and sequencing-based approaches to gene identification and functional analysis in the IBMRIL population. In addition, due to the five generations of intermating during the development of the IBMRIL population, the resolution of QTL mapping is markedly increased (Lee *et al.* 2002).

The IBMRIL population has been used in multiple QTL mapping experiments. QTL contributing to resistance to southern leaf blight have been identified (Balint-Kuri *et al.*, 2007). Disease resistance was mapped in four environments, two of which were artificially inoculated with the disease to increase incidence; four QTL were identified in all of the environments. Upon comparing results of QTL mapping in the IBM advanced intercross lines and conventional RILs, the IBM lines were found to contribute 5 to 50 times greater resolution in mapping. This demonstrates the advantage of the increased number of recombination events in the advanced intercross mating design of the IBMRIL population (Balint-Kurti *et al.* 2007).

Lauter *et al.* (2008) used the IBMRIL population to map variation for the total number of leaves before flowering, and number of leaves below the uppermost ear. These traits were found to be 80% heritable in the RILs, with ranges showing transgressive segregation. This transgressive phenotypic action was surprising, as additive variation explained 40% of the heritable variation. The two traits were highly correlated, and seven total QTL were identified, six of which were common between the two traits. B73 contributed alleles increasing leaf number in all cases, for both traits.

Upon mapping confidence intervals to the genome, loci were resolved to regions of about 1Mb. This study further demonstrates the increased resolution possible in the IBMRIL population (Lauter *et al.* 2008). Other mapping experiments in the IBM have characterized 14 architecture phenotypes (Pressoir *et al.* 2009), as well as carbon and nitrogen use and seed biomass (Zhang *et al.* 2010),

Because so many traits and markers have all been scored in a common "eternal" population, researchers can make use of data from many more traits than would be feasible to measure in a single lab. As a result, data from multiple experiments can be utilized in concert to provide evidence of possible pleiotropic effects on several related traits. In addition, B73 and Mo17 are progenitors of many modern maize varieties. As a result, the genetic variation contained in the IBMRIL population is much more agronomically and biologically relevant than extreme phenotypes and mutations.

B73 x Mo17 near-isogenic lines

In addition to the IBMRIL population, a set of near-isogenic lines (NILs) combining the B73 and Mo17 genotypes was created by Eichten *et al.* in 2011. B73 and Mo17 F1 progeny were backcrossed to a given parent three times, then self-pollinated for four to six generations to create a set of 150 NILs. One hundred of these NILs are predominantly B73 with several introgressions of Mo17, and 50 contain introgressions of B73 in a Mo17 background. Genotyping was performed by Eichten *et al.* to characterize the introgressions, and the population is available for fine-mapping or QTL validation.

Nested association mapping (NAM) population

The maize NAM population was developed from 25 highly diverse founders each crossed to B73 to create 25 families each containing 200 RILs (Yu *et al.* 2008), capturing approximately 136,000 recombination events (McMullen *et al.* 2009). The founders were chosen to capture a wide range of maize diversity, including tropical and temperate lines, sweet corn, and popcorn (McMullen *et al.* 2009). The extensive diversity and known structure of the population as well as the sequencing and marker data available on the founders and inbreds makes this a valuable resource for maize research.

The first QTL mapping project utilizing the entire NAM population was undertaken by Buckler *et al.* (2009) and focused on the genetic basis of flowering time. The 5,000 lines were grown in four locations for two years, providing eight environments. Data were obtained for days to silking as well as days to anthesis, each estimated to be 94% heritable. The time interval between anthesis and silking was also calculated, and showed 78% heritability, as calculated by line BLUPs across all crosses. Depending on the QTL mapping approach (stepwise regression/composite interval mapping, joint stepwise regression/joint inclusive composite interval mapping), between 30 and 50 QTLs were identified, all with small additive effects. The largest QTL for days to silking affected the trait 1.7 days, and for the anthesis-silking interval just 0.4 days. Previously discovered flowering time QTLs, including *vgt1*, were among those QTL identified. Effects were mainly additive, and these results did not support effects for geographic origin, epistasis, or environmental interaction (Buckler *et al.* 2009).

Several other traits have since been investigated using the NAM population. These include 13 different morphological traits (Brown *et al.* 2011), northern leaf blight resistance (Poland *et al.* 2011), southern leaf blight resistance (Kump *et al.* 2011), leaf architecture (Tian *et al.* 2011), and kernel composition (Cook *et al.* 2012). The NAM founders and/or RILs were also utilized in studies encompassing even broader diversity; for example kernel, seed, and zein characteristics (Flint-Garcia *et al.* 2009), aluminum tolerance (Krill *et al.* 2010), photoperiod response (Coles *et al.* 2011), stalk strength (Peiffer *et al.* 2013), and plant height (Peiffer *et al.* 2014). All phenotypic datasets are available for public use via http://www.panzea.org.

Literature cited

Axtell, M. J., 2013 Classification and comparison of small RNAs from plants. Ann. Rev. Plant Biol. 64: 137-159.

Balint-Kurti, P. J., J. C. Zwonitzer, R. J. Wisser, M. L. Carson, M. A. Oropeza-Rosas *et al.*, 2007 Precise mapping of quantitative trait loci for resistance to southern leaf blight, caused by *Cochliobolus heterostrophus* race O, and flowering time using advanced intercross maize lines. Genetics 176: 645-657.

Barton, M. K., 2010 Twenty years on: The inner workings of the shoot apical meristem, a developmental dynamo. Dev. Biol. 341: 95-113.

Bauer, P., M. Lubkowitz, R. Tyers, K. Nemoto, R. B. Meeley *et al.*, 2004 Regulation and a conserved intron sequence of liguleless3/4 Knox Class-I homeobox genes in grasses. Planta 219: 359-368.

Bauman, L. E., J. S. Sinsheimer, E. M. Sobel, and K. Lange 2008 Mixed effects models for quantitative trait loci mapping with inbred strains. Genetics 180: 1743-1761.

Baurle, I. and T. Laux, 2005 Regulation of *WUSCHEL* transcription in the stem cell niche of the *Arabidopsis* shoot meristem. The Plant Cell 17: 2271-2280.

Beavis, W. D., D. Grant, M. Albertsen, and R. Fincher, 1991 Quantitative trait loci for plant height in four maize populations and their associations with qualitative genetic loci. Theor Appl Genet 83: 141-145.

Beavis, W. D., 1998 QTL Analyses: Power, Precision, and Accuracy, pp. 145-161 in *Molecular dissection of complex traits*, edited by A. H. Paterson. CRC Press, Boca Raton, FL.

Berke, T. G. and T. R. Rocheford, 1999 Quantitative trait loci for tassel traits in maize. Crop Sci 39: 1439-1443.

Bommert, P., B. I. Je, A. Goldschmidt, and D. Jackson, 2013 The maize Ga gene *COMPACT PLANT2* functions in CLAVATA signaling to control shoot meristem size. Nature 502: 555-558.

Brown, P. J., N. Upadyayula, G. S. Mahone, F. Tian, P. J. Bradbury *et al.*, 2011 Distinct genetic architectures for male and female inflorescence traits of maize. PLOS Genetics 7: e1002383.

Buckler, E. S., J. B. Holland, P. J. Bradbury, C. B. Acharya, P. J. Brown *et al.*, 2009 The genetic architecture of maize flowering time. Science 325: 714-718.

Callos, J. D., M. DiRado, B. Xu, F. J. Behringer, B. M. Link et al., 1994 The *forever young* gene encodes an oxidoreductase required for proper development of the *Arabidopsis* vegetative shoot apex. Plant J. 6: 835-847.

Clark, S. E., M. P. Running, and E. M. Meyerowitz, 1993 *CLAVATA1*, a regulator of meristem and flower development in *Arabidopsis*. Development 119: 397-418.

Clark, S. E., M. P. Running, and E. M. Meyerowitz, 1995 *CLAVATA3* is a specific regulator of shoot and floral meristem development affecting the same processes as *CLAVATA1*. Development 121: 2057-2067.

Clark, S. E., S. E. Jacobsen, J. Z. Levin, and E. M. Meyerowitz, 1996 The CLAVATA and SHOOT MERISTEMLESS loci competitively regulate meristem activity in *Arabidopsis*. Development 122: 1567-1575.

Coles, N. D., C. T. Zila, and J. B. Holland, 2011 Allelic effect variation at key photoperiod response quantitative trait loci in maize. Crop Science 51: 1036-1049.

Cook, J. P., M. D. McMullen, J. B. Holland, F. Tian, P. Bradbury *et al.*, 2012 Genetic architecture of maize kernel composition in the nested association mapping and inbred association panels. Plant Physiol 158: 824-834.

DeYoung, B. J., K. L. Bickle, K. J. Schrage, P. Muskett, K. Patel *et al.*, 2006 The CLAVATA1-related BAM1, BAM2 and BAM3 receptor kinase-like proteins are required for meristem function in Arabidopsis. Plant J. 45: 1-16.

Douglas, R. N., D. Wiley, A. Sarkar, N. Springer, M. C. P. Timmermans *et al.*, 2010 *ragged seedling2* encodes an ARGONAUTE7-Like protein required for mediolateral expansion, but not dorsiventrality, of maize leaves. The Plant Cell 22: 1441-1451.

Efroni, I., S. K. Han, H. J. Kim, M. F. Wu, E. Steiner et al., 2013 Regulation of leaf maturation by chromatin-mediated modulation of cytokinin responses. Dev. Cell 24: 438-445.

Eichten, S. R., J. M. Foerster, N. de Leon, Y. Kai, C. T. Yeh *et al.*, 2011 B73-Mo17 near-isogenic lines demonstrate dispersed structural variation in maize. Plant Physiol. 156: 1679-1690.

Flint-Garcia, S. A., A. L. Bodnar, and M. P. Scott, 2009 Wide variability in kernel coposition, seed characteristics, and zein profiles among diverse maize inbreds, landraces, and teosinte. Theor Appl Genet 100: 1129-1141.

Forestan, C., and S. Varotto, 2012 The role of PIN auxin efflux carriers in polar auxin transport and accumulation and their effect on shaping maize development. Molecular Plant 5: 787-798.

Foster, T., J. Yamaguchi, B. C. Wong, B. Veit, and S. Hake, 1999 *Gnarley1* is a dominant mutation in the *knox4* homeobox gene affecting cell shape and identity. The Plant Cell 11: 1239-1252.

Galinat, W. C., 1959 The phytomer in relation to floral homologies in the American *Maydeae*. Bot Mus Leafl 19: 1-32. Harvard Univ, Cambridge.

Gallavotti, A., 2013 The role of auxin in shaping shoot architecture. J. Exp. Bot. 64: 2593-2608.

Giulini, A., J. Wang, and D. Jackson, 2004 Control of phyllotaxy by the cytokinin-inducible response regulator homologue *ABPHYL1*. Nature 430: 1031-1034.

Hake, S., B. R. Char, G. Chuck, T. Foster, J. Long *et al.,* 1995 Homeobox genes in the functioning of plant meristems. Phil. Trans. R. Soc. Lond. B 350: 45-51.

Hake, S., E. Vollbrecht, and M. Freeling, 1989 Cloning *Knotted*, the dominant morphological mutant in maize using *Ds2* as a transposon tag. EMBO J. 8: 15-22.

Hay, A., J. Craft, and M. Tsiantis, 2004 Plant hormones and homeoboxes: Bridging the gap? BioEssays 26: 395-404.

Hochholdinger, F. and R. Tuberosa, 2009 Genetic and genomic dissection of maize root development and architecture. Curr. Opin. Plant Biol. 12: 172-177.

Itoh, J. I., H. Kitano, M. Matsuoka, and Y. Nagato, 2000 Shoot organization genes regulate shoot apical meristem organization and the pattern of leaf primordium initiation in rice. The Plant Cell 12: 2161-2174.

Jackson, D., B. Veit and S. Hake, 1994 Expression of maize *KNOTTED1* related homeobox genes in the shoot apical meristem predicts patterns of morphogenesis in the vegetative shoot. Development 120: 405-413.

Jackson, D. and S. Hake, 1999 Control of phyllotaxy in maize by the *abphyl1* gene. Development 126: 315-323.

Kayes, J. M. and S.E. Clark, 1998 *CLAVATA2*, a regulator of meristem and organ development in Arabidopsis. Development 125: 1253-1260.

Kerstetter, R. A., D. Laudencia-Chingcuanco, L. G. Smith, and S. Hake, 1997 Loss-of-function mutations in the maize homeobox gene, *knotted1,* are defective in shoot meristem maintenance. Development 124: 3045-3054.

Kierskowski, D., N. Nakayama, A. L. Routier-Kierzkowska, A. Weber, E. Bayer *et al.,* 2012 Elastic domains regulate growth and organogenesis in the plant shoot apical meristem. Science 335: 1096-1099.

Knauer, S., A. L. Holt, I. Rubio-Somoza, E. J. Tucker, A. Hinze *et al.,* 2013 A protodermal miR394 signal defines a region of stem cell competence in the Arabidopsis shoot meristem. Devel. Cell 24: 125-132.

Krill, A. M., M. Kirst, L. V. Kochian, E. S. Buckler, and O. A. Hoekenga, 2010 Association and linkage analysis of aluminum tolerance genes in maize. PLoS ONE 5: e9958.

Kump, K. L., P. J. Bradbury, R. J. Wisser, E. S. Buckler, A. R. Belcher et al., 2011 Genome-wide association study of quantitative resistance to southern leaf blight in the maize nested association mapping population. Nature Genetics 43: 163-168.

Kwon, C. S. and D. Wagner, 2007 Unwinding chromatin for development and growth: A few genes at a time. Trends Genet. 23: 403-412.

Kyozuka, J., 2007 Control of shoot and root meristem function by cytokinin. Curr. Opin. Plant Biol. 10: 442-446.

Lauter, N., M.J. Moscou, J. Habiger, and S.P. Moose, 2008 Quantitative genetic dissection of shoot architecture traits in maize: towards a functional genomics approach. The Plant Genome 1: 99-110.

Laux, T., K.F.X. Mayer, J. Berger, and G. Jürgens, 1996 The *WUSCHEL* gene is required for shoot and floral meristem integrity in *Arabidopsis*. Development 122: 87-96.

Lawrence, C. J., L. C. Harper, M. L. Schaeffer, T. Z. Sen, T. E. Siegfried *et al.,* 2008 MaizeGDB: The maize model organism database for basic, translational, and applied research. Intl. J. Plant Genomics. 2008:496957.

Lee, M., N. Sharopova, W. D. Beavis, D. Grant, M. Katt *et al.,* 2002. Expanding the genetic map of maize with the intermated B73 × Mo17 (IBM) population. Plant Mol. Biol. 48: 453-461.

Li, L., K. Petsch, R. Shimizu, S. Liu, W. W. Xu *et al.,* 2013 Mendelian and non-mendelian regulation of gene expression in maize. PLOS Genetics 9: e1003202.

Liu, Q., X. Yao, L. Pi, H. Wang, X. Cui *et al.,* 2009 The ARGONAUTE10 gene modulates shoot apical meristem maintenance and establishment of leaf polarity by repressing miR165/166 in Arabidopsis. Plant J. 58: 27-40.

Long, J. A., E. I. Moan, J. I. Medford, and M. K. Barton, 1996 A member of the KNOTTED class of homeodomain proteins encoded by the STM gene of Arabidopsis. Nature 379: 66-69.

Lunde C., S. Hake, 2009 The interaction of knotted1 and thick tassel dwarf1 in vegetative and reproductive meristems of maize. Genetics 181: 1693-1697.

Mayer, K. F. X., H. Schoof, A. Haecker, M. Lenhard, G. Jurgens *et al.,* 1998 Role of *WUSCHEL* in regulating stem cell fate in the *Arabidopsis* shoot meristem. Cell 95: 805-815.

McMullen, M. D., S. Kresovich, H. S. Villeda, P. Bradbury, H. Li *et al.,* 2009 Genetic properties of the maize nested association mapping population. Science 7: 737-740.

Moore, C. R., D.S. Gronwall, N.D. Miller, and E.P. Spalding, 2013 Mapping quantitative trait loci affecting *Arabidopsis thaliana* seed morphology features extracted computationally from images. G3 3: 109-118.

Moose, S. P. and P. H. Sisco, 1994 *Glossy15* controls the epidermal juvenile-to-adult phase transition in maize. The Plant Cell 6: 1343-1355.

Muehlbauer, G. J., J. E. Fowler, and M. Freeling, 1999 Sectors expressing the homeobox gene *liguleless3* implicate a time-dependent mechanism for cell fate acquisition along the proximal-distal axis of the maize leaf. Development 124: 5097-5106.

Nagasaki, H., J. Itoh, K. Hayashi, K. Hibara, N. Satoh-Nagasawa *et al.,* 2007 The small interfering RNA production pathway is required for shoot meristem initiation in rice. Proc. Natl. Acad. Sci. USA 104: 14867-14871.

Nogueira, F. T. S., S. Madi, D. H. Chitwood, M. T. Juarez, and M. C. P. Timmermans, 2007 Two small regulatory RNAs establish opposing fates of a developmental axis. Genes Dev. 21: 750-755.

Omori, F. and Y. Mano, 2007. QTL mapping of root angle in F2 populations from maize 'B73' x teosinte *'Zea luxurians'*. Plant Root 1: 57-65.

Panzea (http://www.panzea.org)

Peaucelle, A., S. A. Braybrook, L. Le Guillou, E. Bron, C. Kuhlemeier *et al.* 2011 Pectin-induced changes in cell wall mechanics underlie organ initiation in Arabidopsis. Curr. Biol. 21: 1720-1726.

Peiffer, J. A., S. A. Flint-Garcia, N. De Leon, M. D. McMullen, S. M. Kaeppler *et al.,* 2013 Genetic architecture of maize stalk strength. PLoS ONE 8: e67066.

Peiffer, J. A., M. C. Romay, M. A. Gore, S. A. Flint-Garcia, Z. Zhang *et al.* 2014 The genetic architecture of maize height. Genetics (doi: 10.1534/genetics.113.159152).

Pernisová, M., P. Klíma, J. Horák, M. Válková, J. Malbeck *et al.*, 2009 Cytokinins modulate auxin-induced organogenesis in plants via regulation of the auxin efflux. Proc. Natl. Acad. Sci. USA 106: 3609-3614.

Poethig, R. S., 1984 Cellular parameters of leaf morphogenesis in maize and tobacco, pp. 235-238 in *Contemporary Problems in Plant Anatomy*, edited by R. A. White and W. C. Dickinson. Academic Press, New York.

Poethig, R. S., E. H. Coe Jr., and M. M. Johri, 1986 Cell lineage patterns in maize embryogenesis: a clonal analysis. Dev Biol 117: 392-404.

Poethig, R. S. and E. J. Szymkowiak, 1995 Clonal analysis of leaf development in maize. Maydica 40: 67-76.

Poland, J. A., P. J. Bradbury, E. S. Buckler, and R. J. Nelson, 2011. Genome-wide nested association mapping of quantitative resistance to northern leaf blight in maize. Proc. Natl. Acad. Sci. USA 108: 6893-6898.

Pressoir, G., P. J. Brown, W. Y. Zhu, N. Upadyayula, T. Rocheford *et al.,* 2009 Natural variation in maize architecture is mediated by allelic differences at the *PINOID* co-ortholog *barren inflorescence2*. Plant J. 58: 618-628.

Reinhardt, D., T. Mandel, and C. Kuhlemeier, 2000 Auxin Regulates the initiation and radial position of plant lateral organs. The Plant Cell 12: 507-518.

Salvi, S., R. Tuberosa, E. Chiapparino, M. Maccaferri, S. Veillet *et al.*, 2002 Toward positional cloning of *Vgt1*, a QTL controlling the transition from the vegetative to the reproductive phase in maize. Plant Mol. Biol. 48: 601-613.

Salvi, S., G. Sponza, M. Morgante, D. Tomes, X. Niu *et al.*, 2007 Conserved noncoding genomic sequences associated with a flowering-time quantitative trait locus in maize. Proc. Natl. Acad. Sci. USA 104: 11376-11381.

Sang, Y., M.Wu, and D. Wagner, 2009 The Stem cell—Chromatin Connection. Seminars in Cell & Developmental Biology 20: 1143-1148.

Scanlon, M. J., R. G. Schneeberger, and M. Freeling, 1996 The maize mutant narrow sheath fails to establish leaf margin identity in a meristematic domain. Development 122: 1683-1691.

Scanlon, M. J., 2000 NARROW SHEATH1 functions from two meristematic foci during founder-cell recruitment in maize leaf development. Development 127: 4573-4585.

Scanlon, M. J., D.C. Henderson, and B. Bernstein, 2002 *SEMAPHORE1* functions during regulation of ancestrally duplicated knox genes and polar auxin transport in maize. Development 129: 2663-2673.

Schauer, S. E., S. E. Jacobsen, D. W. Meinke, and A. Ray, 2002 DICER-LIKE1: Blind men and elephants in Arabidopsis development. Trends Plant Sci. 7: 487-491.

Schnable, P. S., D. Ware, R. S. Fulton, J. C. Stein, F. Wei *et al.*, 2009 The B73 Maize Genome: Complexity, Diversity, and Dynamics. Science 326: 1112-1115.

Schneeberger, R. G., P. W. Becraft, S. Hake, and M. Freeling, 1995 Ectopic expression of the Knox homeo box gene *Rough sheath1* alters cell fate in the maize leaf. Genes Dev. 9: 2292-2304.

Schoof, H., M. Lenhard, A. Haecker, K. F. X. Mayer, G. Jurgens *et al.*, 2000 The stem cell population of *Arabidopsis* shoot meristems is maintained by a regulatory loop between the *CLAVATA* and *WUSCHEL* genes. Cell 100: 635-644.

Shen, W., and L. Xu, 2009 Chromatin remodeling in stem cell maintenance in Arabidopsis thaliana. Molecular Plant 2: 600-609.

Sinha, N., 1999 Leaf development in angiosperms. Ann. Rev. Plant Physiol. Plant Mol. Biol. 50: 419-446.

Smith, L. G., B. Greene, B. Veit, and S. Hake, 1992 A dominant mutation in the maize homeobox gene, Knotted-1, causes its ectopic expression in leaf cells with altered fates. Development 116: 21-30.

Taguchi-Shiobara, F., Z. Yuan, S. Hake, and D. Jackson, 2001 The *fasciated ear2* gene encodes a leucine-rich repeat receptor-like protein that regulates shoot meristem proliferation in maize. Genes Dev. 15: 2755-2766.

Takacs, E. M., J. Li, C. Du, L. Ponnala, D. Janick-Buckner *et al.*, 2012 Ontogeny of the maize shoot apical meristem. The Plant Cell 24: 3219-3234.

Tian, F., P. J. Bradbury, P. J. Brown, H. Hung, Q. Sun *et al.,* 2011 Genome-wide association study of leaf architecture in the maize nested association mapping population. Nature Genetics 43: 159-162.

Timmermans, M. C. P., A. Hudson, P. W. Becraft, and T. Nelson, 1999 ROUGH SHEATH2: a myb protein that represses *knox* homeobox genes in maize lateral organ primordia. Science 284: 151-153.

Tsiantis, M., R. Schneeberger, J. F. Golz, M. Freeling, and J. A. Langdale, 1999 The maize *rough sheath2* gene and leaf development programs in monocot and dicot plants. Science 284: 154-156.

Uchida, N., B. Townsley, K. Chung, and N. Sinha, 2007 Regulation of *SHOOT MERISTEMLESS* genes via an upstream-conserved noncoding sequence coordinates leaf development. Proc. Natl. Acad. Sci. USA 104: 15953-15958.

Upadyayula, N., H. S. da Silva, M. O. Bohn, and T. R. Rocheford, 2006 Genetic and QTL analysis of maize tassel and ear inflorescence architecture. Theor. Appl. Genet. 112: 592-606.

Vanstraelen, M., and E. Benková, 2012 Hormonal interactions in the regulation of plant development. Ann. Rev. Cell Dev. Biol. 28: 463-487.

Vaucheret, H., F. Vazquez, P. Crété, and D. P. Bartel, 2004 The action of ARGONAUTE1 in the miRNA pathway and its regulation by the miRNA pathway are crucial for plant development. Genes Dev. 18: 1187-1197.

Vladutu, C., J. McLaughlin, and R. L. Phillips, 1999 Fine mapping and characterization of linked quantitative trait loci involved in the transition of the maize apical meristem from vegetative to generative structures. Genetics 153: 993-1007.

Vollbrecht, E., B. Veit, N. Sinha, and S. Hake, 1991 The developmental gene *Knotted-1* is a member of a maize homeobox gene family. Nature 350: 241-243.

Vollbrecht, E., L. Reiser, and S. Hake, 2000 Shoot meristem size is dependent on inbred background and presence of the maize homeobox gene, knotted1. Development 127: 3161-3172.

Wagner, Doris, 2003 Chromatin regulation of plant development. Curr. Opin. Plant Biol. 6: 20-28.

Wang, Y. and J. Li, 2008 Molecular basis of plant architecture. Ann. Rev. Plant Biol. 59: 253-279.

Woodward, J. B., N. D. Abeydeera, D. Paul, K. Phillips, M. Rapala-Kozik et al., 2010 A maize thiamine auxotroph is defective in shoot meristem maintenance. The Plant Cell 22: 3305-3317.

Yanai, O., E. Shani, K. Dolezal, P. Tarkowski, R. Sablowski *et al.,* 2005 Arabidopsis KNOXI proteins activate cytokinin biosynthesis. Curr. Biol. 15: 1566-1571.

Yang, X., H. Ma, P. Zhang, J. Yan, Y. Guo *et al.,* 2012 Characterization of QTL for oil content in maize kernel. Theor. Appl. Genet. 125: 1169-1179.

Yu, X., H. Wang, W. Zhong, J. Bai, P. Liu *et al.,* 2013 QTL mapping of leafy heads by genome resequencing in the RIL population of *Brassica rapa.* PLOS ONE 8: e76059.

Zeng, Z. B., 1994 Precision mapping of quantitative trait loci. Genetics 136: 1457-1468.

Zhang, B. H., X. P. Pan, S. B. Cox, G. P. Cobb, and T. A. Anderson, 2006 Evidence that miRNAs are different from other RNAs. Cell. Mol. Life Sci. 63: 246-254.

Zhang, X., S. Madi, L. Borsuk, D. Nettleton, R. J. Elshire *et al.,* 2007 Laser microdissection of narrow sheath mutant maize uncovers novel gene expression in the shoot apical meristem. PLOS Genetics 3: e101.

Zhu, J., S. M. Kaeppler, and J. P. Lynch, 2005 Mapping of QTLs for lateral root branching and length in maize (*Zea mays* L.) under differential phosphorus supply. Theor. Appl. Genet. 111: 688-695.

Table 1. SAM-related maize genes

GENE ID	MAIZE GENE NAME	SYMBOL
GRMZM2G035688	aberrant phyllotaxyl1	abph1
GRMZM2G074097	bladekiller1	blk1
GRMZM2G064732	compact plant2	ct2
GRMZM2G104925	fasciated ear2	fea2
GRMZM2G133331	fasciated ear4	fea4
GRMZM2G452178	gnarley1 (knox4)	gn1
GRMZM2G017087	knotted1	kn1
GRMZM2G002225	knotted1-like homeobox10	knox10
GRMZM2G000743	knotted1-like homeobox3	knox3
GRMZM2G135447	knotted1-like homeobox8	knox8
GRMZM2G020187	leafbladeless1	lbl1
GRMZM2G094241	lg4a/knox11	lg4a
GRMZM5G832409	lg4b/knox5	lg4b
GRMZM2G087741	liguless3	lg3
GRMZM2G069028	narrow sheath1	ns1
GRMZM2G393433	no apical meristem1	nam1
GRMZM2G139700	no apical meristem2	nam2
GRMZM5G892991	ragged seedling1	rgd1
GRMZM2G109987	rolledleaf1	rld1
GRMZM2G042250	rolledleaf2	rld2
GRMZM2G028041	rough sheath1	rs1
GRMZM2G403620	rough sheath2	rs2
GRMZM2G300133	thick tassel dwarf1	td1
GRMZM2G010353	viviparous kernel8	vp8
GRMZM2G133972	WUSCHEL related homeobox 9a	wox9a
GRMZM2G031882	WUSCHEL related homeobox 9b	wox9b
GRMZM2G409881	WUSCHEL related homeobox 9c	wox9c

Chapter 2

Genetic control of maize shoot apical meristem architecture

Abstract

The shoot apical meristem contains a pool of undifferentiated stem cells, and generates all above-ground organs of the plant. During vegetative growth, cells differentiate from the meristem to initiate leaves while the pool of meristematic cells is preserved; this balance is determined in part by genetic regulatory mechanisms. To assess vegetative meristem growth and genetic control in *Zea mays*, we investigated its morphology at multiple time points and identified three stages of growth. We measured meristem height, width, plastochron internode length, and associated traits from 86 individuals of the intermated B73 x Mo17 recombinant inbred line population. For meristem height-related traits, the parents exhibited markedly different phenotypes, with B73 being very tall, Mo17 short, and the population distributed between. In the outer cell layer, differences appeared to be related to number of cells rather than cell size. In contrast, B73 and Mo17 were similar in meristem width traits and plastochron internode length, with transgressive segregation in the population. Multiple loci (6-9 for each trait) were mapped, indicating meristem architecture is controlled by many regions; none of these coincided with previously described mutants impacting meristem development. Major loci for height and width explaining 16% and 19% of the variance were identified on chromosomes 5 and 8, respectively. Significant loci for related traits frequently coincided, while those for unrelated traits did not overlap. Using three near-isogenic lines, a locus explaining 16% of the parental variance in meristem height was validated. Published expression data were leveraged to identify candidate genes in significant regions.

Introduction

Differences in plant morphology in part reflect differences in organ shape, number, and size. Mutant analysis has been an excellent tool to dissect the major regulators controlling plant morphology. In addition, quantitative trait locus (QTL) mapping has been conducted in many plant species and on numerous traits impacting plant morphology - e.g. leaf or leafy head size and shape (Jiang *et al.* 2000, Yu *et al.* 2013, Jun *et al.* 2013, Tian *et al.* 2011), root architecture (Loudet *et al.* 2005, Johnson *et al.* 2000, Courtois *et al.* 2009, Hochholdinger and Tuberosa 2009), fruit size and shape (Causse *et al.* 2004, Frary *et al.* 2000, Grandillo *et al.* 1999), and whole plant or inflorescence architecture (Lauter *et al.* 2008, Clark *et al.* 2006, Upadyayula *et al.* 2006). Most QTL mapping studies have focused on traits that were measured on mature organs, though some have targeted features of the maize embryo (Moore *et al.* 2013, Yang *et al.* 2012). An understanding of the genetic control of the morphology of undifferentiated tissue types may lead to insight into the morphology and development of differentiated tissue types.

The shoot apical meristem (SAM) contains a set of undifferentiated stem cells and forms a vital control center for plant growth and development. It produces all aerial organs of the plant including lateral shoots, leaves and flowers, and together with environmental cues, determines plant architecture (Wang and Li 2008). The morphology of the SAM is constrained by the balance between organogenesis and stem cell maintenance. Without this balance, the meristem either depletes its supply of stem cells during leaf formation, leading to developmental arrest, or over-proliferates stem cells and

fails to initiate leaves (Barton 2010). In maize, the SAM is initiated during the transition stage of embryogenesis, and its dome-like structure begins to form around the coleoptilar stage. The central zone of the meristem contains the stem cells, while organogenesis takes place in the peripheral zone. Based on mutant analysis and transcript profiling, the function of organogenesis takes place before meristem maintenance begins in maize (Takacs *et al.* 2012; Vollbrecht *et al.* 2000). Leaves are formed from the SAM via recruitment of 100-200 leaf initials termed founder cells (Poethig 1984). About five leaves develop in the maize embryo between fertilization and seed maturation and quiescence; leaf development and growth resumes upon germination. Leaf primordia are initiated at regular intervals; the time between leaf initiation is measured in plastochrons (P) (Sharman 1942b; Sylvester *et al.* 1990). The importance of the SAM for growth and development has led to numerous genetic studies investigating SAM function. Most of these studies focused on mutant analysis and uncovered several regulatory processes acting in the SAM. In some cases these mutants resulted in alteration of SAM size and/or shape as well as whole plant morphology.

In *Arabidopsis*, a negative feedback loop between CLAVATA (CLV) and the homeobox gene *WUSHEL (WUS)* is a primary regulator of stem cell number and thereby SAM size (Schoof *et al.* 2000, Wang and Li 2008). Defects in CLV receptor-ligand signaling lead to enlarged meristems (Leyser and Furner 1992; Clark *et al.* 1993, 1995; Kayes and Clark 1998), while plants defective in *WUS* show impaired meristem maintenance (Laux *et al.* 1996). Maize mutants in this pathway include *faciated ear2 (fea2)* (Taguchi-Shiobara *et al.* 2001) and *compact plant2 (ct2)* (Bommert *et al*. 2013),

which were initially identified based on their inflorescence phenotype but also affect the size of the vegetative meristem. Another maize mutant, *thick tassel dwarf (td1)* (Taguchi-Shiobara *et al.* 2001), is similar in function to CLV1 in inflorescence and floral meristems, but in the vegetative SAM is more akin to the BAM genes (DeYoung *et al.* 2006), which have multiple functions throughout development (Lunde and Hake 2009).

Another major category of genes shown to affect meristem size is the *Knotted-1-like homeobox (KNOX)* genes. Maize plants without functional *Knotted-1 (Kn1),* the founding member of this gene family (Hake *et al.* 1989; Vollbrecht *et al.* 1991), are unable to maintain the shoot meristem (Kerstetter *et al.* 1997; Vollbrecht *et al.* 2000). In maize, kn1 mutants display a decrease in meristem size with penetrance dependent on genetic background, providing a clear indication for the presence of natural variation in pathway regulating SAM activity (Vollbrecht *et al.* 2000). Meristem termination phenotypes were also observed in orthologs of kn1, *Arabidopsis STM* (Long *et al.* 1996) and rice *OSH1* (Tsuda *et al.* 2011). Maize *KNOX* genes, such as *rough sheath1*, *gnarley1/KNOX4*, and *liguleless3* (*lg3*) and *lg4* (Schneeberger et al. 1995; Foster et al. 1999; Muehlbauer et al. 1999; Bauer et al. 2004), are expressed specifically in the SAM, but possibly due to redundancy, these mutants are not known to have an effect on SAM size (Hake et al. 2004; Bolduc *et al.* 2014).

KNOX proteins act by controlling the ratio of plant hormones in the SAM to maintain meristematic identity (Kyozuka 2007). Indeed, the regulation and patterning of many plant hormones is vital to the function of the meristem (see Hay *et al.* 2004 and Vanstraelen and Benková 2012 for reviews). Cytokinin promotes cell division, while

auxin promotes organogenesis in the peripheral zone of the meristem (Pernisová *et al.* 2009). Perturbation of cytokinin biosynthesis leads to loss of the SAM (Yanai *et al.* 2005), whereas mutations in cytokinin response regulators, such as the maize mutant *aberrant phyllotaxy1* (*abph1)* cause larger meristems to form (Jackson and Hake 1999; Giulini *et al.* 2004). Without auxin transport the SAM loses its ability to form organs (Reinhardt 2000; see Gallavotti 2013 and Forestan and Varotto 2012 for reviews). Gibberellins and brassinosteroids interact with auxin and cytokinin pathways to regulate their ratio during plant development (Vanstraelen and Benková 2012).

SAM establishment and function are also impacted by the activity of small RNAs (Zhang *et al.* 2006; see Axtell 2013 for microRNA review). During SAM formation in *Arabidopsis*, microRNA394 (miR394) moves from the protoderm to the underlying cell layers to define stem cell location (Knauer *et al.* 2013). In addition, the correct spatiotemporal regulation of class III homeodomain leucine zipper (HD-ZIPIII) transcription factors by miR166 is essential for normal meristem function, As such, key regulators in miRNA biogenesis or function show meristem defects when affected, e.g. *ago1* (Vaucheret *et al.* 2004), *ago10* (Liu *et al.* 2009), and *dcl1* (Schauer et al. 2002). Likewise, maize *leafbladeless* and *ragged seedling2*, which encode essential components in the biogenesis of *trans*-acting small interfering RNAs, regulate meristem function through their effect on auxin response as well as the expression domain of miR166 and HD-ZIPIII transcription factors (Nogueira *et al.* 2007; Douglas *et al.* 2010). Mutants in this pathway in rice, *sho* mutants, display variable morphological differences in the SAM,

the shape of which correlates with variation in phyllotaxy and plastochron timing (Itoh *et al.* 2000; Nagasaki *et al.* 2007), linking SAM architecture to plant morphology.

Chromatin structure and remodeling regulators are parts of yet another process linked to stem cell maintenance (Shen and Xu 2009; for review see Wagner 2003; Kwon and Wagner 2007; Sang *et al.* 2009). Chromatin remodeling pathway components also interact with the CK response pathway (Efroni *et al.* 2013), leading to cross-talk among the regulatory processes.

Besides these regulatory mechanisms that ultimately effect gene expression, several recent studies have revealed downstream processes that impact SAM function. These include enzymes that vary the properties of the cell wall, as well as metabolic processes (Kierskowski *et al.* 2012; Peaucelle *et al.* 2011). For instance, maize *bladekiller1-R* (*blk1-R*), a thiamine auxotroph, is defective in both meristem maintenance and organ initiation and displays progressively decreasing SAM size (Woodward *et al.* 2010).

These processes and pathways act and interact to form a complex regulatory network controlling SAM morphogenesis and maintenance. Although many aspects of the maize SAM have been studied through mutant and expression analysis, the genetic control of natural variation in SAM architecture is unknown.

The objectives of this study were to examine SAM morphology during vegetative development, calculate heritability and segregation of SAM measurements in a RIL population to use for mapping, map QTL to determine the genetic architecture controlling

natural variation in SAM morphology, and to use expression data to identify candidate genes involved in regulating and responding to changes in meristem architecture.

Materials and Methods

Plant materials

Two sets of plant materials were used in this study: 86 lines from the intermated B73 x Mo17 recombinant inbred line (IBMRIL) population and the B73 and Mo17 parents (Table S1; Lee *et al.* 2002); and a set of three near-isogenic lines (NILs) selected from the 150 B73 x Mo17 NIL population (Table S1; Eichten *et al.* 2011). These NILs were backcrossed three times, and self-pollinated for four to six generations.

Plant growth and experimental design

To assess the optimal time for assessing SAM architecture traits, B73 and Mo17 seed was planted in six-inch square pots with five plants per pot in a 1:1 mix of black soil and SunGro potting soil, with the recommended application rate of 2 teaspoons per square foot of Osmocote Plus fertilizer. Plants were grown in a growth chamber with 16 h days at 25C and 20C nights. Sixty B73 and 60 Mo17 individuals were grown for four weeks with up to 10 plants sampled for histology at each time point (7, 10, 14, 17, 21, and 28 days after planting). An additional 40 of each genotype were grown in a second replication and sampled in a similar fashion at 7, 14, 21, and 28 days after planting. Results of these two experiments were combined by calculating the weighted mean and standard error, allowing for the inclusion of the effect of the two separate experiments. Each genotype/week combination was represented by 9-20 measured images with the exception of Mo17 at four weeks, where most of the SAMs had already transitioned and were not included. As a result of this study, two weeks was used as the sampling time

point for the remainder of the analyses, as two-week old SAMs had reached full vegetative size while not yet showing signs of transition (Figure 1D-E, boxes).

For the mapping and validation experiments, seeds were planted in one-inch wide by eight-inch deep tubes placed in 10 x 20 racks using a 1:1 mix of black soil and either MetroMix or SunGro potting soil, with the recommended application rate of 2 teaspoons per square foot of Osmocote Plus fertilizer. Every third row of ten within flats were left empty to allow plants more room to grow, provide even air flow, and reduce edge effects, resulting in a total of 140 plants per rack. Plants were grown for 14 days in growth chambers with 16 h days at 25C and 20C nights.

Eighty-six IBMRILs and the B73 and Mo17 parents were grown twice, each grow-out containing two replications of 10 plants per line, with lines randomized within each replication. All healthy plants were sampled for histology, and 15 to 39 images were measured per RIL, in addition to 83 B73 and 80 Mo17.

For the validation experiment, two B73-like (B034 and B063) and one Mo17-like (M049) NILs (Table S1) were selected to target the SAM_height_6 QTL on chromosome 5. These three lines as well as B73 and Mo17 were grown in 40 small blocks, each consisting of one plant per line and lines randomly distributed within each block. All normally-growing plants were sampled for histology.

Histology

For the IBMRIL population, shoots were dissected at 14 days, fixed in FAA overnight, and embedded in paraffin according to Ruzin (1999). Serial, median

longitudinal 8um sections were cut using a microtome, mounted on slides, stained with toluidine blue, and de-paraffinized. A light microscope and Zeiss AxioVision software were used to capture SAM images.

For the time course study and NIL validation, shoots were dissected at 14 days and fixed in FAA overnight. Tissues were then dehydrated and cleared using a series of ethanol and methyl salicylate according to Jackson and Hake (1999) before being stored in 100% methyl salicylate. Cleared tissue blocks were imaged directly on slides and captured as described above.

SAM architecture measurements

SAM images were measured for SAM width, height, arc length, midpoint width, P1 height, plastochron internode length and arc cell count using ImageJ software (http://rsbweb.nih.gov/ij/). Width was measured from the point of insertion of the P1 leaf into the SAM, known as the P1 cleft (Figure 1A). Height was measured from the apex of the SAM to the width line, and arc length traced the outer distance from the apex to the P1 cleft. Midpoint width was defined as the width of the SAM at the midpoint of the height. P1 height was the distance from the P1 cleft to the tip of the P1. Plastochron internode length (PIL) was the vertical distance from the P2 to P1 cleft. Cells were counted in the L1 layer along the arc length. Average cell size (arc length divided by arc cell count), height:width ratio, and volume as a dome were also calculated as derived traits for each individual sample.

Data analysis

Analysis of the raw phenotype data, including Pearson's correlation coefficients, ANOVAs, and Student's t-test (for comparing NILs to parental inbreds) were conducted in R (http://www.r-project.org/). Heritability on a plot-means basis was calculated as the additive genetic variance of the RIL (Va_RIL) divided by the total phenotypic variance (Vp), according to Bernardo 2010 (p. 153-156).

The genetic map used for QTL mapping was derived from sequenced RNA in the IBMRIL (Li *et al.*, 2013). QTL mapping was performed using QTLCartographer (http://statgen.ncsu.edu/qtlcart/) composite interval mapping (Model 6), with 10 background markers and 5cM windows. To determine a significance threshold, 1000 permutations at $\alpha=0.05$ were conducted on each trait. All traits gave similar results, so the average LOD value of 3 was used as a cutoff to declare QTL significance. Confidence intervals were determined by a 1-LOD drop.

To map the correlation between gene expression in shoot apices and SAM phenotypes, Pearson's correlation coefficients were calculated for each pairwise gene and trait combination across 86 IBMRILs. Significance thresholds were determined for each gene-trait combination individually at a comparison-wise threshold of $p<0.05$ after 1000 permutations. Genes included in this analysis are only those expressed in some stage of the ontogeny of the B73 SAM (Takacs *et al.* 2012), as well as in shoot apices of the IBMRIL (Li *et al.* 2013).

Results

Growth of the maize SAM

To examine the architecture of the maize SAM throughout the vegetative phase of growth, we measured B73 and Mo17 at six time points from one to four weeks after planting. Analysis of SAM width and to a lesser extent SAM height from the P1 cleft (Figure 1A) revealed a similar pattern of SAM development between the two inbreds, with a phase of decelerated growth rate surrounded by two periods of more rapid expansion (Figure 1D-E). Thus, in addition to its role in organ initiation, the SAM seems to dynamically alter the rate of expansion of its stem cell pool throughout vegetative development. After the initial expansion of the SAM, this phase of delayed growth started around 14 days after planting for B73, and around 10 days for Mo17 (Figure 1D-E, boxes indicate leveling off of growth rate).

Another period of SAM expansion took place around 18-19 days for Mo17 and between 21-28 days (exact time point not known) for B73, or about 10 days prior to transition. During this time, the SAM again accumulated stem cells before it began to transition to an inflorescence meristem, as defined here by the presence of branch and spikelet pair meristems. Throughout this phase the SAM rapidly became wider and taller (Figure 1D-E), and its relative position in the plant began to shift upwards by 1-2cm. At 28 days after planting, most (89%) Mo17 SAMs had reached transition, compared with 0% for B73.

Fourteen days after planting (horizontal boxes in Figure 1D-E) was selected as a common time at which to measure the vegetative size of the SAM in its phase of stem cell pool maintenance rather than proliferation, as both B73 and Mo17 SAMs had reached the plateau of full vegetative size at this age, but neither inbred at this time point had started to expand prior to transition.

Quantitative variation for SAM architecture in maize

To determine the heritability of natural variation for a variety of SAM architecture traits, we examined B73 and Mo17 and a subset of 86 individuals of the IBMRIL population (Table S1). Measurements of ten traits were initially used to characterize SAM architecture: height, arc length, width, and midpoint width from the P1 cleft; cell number in the L1 layer along the arc length; length of P1; plastochron internode length (PIL); and the derived traits of cell size, height:width ratio, and volume (Figure 1A-C). The measurements of SAM traits in B73 and Mo17 were compared to the distributions observed in the RIL population to determine the type of segregation occurring for each trait (Table 1).

Distributions of the meristem traits followed two main patterns, exemplified by width and height (Figures 2A and S1). For many SAM traits (height, height:width ratio, volume, arc cell count and arc length), B73 and Mo17 exhibited substantially different values ($p<0.001$; Table 1, Figures 2A and S1). The distributions of these traits in the IBMRIL showed a range of between-parent values and a positive skew, with more lines having values closer to the shorter SAM in Mo17. This could indicate that several alleles

are needed in combination to create the extreme height observed in B73. Several other traits (SAM width, midpoint width, and PIL) displayed normal distributions (Figures 2A and S1). The phenotype of B73 and Mo17 was quite similar for these traits, while the RILs showed substantial transgressive segregation (Table 1, Figures 2A and S1).

In addition to the extreme values of B73 and Mo17 observed for SAM height and related traits, these parental lines were also unique in their height:width ratio. Most RIL showed a height:width ratio very near 1 (average 0.99, Table 1). However, the B73 SAM was much taller than wide (ratio of 1.37, or 3.44 standard deviations away from the mean), and Mo17 was wider than its height (ratio of 0.74; -2.34 sd). Only one Mo17-like IBMRIL showed a ratio insignificantly outside of these parental values.

Heritability estimates for SAM architecture were medium to high, ranging from 0.54 to 0.88 for significant traits (0.86 for height, 0.72 for width; Table 1). Several of the SAM architecture traits measured are likely to be under common genetic control mechanisms, as correlations among the RILs (Figure 2B) provided evidence for clusters of related traits. Some of these relationships reflected derived traits or related measurements. One group of correlated traits included height, arc length, volume and height:width ratio, and the second group of correlated traits included width and mid-point width. These two groups showed high trait correlation within the groups and low correlation between them. All of the remaining three traits showed low correlation to the first two main phenotypic groups. PIL showed some correlation with SAM height, volume, and arc length, but largely captured unique variation. SAM arc length was primarily due to changes in cell number rather than size, as SAM arc cell number was

significantly different between the parents and across the population, correlated with other SAM height and arc length, and heritable.

Arc cell size and P1 height had the lowest heritability estimates and were not significant (at $p<0.01$) among the RILs (Table 1). In the case of arc cell size, this may be due to deviation in cell size along the length of an individual SAM's arc length, or a lack of biological variation in the trait. In addition, it should be noted that relative arc cell size and count may likely differ from that of the meristematic cells in the central zone of the SAM. For P1 height, considerable growth occurs in a single primordium throughout the duration of any single plastochron, such that a P1 primordial early in the plastochron is much smaller than the same P1 leaf later in the plastochron, causing the trait to have substantial variation outside of genetic effect. Due to their low heritability these traits were not used for further analyses.

Mapping QTL associated with SAM architecture

To identify regions of the genome associated with variation for SAM architecture, a QTL mapping analysis was conducted with all phenotypic measurements in the IBMRIL population combined with genetic marker data (7,856 SNP markers, Li *et al.* 2013). Between six and nine QTL were identified for every SAM trait, each contributing 4-23% of the trait variation (Table 2, S3). The multiple regression model based on the combined significant QTL explained 55-74% of the total variation for each of the SAM traits (Table 2).

Eight QTL were identified for SAM height, six of which were shared with arc length and/or volume QTL (Table 3). SAM height QTL were located on chromosomes 1, 2, 3, 5, and 6, with two each located on chromosomes 1 and 5, and the highest LOD and effect-size QTL located on chromosome 5. The SAM_height_6 QTL on chromosome 5 (see Table 3) explained 16% of the variation in SAM height, and was also highly significant for all three related traits.

Eight QTL were mapped for SAM width, six of which were in common with midpoint width QTL (Figure S2, Table S2). SAM width QTL showed wider confidence intervals and were located across seven chromosomes (all but 1, 6, and 7). The most significant QTL for SAM width was shared by midpoint width and mapped to chromosome 8, and explained 19% of the variation.

The SAM architecture QTL regions were relatively well defined, with an average of 9.51 cM per QTL. Highly correlated SAM traits often showed QTL coincidence: QTLs for SAM height were commonly found in the same locations as those for SAM arc length and volume, and SAM width and midwidth co-localized (Table S3, Figure 3). Peaks significant for only a subset of correlated phenotypes frequently harbored smaller non-significant peaks for the correlated traits. None of the SAM height or height-related QTL was mapped to the same locations as SAM width or midwidth (Figure 3).

Traits that showed correlation among multiple different measures of SAM architecture reflected this in their QTL locations. For example, PIL was weakly correlated with other SAM traits but seemed to reflect some unique measures of SAM architecture. As predicted, five of nine QTL for PIL mapped to unique locations, while

the other four coincided with height and/or arc length, volume, or midpoint width (Table S3).

The ability to map QTL for SAM architecture was independent of whether parental phenotypes showed distinct differences in the trait of interest (Tables 1-2; Figure 2A), supporting the idea that QTL mapping can be successful in populations originating from similar parental phenotypes when transgressive segregation is present.

Validation of a strong-effect SAM height QTL

We sought to validate the existence of SAM_height_6, a strong-effect QTL (16% variation explained, LOD 9.25) on chromosome 5 at 892.81 - 895 cM (Tables 3 and S3) using a set of three near-isogenic lines (NILs; Eichten *et al.* 2011). Two NILs (B034 and B063) had a largely B73 genome with regions of Mo17 introgression while the other line (M049) was mostly Mo17 with at least one introgressed region of B73. In each of these NILs, the introgression on chromosome 5 spanned the entire QTL confidence interval. Other introgressed regions (different for each NIL and not overlapping with other SAM height QTL) were present in the background, but these were minimal: B034, B063, and M049 contained 2.35, 3.87, and 2.56% total introgression, respectively. At least 33 individuals were measured for the parents and each of these three NIL genotypes. The NIL genotypes were significantly different from the parents in the expected direction (Figure 4C-D) based on the introgressed region (Figure 4A-B). This analysis supports the existence of this SAM height QTL on chromosome 5 and suggests that it contributed

15% (16 of 105μm) of the variation in SAM height (Figure 4C-D) based on B-like NILs. M049 showed a slightly smaller than predicted effect.

Identifying potential candidate genes in QTL regions

Three traits - SAM height, width, and PIL - representing the three different groups of correlated traits were further examined for potential candidate genes with the expression data. First, correlation analysis was conducted between gene expression in shoot apices (Li *et al.* 2013) and SAM architecture traits across the same set of IBMRILs to identify whether expression levels of some genes are correlated to SAM morphology differences and whether these genes are within genomic regions defined by the mapped QTL. There were 41, 33, and 9 cases for the three traits (Figure 5 A, B, and C, respectively) where significantly correlated gene expression coincided with genes located under QTL for that trait. These 83 genes include annotations related to sucrose and metal transport, homeobox genes, and growth-related factors (Table S4). These genes may be targets of future research in SAM growth and stem cell pool homeostasis, as well as potentially the control of maize vegetative development.

As these 83 genes would be expected to be expressed in the SAM and play a role in SAM formation or function, expression of these genes was examined across SAM ontogeny in B73 using expression data from Takacs *et al.* 2012. Levels and patterns of expression across SAM ontogeny varied greatly (Figure S2). Some genes were expressed in a stage-specific manner, while others showed increasing or decreasing expression levels throughout the development of the SAM. Using expression patterns may be one

additional way to narrow down candidate genes for future studies targeting specific gene families and interactions.

Discussion

The maize SAM has three stages of development during vegetative plant growth

The morphology and growth rate of the maize SAM are not static. The most evident examples of dynamic growth are the changes take place in the SAM prior to or at reproductive transition, among them the enlargement of the apex as the growth rate increases, a change in phyllotaxy and suppression of internodes in the flower, and an increased rate of initiation of primordia accompanied by decreased size of primordia at initiation (Lyndon and Battey 1985). In *Sinapis alba* these changes have been detected as early as 24 hours after long day floral induction; flower primordia initiated around 60 hours after (Bernier 1997). The dramatic enlargement of the SAM prior to initiation is thought to be due to an increase in the number of stem cells in the central part of the SAM to support the shift in phyllotaxy during flower formation (Ormenese *et al.* 2002).

In studying the dynamic growth of the SAM up until the point of reproductive transition (as defined here by the formation of spikelet pair meristems), we characterized the changes that took place during the vegetative growth of the plant. The time points analyzed indicated three distinct stages of vegetative SAM growth: an initial proliferation of the stem cell pool where SAM size increased, a maintenance phase where a balance was maintained between organ initiation and SAM maintenance, and finally a second expansion of the SAM in preparation for transition.

Previous research outlined in Chuck and Hake (2005) and Poethig (1990) indicate that the size of the shoot or even factors produced by the root system may be the

important features in regulating the timing of reproductive development, in concert with the genetic pathways implicated in phase change. Sharman (1942a) too suggested that some minimum condition must be reached within the apex that tips a balance, causing the abrupt change from vegetative to reproductive growth. Perhaps part of that balance lies in the size of the SAM and the accumulation of an excess of cells in the meristematic pool that then triggers floral transition. This would explain the relative timeframe of the stages of SAM development of different inbreds during vegetative development, with earlier-flowering inbreds progressing faster through the stages of SAM growth (Thompson and Muehlbauer, unpublished data).

Arc length of the tunica layer (L1) is influenced by cell number

A larger SAM may be due to either an increase in cell number, cell size, or both. To comprehensively address which of these is the case in maize, the size and shape of cells in all regions of the SAM should be carefully examined. Due to the difficulty of obtaining accurate data for the more internal cells of the SAM, we investigated only cell number and size along the arc length in the L1 layer. Despite a wide range of SAM architecture present in the IBMRIL population and its parents, the size of these cells was not significantly different among genotypes ($p>0.05$) and showed relatively low heritability ($h^2=0.43$). Conversely, the number of cells present in this layer was found to be highly significant ($p<0.001$) and slightly more heritable ($h^2=0.66$; see Table 1). B73 and Mo17, the inbred parents of the population, exhibited very different morphologies as reflected by SAM height and arc length; this difference between the parents and

throughout the population correlates with the increased number of cells but not with cell size. Thus, for the outermost layer of cells in the meristem, the differences observed in overall SAM size in the IBMRIL and its inbred parents were primarily related to the number of cells present, not cell size.

SAM architecture is controlled by many QTL

Multiple QTL were identified for each of the traits analyzed. In a small population such as the subset utilized here, QTL analysis will tend to underestimate the number of loci contributing to the trait and overestimate the size of the effects (Beavis 1998). This indicates that the genetic control of maize SAM architecture may actually be controlled by even more QTL that were not identified. Similar results have been found for natural variation in other morphological characteristics, such as leaf shape in Antirrhinum (Langlade *et al.* 2005), tomato (Chitwood *et al.* 2013), and maize (Tian *et al.* 2011), as well as floral shape in Arabidopsis (Juenger *et al.* 2000). Also in maize, large numbers of small-effect additive QTL have been shown to be the basis of control of flowering time (Buckler *et al.* 2009), though larger-effect loci were identified for inflorescence traits (Brown *et al.* 2011).

Genes controlling natural variation differ from those known to affect mutant morphologies

Many genes have been previously identified as affecting SAM size based on mutant phenotypes, including *Knotted-1* (Vollbrecht *et al.* 2000), *abphyl1* (Jackson and

Hake 1999), *Extra cell layers1* (Kessler *et al.* 2006), *bladekiller1-R* (Woodward *et al.* 2010), *fasciated ear2* (*fea2*) (Taguchi-Shiobara *et al.* 2001), and *compact plant2* (Bommert *et al.* 2013). Several main processes have also been implicated in the initiation, function, or maintenance of the SAM, including the CLV-WUS feedback loop, KNOX, plant hormones, small RNAs, and chromatin structure and remodeling. However, genes known to be involved in these processes or directly impact the SAM did not coincide with the QTL we identified. This could indicate that these genes don't play a significant role in the control of natural variation in maize SAM architecture, or perhaps that some of these genes do not show significant variation within the IBMRIL.

One of these genes, *fea2*, was implicated in a previous QTL study for kernel row number, a trait that correlated with inflorescence meristem size (Bommert *et al.* 2013). As mentioned, this gene was not identified as a QTL candidate for SAM size. In addition, expression of *fea2* was not correlated with SAM size across the RILs examined, and significant expression differences were not observed in shoot apex tissues between extreme groups in SAM size, even between B73 and Mo17. This supports the hypothesis that known SAM genes are simply not significantly different in the lines examined for their impact on the shoot meristem specifically.

Another reason for the lack of QTL coinciding with previously identified genes affecting SAM size is that mutations in these genes are often quite severe, affecting the expression of many downstream genes and having pleiotropic effects on plant growth and development. It may well be that downstream targets of these major genes are more likely to be implicated in controlling the range of natural variation observed in SAM

architecture. Our results point to many basic physical structural functions on a cellular level: metal, sugar, and miscellaneous transport; cell organization and cell wall synthesis; lipid metabolism; and signaling. These pathways may be more likely to be responsible for the "fine-tuning" of the size and shape of the SAM.

Despite the lack of overlap with genes affecting SAM size, the 83 candidate genes identified did include annotations previously implicated in SAM function. Two classical maize genes (Schnable and Freeling 2011), *knotted interacting protein1* and *sucrose export defective1*, were among this subset, along with a gene annotated as a homeobox gene. Knotted-interacting and homeobox genes may play a role in shaping the maize SAM, as genes in these families have been shown to be involved in SAM function (Hake *et al.* 1995, Kerstetter *et al.* 1994, Jackson *et al.* 1994, Belles-Boix *et al.* 2006) and alter leaf morphology and internode patterning (Nishimura *et al.* 2000, Smith and Hake 2003, Rosin *et al.* 2003). Several sucrose and metal transport annotations (as well as 16 other miscellaneous transport annotations) were also observed in the candidate subset; these classes of genes are differentially expressed in the apex cells of narrow sheath mutant plants (Zhang *et al.* 2007), which are paralogous to the WUSCHEL1-like homeobox transcription factors. An ethylene metabolism gene, three RNA transcription regulators, and two elongation factor protein genes were also among the potential candidates.

Interestingly, though several genes that encode transporters for auxin, cytokinin, and gibberellin have been shown to be involved in the formation and function of the SAM (Kessler and Sinha 2004, Hay *et al.* 2002, Scanlon *et al.* 2002, Rupp *et al.* 2002), these families were not identified in our analysis. Again, though it may be that these

genes are not relevant to SAM architecture, an alternative explanation is that they simply are not differentially expressed in the IBMRIL population. In either case, our results support the presence of multiple undiscovered genes contributing to natural variation in meristem morphology that warrant further study.

Literature cited

Axtell, M. J., 2013 Classification and comparison of small RNAs from plants. Ann. Rev. Plant Biol. 64: 137-159.

Barton, M. K., 2010 Twenty years on: The inner workings of the shoot apical meristem, a developmental dynamo. Dev. Biol. 341: 95-113.

Bauer, P., M. Lubkowitz, R. Tyers, K. Nemoto, R. B. Meeley *et al.,* 2004 Regulation and a conserved intron sequence of liguleless3/4 Knox Class-I homeobox genes in grasses. Planta 219: 359-368.

Beavis, W. D., 1998 QTL Analyses: Power, Precision, and Accuracy, pp. 145-161 in *Molecular dissection of complex traits*, edited by A. H. Paterson. CRC Press, Boca Raton, FL.

Bernardo, R., 2010 *Breeding for quantitative traits in plants*. Stemma Press, Woodbury, MN.

Belles-Boix, E., O. Hamant, S. M. Witiak, H. Morin, J. Traas *et al.,* 2006 *KNAT6:* An *Arabidopsis* homeobox gene involved in meristem activity and organ separation. The Plant Cell 18: 1900-1907.

Bernier, G., 1997 Growth changes in the shoot apex of *Sinapis alba* during transition to flowering. J. Exp. Bot. 48: 1071-1077.

Bolduc, N., R. G. Tyers, M. Freeling, and S. Hake. 2014 Unequal redundancy in maize knotted1 homeobox genes. Plant Physiol. 164: 229-238.

Bommert, P., B. I. Je, A. Goldschmidt, and D. Jackson, 2013 The maize Ga gene *COMPACT PLANT2* functions in CLAVATA signaling to control shoot meristem size. Nature 502: 555-558.

Brown, P. J., N. Upadyayula, G. S. Mahone, F. Tian, P. J. Bradbury *et al.,* 2011 Distinct genetic architectures for male and female inflorescence traits of maize. PLOS Genetics 7: e1002383.

Buckler, E. S., J. B. Holland, P. J. Bradbury, C. B. Acharya, P. J. Brown *et al.,* 2009 The genetic architecture of maize flowering time. Science 325: 714-718.

Causse, M., P. Duffe, M.C. Buret, R. Damidaux, D. Zamir *et al.,* 2004 A genetic map of candidate genes and QTLs involved in tomato fruit size and composition. J. Exp. Bot. 55: 1671-1685.

Chitwood, D. H., R. Kumar, L. R. Headland, A. Ranjan, M. F. Covington *et al.*, 2013 A quantitative genetic basis for leaf morphology in a set of precisely defined tomato introgression lines. The Plant Cell 25: 2465-2481.

Chuck, G. and S. Hake, 2005 Regulation of developmental transitions. Curr. Opin.Plant Biol. 8: 67-70.

Clark, S. E., M. P. Running, and E. M. Meyerowitz, 1993 *CLAVATA1*, a regulator of meristem and flower development in *Arabidopsis.* Development 119: 397-418.

Clark, S. E., M. P. Running, and E. M. Meyerowitz, 1995 *CLAVATA3* is a specific regulator of shoot and floral meristem development affecting the same processes as *CLAVATA1*. Development 121: 2057-2067.

Clark, R. M., T. N. Wagler, P. Quijada, and J. Doebley, 2006 A distant upstream enhancer at the maize domestication gene *tb1* has pleiotropic effects on plant and inflorescent architecture. Nature Genetics 38: 594-597.

Courtois, B., N. Ahmadi, F. Khowaja, A. H. Price, J. F. Rami *et al.*, 2009 Rice root genetic architecture: meta-analysis from a drought QTL database. Rice 2: 115-128.

DeYoung, B. J., K. L. Bickle, K. J. Schrage, P. Muskett, K. Patel *et al.*, 2006 The CLAVATA1-related BAM1, BAM2 and BAM3 receptor kinase-like proteins are required for meristem function in Arabidopsis. Plant J. 45: 1-16.

Douglas, R. N., D. Wiley, A. Sarkar, N. Springer, M. C. P. Timmermans *et al.*, 2010 *ragged seedling2* encodes an ARGONAUTE7-Like protein required for mediolateral expansion, but not dorsiventrality, of maize leaves. The Plant Cell 22: 1441-1451.

Efroni, I., S. K. Han, H. J. Kim, M. F. Wu, E. Steiner et al., 2013 Regulation of leaf maturation by chromatin-mediated modulation of cytokinin responses. Dev. Cell 24: 438-445.

Eichten, S. R., J. M. Foerster, N. de Leon, Y. Kai, C. T. Yeh *et al.*, 2011 B73-Mo17 near-isogenic lines demonstrate dispersed structural variation in maize. Plant Physiol. 156: 1679-1690.

Forestan, C., and S. Varotto, 2012 The role of PIN auxin efflux carriers in polar auxin transport and accumulation and their effect on shaping maize development. Molecular Plant 5: 787-798.

Foster, T., J. Yamaguchi, B. C. Wong, B. Veit, and S. Hake, 1999 *Gnarley1* is a dominant mutation in the *knox4* homeobox gene affecting cell shape and identity. The Plant Cell 11: 1239-1252.

Frary, A., T. C. Nesbitt, A. Frary, S. Grandillo, E. can der Knaap *et al.,* 2000 fw2.2: A quantitative trait locus key to the evolution of tomato fruit size. Science 289: 85-88.

Gallavotti, A., 2013 The role of auxin in shaping shoot architecture. J. Exp. Bot. 64: 2593-2608.

Giulini, A., J. Wang, and D. Jackson, 2004 Control of phyllotaxy by the cytokinin-inducible response regulator homologue *ABPHYL1*. Nature 430: 1031-1034.

Grandillo, S., H.M. Ku, and S.D. Tanksley, 1999 Identifying the loci responsible for natural variation in fruit size and shape in tomato. Theor. Appl. Genet. 99: 978-987.

Hake, S., B. R. Char, G. Chuck, T. Foster, J. Long *et al.,* 1995 Homeobox genes in the functioning of plant meristems. Phil. Trans. R. Soc. Lond. B 350: 45-51.

Hake, S., E. Vollbrecht, and M. Freeling, 1989 Cloning *Knotted*, the dominant morphological mutant in maize using *Ds2* as a transposon tag. EMBO J. 8: 15-22.

Hake, S., H. M. S. Smith, H. Holtan, E. Magnani, G. Mele *et al.,* 2004 The role of Knox genes in plant development. Ann. Rev. Cell Dev. Biol. 20: 125-151.

Hay, A., H. Kaur, A. Phillips, P. Hedden, S. Hake *et al.,* 2002 The gibberelllin pathway mediates KNOTTED1-type homeobox function in plants with different body plans. Curr. Biol. 12: 1557-1565.

Hay, A., J. Craft, and M. Tsiantis, 2004 Plant hormones and homeoboxes: Bridging the gap? BioEssays 26: 395-404.

Hochholdinger, F. and R. Tuberosa, 2009 Genetic and genomic dissection of maize root development and architecture. Curr. Opin. Plant Biol. 12: 172-177.

ImageJ (http://rsbweb.nih.gov/ij/)

Itoh, J. I., H. Kitano, M. Matsuoka, and Y. Nagato, 2000 Shoot organization genes regulate shoot apical meristem organization and the pattern of leaf primordium initiation in rice. The Plant Cell 12: 2161-2174.

Jackson, D., B. Veit and S. Hake, 1994 Expression of maize *KNOTTED1* related homeobox genes in the shoot apical meristem predicts patterns of morphogenesis in the vegetative shoot. Development 120: 405-413.

Jackson, D. and S. Hake, 1999 Control of phyllotaxy in maize by the *abphyl1* gene. Development 126: 315-323.

Jiang, C., R. J. Wright, S. S. Woo, T. A. DelMonte, and A. H. Paterson, 2000 QTL analysis of leaf morphology in tetraploid *Gossypium* (cotton). Theor. Appl. Genet. 100: 409-418.

Johnson, W. C., L.E. Jackson, O. Ochoa, R. van Wijk, J. Peleman *et al.*, 2000 Lettuce, a shallow-rooted crop, and *Lactuca serriola*, its wild progenitor, differ at QTL determining root architecture and deep soil water exploration. Theor. Appl. Genet. 101: 1066-1073.

Juenger, T., M. Purugganan, and T. F. C. Mackay, 2000 Quantitative trait loci for floral morphology in *Arabidopsis thaliana*. Genetics 156: 1379-1392.

Jun, T. H., K. Freewalt, A. P. Michel, and R. Mian, 2013 Identification of novel QTL for leaf traits in soybean. Plant Breeding 133: 61-66.

Kayes, J. M. and S.E. Clark, 1998 *CLAVATA2*, a regulator of meristem and organ development in Arabidopsis. Development 125: 1253-1260.

Kerstetter, R. A., D. Laudencia-Chingcuanco, L. G. Smith, and S. Hake, 1997 Loss-of-function mutations in the maize homeobox gene, *knotted1*, are defective in shoot meristem maintenance. Development 124: 3045-3054.

Kerstetter, R. A., E. Vollbrecht, B. Lowe, B. Veit, J. Yamaguchi *et al.*, 1994 Sequence analysis and expression patterns divide the Maize *knotted1*-like homeobox genes into two classes. The Plant Cell 6: 1877-1887.

Kessler, S. and N. Sinha, 2004 Shaping up: the genetic control of leaf shape. Curr. Opin. Plant Biol. 7: 65-72.

Kessler, S., B. Townsley, and N. Sinha, 2006 L1 Division and differentiation patterns influence shoot apical meristem maintenance. Plant Physiol. 141: 1349-1362.

Kierskowski, D., N. Nakayama, A. L. Routier-Kierzkowska, A. Weber, E. Bayer *et al.*, 2012 Elastic domains regulate growth and organogenesis in the plant shoot apical meristem. Science 335: 1096-1099.

Knauer, S., A. L. Holt, I. Rubio-Somoza, E. J. Tucker, A. Hinze *et al.*, 2013 A protodermal miR394 signal defines a region of stem cell competence in the Arabidopsis shoot meristem. Devel. Cell 24: 125-132.

Kwon, C. S. and D. Wagner, 2007 Unwinding chromatin for development and growth: A few genes at a time. Trends Genet. 23: 403-412.

Kyozuka, J., 2007 Control of shoot and root meristem function by cytokinin. Curr. Opin. Plant Biol. 10: 442-446.

Langlade, N. B., X. Feng, T. Dransfield, L. Copsey, A. I. Hanna *et al.,* 2005 Evolution through genetically controlled allometry space. Proc. Natl. Acad. Sci. USA 102: 10221-10226.

Lauter, N., M.J. Moscou, J. Habiger, and S.P. Moose, 2008 Quantitative genetic dissection of shoot architecture traits in maize: towards a functional genomics approach. The Plant Genome 1: 99-110.

Laux, T., K.F.X. Mayer, J. Berger, and G. Jürgens, 1996 The *WUSCHEL* gene is required for shoot and floral meristem integrity in *Arabidopsis*. Development 122: 87-96.

Lee, M., N. Sharopova, W. D. Beavis, D. Grant, M. Katt *et al.,* 2002. Expanding the genetic map of maize with the intermated B73 × Mo17 (IBM) population. Plant Mol. Biol. 48: 453-461.

Leyser, H. M. O. and I. J. Furner, 1992 Characterisation of three shoot apical meristem mutants of *Arabidopsis thaliana.* Development 116: 397-403.

Li, L., K. Petsch, R. Shimizu, S. Liu, W. W. Xu *et al.,* 2013 Mendelian and non-mendelian regulation of gene expression in maize. PLOS Genetics 9: e1003202.

Liu, Q., X. Yao, L. Pi, H. Wang, X. Cui *et al.,* 2009 The ARGONAUTE10 gene modulates shoot apical meristem maintenance and establishment of leaf polarity by repressing miR165/166 in Arabidopsis. Plant J. 58: 27-40.

Long, J. A., E. I. Moan, J. I. Medford, and M. K. Barton, 1996 A member of the KNOTTED class of homeodomain proteins encoded by the STM gene of Arabidopsis. Nature 379: 66-69.

Loudet, O., V. Gaudon, A. Trubuil, and F. Daniel-Vedele, 2005 Quantitative trait loci controlling root growth and architecture in *Arabidopsis thaliana* confirmed by heterogeneous inbred family. Theor. Appl. Genet. 110: 742-753.

Lunde C., S. Hake, 2009 The interaction of knotted1 and thick tassel dwarf1 in vegetative and reproductive meristems of maize. Genetics 181: 1693-1697.

Lyndon, R. F., and N. H. Battey, 1985 The growth of the shoot apical meristem during flower initiation. Biologia Plantarum (Praha) 27: 339-349.

Moore, C. R., D.S. Gronwall, N.D. Miller, and E.P. Spalding, 2013 Mapping quantitative trait loci affecting *Arabidopsis thaliana* seed morphology features extracted computationally from images. G3 3: 109-118.

Muehlbauer, G. J., J. E. Fowler, and M. Freeling, 1999 Sectors expressing the homeobox gene liguleless3 implicate a time-dependent mechanism for cell fate acquisition along the proximal-distal axis of the maize leaf. Development 124: 5097-5106.

Nagasaki, H., J. Itoh, K. Hayashi, K. Hibara, N. Satoh-Nagasawa *et al.,* 2007 The Small interfering RNA production pathway is required for shoot meristem initiation in rice. Proc. Natl. Acad. Sci. USA 104: 14867-14871.

Nishimura, A., M. Tamaoki, T. Sakamoto, and M. Matsuoka, 2000 Over-expression of tobacco *knotted1*-type class1 homeobox genes alters various leaf morphology. Plant Cell Physiol. 41: 583-590.

Nogueira, F. T. S., S. Madi, D. H. Chitwood, M. T. Juarez, and M. C. P. Timmermans, 2007 Two small regulatory RNAs establish opposing fates of a developmental axis. Genes & Dev. 21: 750-755.

Ormenese, S., A. Havelange, G. Bernier, C. van der Schoot, 2002 The shoot apical meristem of *Sinapis alba* L. expands it central symplasmic field during the floral transition. Planta 215: 67-78.

Peaucelle, A., S. A. Braybrook, L. Le Guillou, E. Bron, C. Kuhlemeier *et al.* 2011 Pectin-induced changes in cell wall mechanics underlie organ initiation in Arabidopsis. Curr. Biol. 21: 1720-1726.

Pernisová, M., P. Klíma, J. Horák, M. Válková, J. Malbeck *et al.*, 2009 Cytokinins modulate auxin-induced organogenesis in plants via regulation of the auxin efflux. Proc. Natl. Acad. Sci. USA 106: 3609-3614.

Poethig, R. S., 1984 Cellular parameters of leaf morphogenesis in maize and tobacco, pp. 235-238 in *Contemporary Problems in Plant Anatomy*, edited by R. A. White and W. C. Dickinson. Academic Press, New York.

Poethig, R. S., 1990 Phase change and the regulation of shoot morphogenesis in plants. Science 250: 923-930.

QTL Cartographer (http://statgen.ncsu.edu/qtlcart/)

R (http://www.r-project.org/)

Reinhardt, D., T. Mandel, and C. Kuhlemeier, 2000 Auxin Regulates the initiation and radial position of plant lateral organs. The Plant Cell 12: 507-518.

Rosin, F. M., J. K. Hart, H. T. Horner, P. J. Davies, and D. J. Hannapel, 2003 Overexpression of a *Knotted*-like homeobox gene of potato alters vegetative development by decreasing gibberellin accumulation. Plant Physiol. 132: 106-117.

Rupp, H. M., M. Frank, T. Werner, M. Strnad, and T. Schmulling, 2002 Increased steady state mRNA levels of the *STM* and *KNAT1* homeobox genes in cytokinin overproducing *Aravidopsis thaliana* indicate a role for cytokinins in the shoot apical meristem. Plant J. 18: 557-563.

Ruzin, S. E., 1999 *Plant microtechnique and microscopy*. Oxford University Press, Oxford, NY.

Sang, Y., M.Wu, and D. Wagner, 2009 The Stem cell—Chromatin Connection. Seminars in Cell & Developmental Biology 20(9): 1143-1148.

Scanlon, M. J., D.C. Henderson, and B. Bernstein, 2002 *SEMAPHORE1* functions during regulation of ancestrally duplicated knox genes and polar auxin transport in maize. Development 129: 2663-2673.

Schauer, S. E., S. E. Jacobsen, D. W. Meinke, and A. Ray, 2002 DICER-LIKE1: Blind men and elephants in Arabidopsis development. Trends Plant Sci. 7: 487-491.

Schnable, J. C. and M. Freeling, 2011 Genes identified by visible mutant phenotypes show increased bias toward one of two subgenomes of maize. PLOS ONE 6: e17855.

Schneeberger, R. G., P. W. Becraft, S. Hake, and M. Freeling, 1995 Ectopic expression of the Knox homeo box gene *Rough sheath1* alters cell fate in the maize leaf. Genes Dev. 9: 2292-2304.

Schoof, H., M. Lenhard, A. Haecker, K. F.X. Mayer, G. Jurgens *et al.*, 2000 The stem cell population of *Arabidopsis* shoot meristems is maintained by a regulatory loop between the *CLAVATA* and *WUSCHEL* genes. Cell 100: 635-644.

Sharman, B. C., 1942a Onset of reproductive phase in grasses and cereals. Nature 150: 208.

Sharman, B. C., 1942b Developmental anatomy of the shoot of *Zea mays.* Ann. Bot. 6: 245-283.

Shen, W., and L. Xu, 2009 Chromatin remodeling in stem cell maintenance in Arabidopsis thaliana. Molecular Plant 2: 600-609.

Smith, H. M. S. and S. Hake, 2003 The interaction of two homeobox genes, *BREVIPEDICELLUS* and *PENNYWISE*, regulates internode patterning in the Arabidopsis inflorescence. The Plant Cell 15: 1717-1727.

Sylvester, A. W., W. Z. Cande, and M. Freeling, 1990 Division and differentiation during normal and liguleless-1 maize leaf development. Development 110: 985-1000.

Taguchi-Shiobara, F., Z. Yuan, S. Hake, and D. Jackson, 2001 The *fasciated ear2* gene encodes a leucine-rich repeat receptor-like protein that regulates shoot meristem proliferation in maize. Genes Dev. 15: 2755-2766.

Takacs, E. M., J. Li, C. Du, L. Ponnala, D. Janick-Buckner *et al.,* 2012 Ontogeny of the maize shoot apical meristem. The Plant Cell 24: 3219-3234.

Tian, F., P. J. Bradbury, P. J. Brown, H. Hung, Q. Sun *et al.,* 2011 Genome-wide association study of leaf architecture in the maize nested association mapping population. Nature Genetics 43: 159-162.

Tsuda, K., Y. Ito, Y. Sato, and N. Kurata, 2011 Positive autoregulation of a KNOX gene is essential for shoot apical meristem maintenance in rice. The Plant Cell 23: 4368-4381.

Upadyayula, N., H. S. da Silva, M. O. Bohn, and T. R. Rocheford, 2006 Genetic and QTL analysis of maize tassel and ear inflorescence architecture. Theor. Appl. Genet. 112: 592-606.

Vanstraelen, M., and E. Benková, 2012 Hormonal interactions in the regulation of plant development. Ann. Rev. Cell Dev. Biol. 28: 463-487.

Vaucheret, H., F. Vazquez, P. Crété, and D. P. Bartel, 2004 The action of ARGONAUTE1 in the miRNA pathway and its regulation by the miRNA pathway are crucial for plant development. Genes Dev. 18: 1187-1197.

Vollbrecht, E., B. Veit, N. Sinha, and S. Hake, 1991 The developmental gene *Knotted-1* is a member of a maize homeobox gene family. Nature 350: 241-243.

Vollbrecht, E., L. Reiser, and S. Hake, 2000 Shoot meristem size is dependent on inbred background and presence of the maize homeobox gene, knotted1. Development 127: 3161-3172.

Wagner, Doris, 2003 Chromatin regulation of plant development. Curr. Opin. Plant Biol. 6: 20-28.

Wang, Y. and J. Li, 2008 Molecular basis of plant architecture. Ann. Rev. Plant Biol. 59: 253-279.

Woodward, J. B., N. D. Abeydeera, D. Paul, K. Phillips, M. Rapala-Kozik et al., 2010 A maize thiamine auxotroph is defective in shoot meristem maintenance. The Plant Cell 22: 3305-3317.

Yanai, O., E. Shani, K. Dolezal, P. Tarkowski, R. Sablowski *et al.,* 2005 Arabidopsis KNOXI proteins activate cytokinin biosynthesis. Curr. Biol. 15: 1566-1571.

Yang, X., H. Ma, P. Zhang, J. Yan, Y. Guo *et al.,* 2012 Characterization of QTL for oil content in maize kernel. Theor. Appl. Genet. 125: 1169-1179.

Yu, X., H. Wang, W. Zhong, J. Bai, P. Liu *et al.,* 2013 QTL mapping of leafy heads by genome resequencing in the RIL population of *Brassica rapa.* PLOS ONE 8(10): e76059.

Zhang, B. H., X. P. Pan, S. B. Cox, G. P. Cobb, and T. A. Anderson, 2006 Evidence that miRNAs are different from other RNAs. Cellular and Molecular Life Sciences 63: 246-254.

Zhang, X., S. Madi, L. Borsuk, D. Nettleton, R. J. Elshire *et al.,* 2007 Laser microdissection of narrow sheath mutant maize uncovers novel gene expression in the shoot apical meristem. PLOS Genetics 3: e101.

Table 1. Summary of SAM architecture traits in the IBMRIL population and parents.

	PARENTS		RILs			
MERISTEM TRAIT	B73	Mo17	MEAN	RANGE	P-VALUE[a]	HERITABILITY
HEIGHT (μm)	188	104	133	103 - 178	<0.001	0.86
ARC LENGTH (μm)	216	141	165	134 - 205	<0.001	0.82
WIDTH (μm)	138	142	135	116 - 155	<0.001	0.72
MIDPOINT WIDTH (μm)	116	120	115	99 - 130	<0.001	0.71
HEIGHT OF P1 (μm)	50	49	53	28 - 74	0.032	0.14
CELL COUNT IN ARC (cells)	17.0	12.3	13.9	11.1 - 17.8	<0.001	0.66
VOLUME (million μm^3)	5.10	1.50	2.40	1.41 - 4.39	<0.001	0.83
HEIGHT:WIDTH RATIO	1.37	0.74	0.99	0.74 - 1.35	<0.001	0.88
ARC CELL SIZE (μm)	13.2	11.7	12.2	10.2 - 14.5	NS	0.43
PLASTOCHRON INTERNODE (μm)	70	67	68	56 - 84	<0.001	0.54

[a]significance of the effect of genotype within the RIL population.

Table 2. Summary of SAM trait QTL.

MERISTEM TRAIT	# OF QTL (+)[a]	RANGE OF PVE[b]	EFFECT RANGE[c]	MODEL PVE
HEIGHT (μm)	8 (6)	4-16%	3.02 - 6.1	0.68
ARC LENGTH (μm)	8 (7)	5-9%	3.49 - 4.75	0.69
WIDTH (μm)	8 (4)	6-19%	2.38 - 4.87	0.61
MIDPOINT WIDTH (μm)	8 (5)	7-12%	2.04 - 2.94	0.60
CELL COUNT IN ARC (cells)	9 (6)	4-23%	0.34 - 0.79	0.74
VOLUME (million μm^3)	7 (6)	5-16%	1.50 - 2.71E5	0.55
HEIGHT:WIDTH RATIO	6 (4)	6-20%	0.24 - 0.57	0.55
PLASTOCHRON INTERNODE (μm)	9 (5)	5-21%	1.47 - 4.23	0.66

[a]Numbers in parenthesis indicate QTL with positive effect in B73.

[b]Phenotypic Variation Explained

[c]Effect ranges shown are absolute values.

Table 3. QTL for SAM height.

QTL	CHROMOSOME	LOD	PVE[a]	EFFECT[b]	cM RANGE[c]	COINCIDENT SAM QTLs
SAM_height_1	1	4.80	7%	4.06	717.91 - 729.41	
SAM_height_2	1	3.45	5%	3.62	1041.41 - 1052.91	Arc length, Plastochron internode
SAM_height_3	2	3.96	6%	3.74	301.21 - 310.91	Arc length
SAM_height_4	3	4.90	9%	-4.58	791.21 - 813.11	Arc length, Volume
SAM_height_5	5	4.82	7%	4.33	772.71 - 781.71	Arc length, Volume
SAM_height_6	5	9.25	16%	6.10	892.81 - 895.01	Arc length, Volume
SAM_height_7	6	5.62	9%	4.49	303.01 - 317.71	Arc length, Volume
SAM_height_8	6	3.03	4%	-3.02	489.71 - 499.31	

[a]Phenotypic Variation Explained

[b]Effect is substitution of Mo17 allele with B73.

[c]QTL intervals calculated by 1-LOD drop.

Table S1. Genotypes used for IBM subset and NILs.

IBM 86		NIL
MO001	MO264	B034
MO005	MO265	B063
MO007	MO266	M049
MO008	MO267	
MO010	MO269	
MO012	MO272	
MO014	MO275	
MO015	MO276	
MO016	MO281	
MO017	MO284	
MO021	MO287	
MO022	MO288	
MO023	MO296	
MO024	MO297	
MO025	MO298	
MO028	MO310	
MO029	MO311	
MO030	MO315	
MO031	MO317	
MO032	MO322	
MO033	MO323	
MO034	MO325	
MO035	MO326	
MO039	MO328	
MO040	MO337	
MO044	MO341	
MO046	MO344	
MO048	MO345	
MO051	MO346	
MO052	MO352	
MO054	MO354	
MO057	MO355	
MO058	MO357	
MO060	MO360	
MO061	MO364	
MO062	MO365	
MO066	MO368	
MO067	MO369	

MO074	MO378
MO075	MO379
MO077	MO382
MO079	MO383
MO262	MO384

Table S2. Correlation values for SAM traits.

	HEIGHT	ARC LENGTH	WIDTH	MIDPOINT WIDTH	P1 HEIGHT	ARC CELL COUNT	VOLUME	HEIGHT:WIDTH RATIO	ARC CELL SIZE	PLASTOCHRON INTERNODE
HEIGHT	1	0.00	0.09	0.11	0.22	0.00	0.00	0.00	0.06	0.00
ARC LENGTH	0.98	1	0.00	0.00	0.17	0.00	0.00	0.00	0.03	0.00
WIDTH	0.18	0.34	1	0.00	0.06	0.10	0.00	0.00	0.04	0.03
MIDPOINT WIDTH	0.17	0.34	0.96	1	0.30	0.05	0.00	0.00	0.09	0.01
P1 HEIGHT	0.13	0.15	0.20	0.11	1	0.54	0.08	0.94	0.53	0.01
ARC CELL COUNT	0.73	0.73	0.18	0.21	0.07	1	0.00	0.00	0.00	0.08
VOLUME	0.97	0.98	0.39	0.36	0.19	0.72	1	0.00	0.03	0.00
HEIGHT:WIDTH RATIO	0.82	0.71	-0.41	-0.39	-0.01	0.57	0.67	1	0.51	0.05
ARC CELL SIZE	0.20	0.23	0.22	0.18	0.07	-0.47	0.23	0.07	1	0.02
PLASTOCHRON INTERNODE	0.38	0.40	0.23	0.26	0.28	0.19	0.40	0.21	0.25	1

Values below the diagnonal are correlation coefficient r; above the diagonal are p-values for significance of the correlation

Table S3. All QTL for SAM traits.

QTL	CHR	LOD	PVE[a]	EFFECT[b]	cM RANGE[c]	COINCIDENT SAM QTLs
SAM_arc_cell_count_1	1	3.1	4.4%	0.34	480.51 - 491.81	
SAM_arc_cell_count_2	1	12.7	22.9%	0.79	802.61 - 804.01	
SAM_arc_cell_count_3	3	3.7	5.6%	-0.35	648.01 - 661.01	
SAM_arc_cell_count_4	5	11.4	20.3%	-0.74	300.61 - 305.41	
SAM_arc_cell_count_5	6	6.0	9.4%	0.49	294.61 - 303.51	
SAM_arc_cell_count_6	6	5.2	8.2%	0.53	414.41 - 424.61	
SAM_arc_cell_count_7	9	4.7	6.9%	0.40	713.61 - 720.91	
SAM_arc_cell_count_8	10	6.6	10.2%	-0.53	396.21 - 402.61	
SAM_arc_cell_count_9	10	4.8	7.3%	0.45	514.61 - 528.61	
SAM_arc_length_1	1	3.4	5.2%	3.49	703.71 - 713.31	
SAM_arc_length_2	1	3.4	5.4%	3.60	1045.61 - 1052.91	Height, Plastochron difference
SAM_arc_length_3	2	4.0	6.1%	3.67	300.11 - 310.91	Height
SAM_arc_length_4	3	3.5	6.7%	-3.81	791.21 - 813.11	Height, Volume
SAM_arc_length_5	5	5.2	9.1%	4.75	772.71 - 781.71	Height, Volume
SAM_arc_length_6	5	5.4	8.7%	4.61	890.81 - 897.01	Height, Volume, Plastochron difference
SAM_arc_length_7	6	4.3	6.7%	3.84	303.01 - 311.31	Height, Volume
SAM_arc_length_8	10	5.5	8.9%	4.36	553.41 - 561.21	
SAM_height/width_1	2	4.2	7.3%	0.03	3.21 - 12.61	Width
SAM_height/width_2	3	6.1	10.5%	-0.04	747.81 - 756.81	
SAM_height/width_3	6	3.5	5.6%	-0.04	182.01 - 190.61	
SAM_height/width_4	6	10.3	19.9%	0.08	212.01 - 220.11	
SAM_height/width_5	7	4.9	8.0%	0.03	345.41 - 358.81	
SAM_height/width_6	9	6.1	10.4%	0.04	395.71 - 402.31	
SAM_height_1	1	4.8	7.2%	4.06	717.91 - 729.41	
SAM_height_2	1	3.5	5.2%	3.62	1041.41 - 1052.91	Arc length, Plastochron difference
SAM_height_3	2	4.0	5.7%	3.74	301.21 - 310.91	Arc length

SAM_height_4	3	4.9	8.8%	-4.58	791.21 - 813.11	Arc length, Volume
SAM_height_5	5	4.8	7.5%	4.33	772.71 - 781.71	Arc length, Volume
SAM_height_6	5	9.3	15.7%	6.10	892.81 - 895.01	Arc length, Volume
SAM_height_7	6	5.6	8.7%	4.49	303.01 - 317.71	Arc length, Volume
SAM_height_8	6	3.0	4.3%	-3.02	489.71 - 499.31	
SAM_midpoint_width_1	2	4.2	7.5%	-2.20	566.21 - 579.81	Width
SAM_midpoint_width_2	4	7.0	12.1%	2.95	111.91 - 119.51	Width
SAM_midpoint_width_3	5	4.5	7.2%	2.04	496.51 - 500.11	Width
SAM_midpoint_width_4	8	6.7	11.3%	2.57	773.51 - 779.71	Width
SAM_midpoint_width_5	9	5.3	8.3%	-2.54	419.31 - 434.71	Width
SAM_midpoint_width_6	9	4.5	7.3%	-2.34	419.31 - 436.61	Width
SAM_midpoint_width_7	9	5.1	8.2%	2.23	561.61 - 570.21	Plastochron difference
SAM_midpoint_width_8	10	6.0	9.9%	2.50	116.21 - 126.11	Width
SAM_volume_1	1	7.1	11.5%	229920	621.91 - 628.51	
SAM_volume_2	1	6.6	10.9%	231501	1022.41 - 1026.41	Plastochron difference
SAM_volume_3	3	5.9	9.7%	-218720	783.91 - 796.31	Arc length, Height
SAM_volume_4	5	8.6	15.2%	257084	771.11 - 779.71	Arc length, Height
SAM_volume_5	5	9.3	16.5%	270943	890.81 - 892.81	Arc length, Height
SAM_volume_6	6	8.4	14.6%	235227	304.51 - 311.31	Arc length, Height
SAM_volume_7	8	3.4	5.3%	150494	706.81 - 721.31	
SAM_width_1	2	5.1	7.8%	-2.71	6.01 - 12.61	Height/width
SAM_width_2	2	8.1	13.6%	-3.58	567.61 - 579.81	Midpoint width
SAM_width_3	3	3.8	5.6%	-2.38	911.71 - 923.51	
SAM_width_4	4	7.6	12.0%	3.24	109.31 - 119.51	Midpoint width
SAM_width_5	5	6.6	10.2%	3.12	501.01 - 506.61	Midpoint width
SAM_width_6	8	10.9	19.3%	4.87	770.21 - 778.41	Midpoint width
SAM_width_7	9	4.4	6.5%	-2.72	428.51 - 436.61	Midpoint width
SAM_width_8	10	8.2	13.5%	3.52	119.21 - 126.11	Midpoint width

SAM_plastochron_internode_1	1	4.5	7.0%	-1.79	1037.41 - 1051.51	Height, Arc length
SAM_plastochron_internode_2	1	4.0	6.0%	1.68	1221.81 - 1225.81	Volume
SAM_plastochron_internode_3	3	6.4	12.0%	-3.59	589.11 - 599.11	
SAM_plastochron_internode_4	3	10.6	21.0%	4.23	606.51 - 617.31	
SAM_plastochron_internode_5	3	4.0	6.0%	1.56	764.51 - 776.01	
SAM_plastochron_internode_6	4	8.0	15.0%	2.47	14.91 - 26.11	
SAM_plastochron_internode_7	4	3.3	5.0%	-1.47	727.31 - 732.51	
SAM_plastochron_internode_8	5	6.1	10.0%	-2.11	897.01 - 911.71	Arc length
SAM_plastochron_internode_9	9	3.8	6.0%	-1.56	566.61 - 574.21	Midpoint width

[a]Phenotypic Variation Explained

[b]Effect is substitution of Mo17 allele with B73.

[c]QTL intervals calculated by 1-LOD drop.

Table S4a. Names, locations, and RPM values of genes in figures S2-4.

			LOCATION			EXPRESSION (RPM) ACROSS SAM ONTOGENY					
GENE	QTL	TRAIT[a]	CHR[b]	GENE START	GENE END	PROEMBRYO	TRANSITION	COLEOPTILE	L1	SEEDLING 14D	LM 14D
GRMZM2G002548	3	W	3	210103369	210107016	7.6	7.8	9.7	9.7	7.2	7.8
GRMZM2G003640	2	H, PI	1	256296778	256306481	25.1	34.7	23.1	22.6	39.8	32.1
GRMZM2G006565	2	W	2	178079687	178081285	NA	NA	1.7	2.9	NA	NA
GRMZM2G009785	5	W	5	133501928	133518495	1.7	2.6	2.8	3.3	1.9	2.3
GRMZM2G011479	3	PI	3	170535673	170538860	1.8	3.4	2.9	3.5	2.4	NA
GRMZM2G018103	6	H	5	213281458	213284285	86.2	55.6	121.5	86.4	103.4	86.2
GRMZM2G018403	5	W	5	139625549	139629866	1.5	2.6	1.2	2.1	NA	5.4
GRMZM2G021704	4	H	3	197320843	197325616	1.9	3.7	3.3	6.4	4.2	4.4
GRMZM2G024211	5	H	5	203173179	203174837	5.1	3.4	12.1	8.6	3.9	2.6
GRMZM2G042099	4	H	3	198517884	198535509	17.4	11.3	9.3	13.4	10.0	5.9
GRMZM2G042412	5	PI	3	193588524	193589318	2.2	22.7	4.8	NA	1.3	NA
GRMZM2G042548	4	H	3	198566641	198569108	3.1	1.8	1.9	2.2	NA	4.1
GRMZM2G045366	4	H	3	197516992	197521537	3.1	NA	2.8	2.7	2.1	4.1
GRMZM2G045404	5	H	5	203651899	203655593	1.7	1.1	1.2	1.1	1.1	2.4
GRMZM2G049536	1	W	2	1139211	1141681	15.6	12.9	13.1	7.7	4.4	12.6
GRMZM2G049888	2	PI	1	289269773	289272986	3.5	2.6	3.3	2.2	NA	NA
GRMZM2G051894	2	H, PI	1	254797250	254802782	3.3	3.4	3.0	3.2	3.0	1.4
GRMZM2G053027	1	H	1	196203304	196214408	12.1	23.3	27.1	17.0	56.4	12.6
GRMZM2G055898	4	H	3	198383505	198387549	NA	NA	NA	NA	4.7	3.9
GRMZM2G056303	2	H, PI	1	254688533	254690378	NA	NA	1.0	NA	NA	NA
GRMZM2G057753	8	W	10	6397188	6398813	NA	NA	NA	NA	2.0	1.1
GRMZM2G060167	5	W	5	140079348	140084522	15.0	26.0	42.1	36.0	57.9	39.3

GRMZM2G061876	5	W	5	128783450	128798039	4.6	3.5	1.4	2.9	NA	NA
GRMZM2G062199	5	W	5	131619811	131624597	5.2	5.2	3.9	1.7	4.7	10.1
GRMZM2G064212	1	W	2	1036162	1039699	8.1	7.1	5.8	7.1	6.0	4.8
GRMZM2G069594	1	H	1	196439361	196441662	182.9	128.3	45.2	37.3	29.2	31.3
GRMZM2G073826	5	W	5	135301776	135303063	3.5	4.3	7.5	13.7	8.4	29.9
GRMZM2G077079	2	PI	1	290957733	290965627	5.9	12.3	3.1	6.2	3.9	5.3
GRMZM2G088427	2	H, PI	1	254427709	254429811	5.4	NA	NA	4.4	3.3	4.8
GRMZM2G095082	5	W	5	141166083	141174627	NA	NA	NA	NA	NA	1.8
GRMZM2G106881	3	H	2	16125764	16131844	10.9	8.1	9.6	17.1	9.4	14.5
GRMZM2G111529	5	W	5	144098266	144117111	7.3	3.2	2.2	3.1	NA	1.1
GRMZM2G114675	5	W	5	143670639	143672877	10.1	79.8	18.8	23.0	53.0	54.8
GRMZM2G118098	5	W	5	130495184	130501387	35.2	32.9	16.9	15.5	11.8	36.8
GRMZM2G118385	7	PI	4	200185081	200190254	9.1	8.0	5.2	9.3	4.7	16.6
GRMZM2G119725	5	W	5	131456304	131460761	4.4	4.2	3.2	3.2	6.8	14.2
GRMZM2G119906	2	W	2	178223921	178225458	13.6	35.3	44.9	23.5	24.2	26.5
GRMZM2G119950	2	W	2	178225719	178231561	85.8	92.5	43.1	30.1	60.1	63.6
GRMZM2G123277	4	H	3	197947785	197952726	2.8	1.5	1.4	1.3	NA	NA
GRMZM2G127431	4	H	3	198039992	198041529	NA	19.4	5.1	2.5	7.3	NA
GRMZM2G128688	4	H	3	198666832	198683812	17.4	12.9	10.1	7.8	2.1	4.6
GRMZM2G130425	5	W	5	137390805	137394317	14.5	10.1	45.2	52.7	11.3	44.3
GRMZM2G134857	7	PI	4	199711316	199712804	2.5	5.5	2.9	NA	21.3	NA
GRMZM2G140582	5	W	5	138797716	138799635	5.6	1.7	4.5	5.1	NA	NA
GRMZM2G148404	8	W	10	6372733	6373839	11.1	109.0	76.4	60.2	315.6	79.2
GRMZM2G149788	4	PI	3	175517604	175525186	2.4	1.8	1.0	NA	1.4	NA
GRMZM2G150098	1	W	2	1624189	1628276	7.5	48.2	28.9	21.4	3.8	11.5

GRMZM2G150471	8	H	6	151227212	151233907	47.2	33.8	26.3	27.6	16.6	21.8
GRMZM2G154437	1	W	2	273517	274882	31.2	40.2	9.6	22.3	17.6	15.8
GRMZM2G158568	5	H	5	203313494	203315969	130.2	149.5	91.3	77.9	55.6	80.5
GRMZM2G159849	5	W	5	144888445	144889692	2.7	6.7	4.3	4.9	4.7	3.2
GRMZM2G163761	2	H, PI	1	256513586	256515267	NA	21.7	14.7	29.0	13.3	20.1
GRMZM2G164405	3	H	2	15889503	15893155	5.6	NA	NA	NA	NA	NA
GRMZM2G164413	3	H	2	15895715	15898391	29.6	31.5	20.7	14.2	15.3	14.2
GRMZM2G164428	3	H	2	15908515	15909994	9.7	10.8	5.7	4.8	9.0	NA
GRMZM2G165383	4	W	4	4851331	4855715	26.4	29.3	9.4	10.1	3.6	8.9
GRMZM2G165461	4	W	4	4861353	4862359	20.6	40.4	9.4	6.1	28.4	4.3
GRMZM2G165535	1	W	2	958698	961773	NA	1.6	1.4	3.0	NA	3.5
GRMZM2G166345	6	W	8	170316262	170329055	77.7	47.7	36.1	31.8	11.4	19.7
GRMZM2G175728	3	H	2	16302477	16307549	3.0	2.7	3.7	6.1	1.4	3.3
GRMZM2G176699	4	H	3	198597189	198606005	4.3	3.9	4.2	10.9	7.4	3.3
GRMZM2G177929	4	H	3	199250797	199253250	NA	NA	NA	NA	2.8	NA
GRMZM2G177970	4	H	3	199239431	199244210	4.6	8.7	4.7	6.4	NA	3.6
GRMZM2G178996	6	H	5	213546478	213549935	2.3	1.6	3.9	5.5	3.3	2.9
GRMZM2G179658	6	H	5	213747274	213751377	5.6	19.3	10.9	4.0	9.6	3.4
GRMZM2G179662	6	H	5	213757019	213765542	26.4	14.8	14.9	13.5	21.5	16.9
GRMZM2G180435	6	H	5	214081527	214081829	NA	NA	NA	1.1	2.7	3.6
GRMZM2G311919	5	W	5	143183402	143198584	4.3	NA	NA	NA	NA	2.0
GRMZM2G318635	6	H	5	213291570	213301733	NA	NA	1.2	2.6	2.1	NA
GRMZM2G323622	4	H	3	199019124	199026441	31.8	87.9	42.6	29.7	243.6	40.3
GRMZM2G341089	3	H	2	15269254	15273461	25.9	28.0	34.4	33.3	44.2	27.6
GRMZM2G352695	2	H, PI	1	254802552	254808367	1.8	2.4	2.0	2.0	2.4	NA

GRMZM2G377589	5	PI	3	194474412	194477783	1.8	1.7	NA	1.0	NA	1.3
GRMZM2G382104	1	W	2	719918	730201	9.3	7.1	13.8	5.0	1.8	6.5
GRMZM2G382341	5	H	5	203620982	203625743	8.6	3.6	7.1	7.0	5.8	15.5
GRMZM2G386643	1	W	2	843985	848903	41.4	23.1	36.7	28.7	12.0	26.4
GRMZM2G399921	5	H	5	203397973	203398690	2.7	11.3	NA	NA	NA	5.8
GRMZM2G416216	2	W	2	177897419	177899409	NA	NA	1.3	1.0	1.7	NA
GRMZM2G457621	1	W	2	1359310	1360881	NA	NA	NA	NA	NA	1.1
GRMZM2G459110	5	H	5	203304149	203308763	1.0	1.0	NA	NA	NA	NA
GRMZM2G460078	5	PI	3	195105902	195126859	21.8	17.0	11.0	5.1	4.1	1.1
GRMZM2G469142	6	H	5	213915512	213917618	3.8	3.4	3.3	1.2	2.8	3.1
GRMZM2G531719	5	H	5	203626113	203626730	2.0	17.7	7.7	22.2	6.1	7.8

[a]W=Width, H=Height, PI=Plastochron Internode

[b]CHR=Chromosome

Table S4b. Annotations of genes in S2-4.

GENE	MAIZE ANNOTATION	ARABIDOPSIS ANNOTATION
GRMZM2G002548	NA	homeobox-1
GRMZM2G003640	LOC732725	dual_specificity_protein_phosphatase_1
GRMZM2G006565	NA	UDP-Glycosyltransferase_superfamily_protein
GRMZM2G009785	Sucrose_export_defective_1	sucrose_export_defective_1_(SXD1)
GRMZM2G011479	hypothetical_protein_LOC100278407	SNARE_associated_Golgi_protein_family
GRMZM2G018103	hypothetical_protein_LOC100191588	Serinc-domain_containing_serine_and_sphingolipid_biosynthesis_protein
GRMZM2G018403	50S_ribosomal_protein_L21	Ribosomal_protein_L21
GRMZM2G021704	hypothetical_protein_LOC100193190	pyrimidin_4
GRMZM2G024211	hypothetical_protein_LOC100193276	alpha/beta-Hydrolases_superfamily_protein
GRMZM2G042099	hypothetical_protein_LOC100191812	Protein_of_unknown_function_DUF1084_(InterPro:IPR009457)
GRMZM2G042412	copper_transporter_1	Ctr_copper_transporter_family
GRMZM2G042548	LOC100285171	DNA_binding
GRMZM2G045366	Integrin-linked_protein_kinase_(EC_2.7.11.1)	Integrin-linked_protein_kinase_family
GRMZM2G045404	dual_specificity_protein_phosphatase_4	indole-3-butyric_acid_response_5
GRMZM2G049536	GINS_complex_subunit_1	partner_of_SLD_five_1
GRMZM2G049888	hypothetical_protein_LOC100384848	Tetratricopeptide_repeat_(TPR)-like_superfamily_protein
GRMZM2G051894	hypothetical_protein_LOC100279225	ARM_repeat_superfamily_protein
GRMZM2G053027	hypothetical_protein_LOC100194362	RING/U-box_superfamily_protein
GRMZM2G055898	hypothetical_protein_LOC100217062	unknown_protein
GRMZM2G056303	hypothetical_protein_LOC100383217	cyclin_d5
GRMZM2G057753	NA	ovate_family_protein_13

GRMZM2G060167	hypothetical_protein_LOC100383365	Protein_of_unknown_function_(DUF3133)
GRMZM2G061876	NA	elongation_factor_family_protein
GRMZM2G062199	Putative_uncharacterized_protein	unknown_protein
GRMZM2G064212	autophagy-related_4	Peptidase_family_C54_protein
GRMZM2G069594	60S_ribosomal_protein_L38	Ribosomal_L38e_protein_family
GRMZM2G073826	Putative_uncharacterized_protein	myb_domain_protein_3r-4
GRMZM2G077079	NA	N2;N2-dimethylguanosine_tRNA_methyltransferase
GRMZM2G088427	NA	AP2/B3-like_transcriptional_factor_family_protein
GRMZM2G095082	hypothetical_protein_LOC100192599	thylakoid_rhodanese-like
GRMZM2G106881	NA	zinc_finger_protein-related
GRMZM2G111529	hypothetical_protein_LOC100383026	glucan_synthase-like_4
GRMZM2G114675	hypothetical_protein_LOC100382415	Heavy_metal_transport/detoxification_superfamily_protein
GRMZM2G118098	hypothetical_protein_LOC100279503	FUNCTIONS_IN:_molecular_function_unknown
GRMZM2G118385	LOC100282323	RWD_domain-containing_protein
GRMZM2G119725	lys_ketoglu_reductase_trans-splicing_related_1	Protein_of_unknown_function_(DUF707)
GRMZM2G119906	hypothetical_protein_LOC100278908	unknown_protein
GRMZM2G119950	hypothetical_protein_LOC100194208	unknown_protein
GRMZM2G123277	hypothetical_protein_LOC100272531	trehalose-phosphatase/synthase_7
GRMZM2G127431	hypothetical_protein_LOC100383186	ovate_family_protein_4
GRMZM2G128688	hypothetical_protein_LOC100382669	elongation_factor_family_protein
GRMZM2G130425	hypothetical_protein_LOC100384140	Transducin_family_protein_/_WD-40_repeat_family_protein
GRMZM2G134857	hypothetical_protein_LOC100277899	unknown_protein
GRMZM2G140582	hypothetical_protein_LOC100384252	B-cell_receptor-associated_31-like

GRMZM2G148404	hypothetical_protein_LOC100381686	unknown_protein
GRMZM2G149788	NA	DHHC-type_zinc_finger_family_protein
GRMZM2G150098	pyruvate_kinase,_cytosolic_isozyme	Pyruvate_kinase_family_protein
GRMZM2G150471	hypothetical_protein_LOC100274373	Integral_membrane_Yip1_family_protein
GRMZM2G154437	hypothetical_protein_LOC100193156	BTB-POZ_and_MATH_domain_2
GRMZM2G158568	60S_ribosomal_protein_L31	Ribosomal_protein_L31e_family_protein
GRMZM2G159849	hypothetical_protein_LOC100191299	peroxin_7
GRMZM2G163761	knotted_interacting_protein1	BEL1-like_homeodomain_11
GRMZM2G164405	Acc_synthase	1-aminocyclopropane-1-carboxylic_acid_(acc)_synthase_6
GRMZM2G164413	LOC100283711	Transmembrane_proteins_14C
GRMZM2G164428	NA	Ovate_family_protein
GRMZM2G165383	phosphoserine_phosphatase	3-phosphoserine_phosphatase
GRMZM2G165461	LOC100281623	SPIRAL1-like2
GRMZM2G165535	hypothetical_protein_LOC100272867	phosphomannomutase
GRMZM2G166345	LOC100282083	Nucleic_acid-binding;_OB-fold-like_protein
GRMZM2G175728	LOC100283786	copper_chaperone_for_SOD1
GRMZM2G176699	hypothetical_protein_LOC100272521	transferases;_transferring_glycosyl_groups
GRMZM2G177929	hypothetical_protein_LOC100381442	IQ-domain_26
GRMZM2G177970	hypothetical_protein_LOC100272291	Nucleotidylyl_transferase_superfamily_protein
GRMZM2G178996	NA	Actin-binding_FH2_(Formin_Homology)_protein
GRMZM2G179658	NA	alpha/beta-Hydrolases_superfamily_protein
GRMZM2G179662	NA	protein_kinase_family_protein_/_WD-40_repeat_family_protein
GRMZM2G180435	NA	Late_embryogenesis_abundant_(LEA)_hydroxyproline-rich_glycoprotein_family

GRMZM2G311919	NA	Chalcone-flavanone_isomerase_family_protein
GRMZM2G318635	NA	Tetratricopeptide_repeat_(TPR)-like_superfamily_protein
GRMZM2G323622	NA	P-loop_ns_triphosphate_hydrolases_protein_with_CH_domain
GRMZM2G341089	ubiquitin-conjugating_enzyme_E2_I	sumo_conjugation_enzyme_1
GRMZM2G352695	hypothetical_protein_LOC100381420	calcium_ATPase_2
GRMZM2G377589	hypothetical_protein_LOC100217155	Polynucleotidyl_transferase;_ribonuclease_H-like_superfamily_protein
GRMZM2G382104	UPF0497_membrane_protein_1	Protein_kinase_protein_with_tetratricopeptide_repeat_domain
GRMZM2G382341	NA	fimbrin-like_protein_2
GRMZM2G386643	hypothetical_protein_LOC100381735	C2_calcium/lipid-binding_plant_phosphoribosyltransferase_family_protein
GRMZM2G399921	NA	arabinogalactan_protein_23_(TAIR:AT3G57690.1)
GRMZM2G416216	hypothetical_protein_LOC100384078	RING/U-box_superfamily_protein
GRMZM2G457621	hypothetical_protein_LOC100272838	unknown_protein
GRMZM2G459110	NA	unknown_protein
GRMZM2G460078	LOC100282439	AMP-dependent_synthetase_and_ligase_family_protein
GRMZM2G469142	alginate_regulatory_protein_AlgP	unknown_protein
GRMZM2G531719	NA	endonuclease/exonuclease/phosphatase_family_protein

Figure 1. SAM phenotypes and timepoints examined. A-C: Median longitudinal sections of the SAM in inbred lines B73 (**B**) and Mo17 (**C**), indicating measurements taken (**A**). B73 and Mo17 display markedly different meristem height but similar width. **D-E:** Changes in SAM height (**D**) and width (**E**) during vegetative development in B73 (blue/darker) and Mo17 (red/lighter), 7-28 days after planting. Highlighted boxes represent vegetative plateau; horizontal box designates this overlap at 14 days. Mo17 transitions around 28 days after planting (not measured once transitioned). Error bars are weighted standard error.

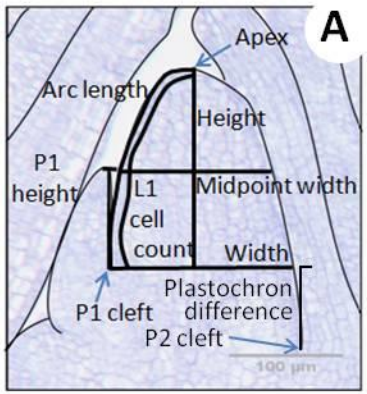
A
Apex
Arc length
Height
P1
height
L1
cell
count
Midpoint width
Width
Plastochron
difference
P1 cleft
P2 cleft
100 µm

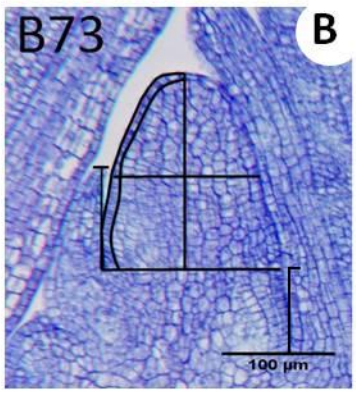
B73
B
100 µm

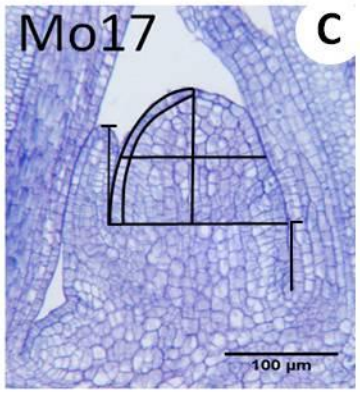
Mo17
C
100 µm

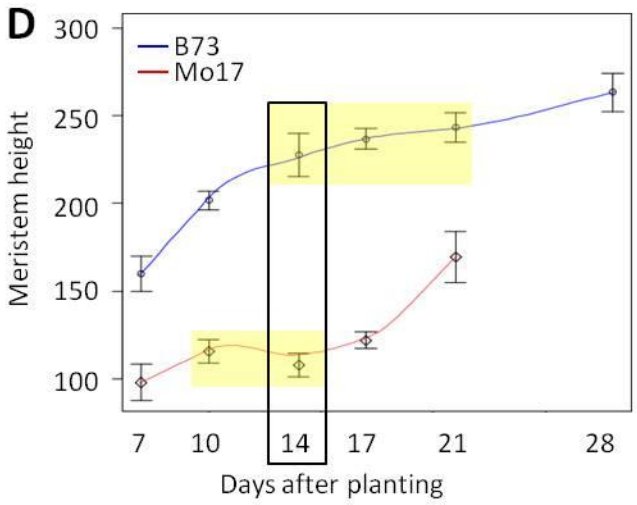
D
300
250
200
150
100
B73
Mo17
Meristem height
7
10
14
17
21
28
Days after planting

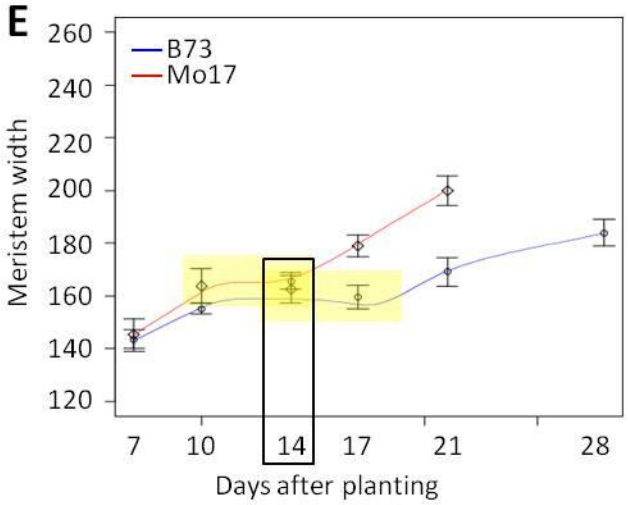
E
260
240
220
200
180
160
140
120
B73
Mo17
Meristem width
7
10
14
17
21
28
Days after planting

Figure 2. Distribution and relationship of traits. A: Density distributions of SAM height (blue/wider) and width (red/taller) in line means of the IBMRIL population. B73 and Mo17 are indicated as B and M, respectively. **B:** Relationship of all SAM traits, both measured and derived, in the IBMRIL. SAM height, arc length, and volume are all highly correlated ($r>0.98$), as are width and midpoint width ($r>0.94$). Strengths of correlations are shown with absolute values; negative correlations are designated in the lower half of the matrix by "-".

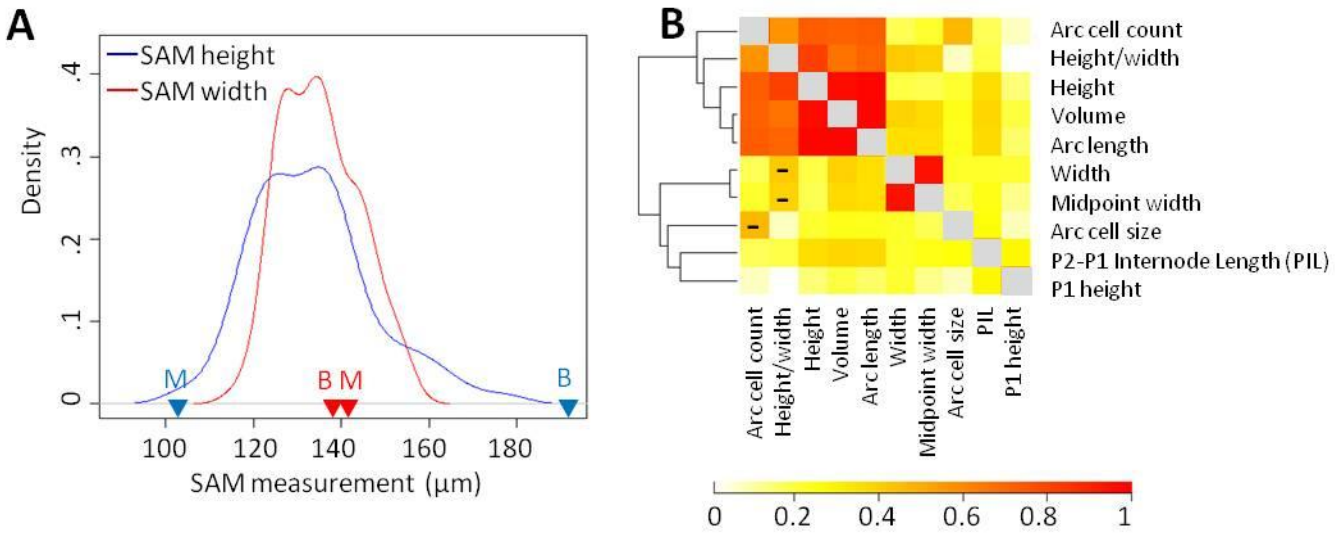
A
SAM height
SAM width
Density
0
.1
.2
.3
.4
M
B M
B
100
120
140
160
180
SAM measurement (µm)
B
Arc cell count
Height/width
Height
Volume
Arc length
Width
Midpoint width
Arc cell size
P2-P1 Internode Length (PIL)
P1 height
PIL
0
0.2
0.4
0.6
0.8
1

Figure 3. Mapping results across 10 chromosomes for the 8 SAM architecture traits. The dashed line represents the significance threshold at LOD=3 , and LOD axis ranged from 0 to 14.3 for each trait. Height, volume, and arc length (all highly related traits) share many QTL, while width and midpoint width share a different set of QTL. Arc cell count and plastochron timing have some QTLs in common with other traits, but many are unique loci.

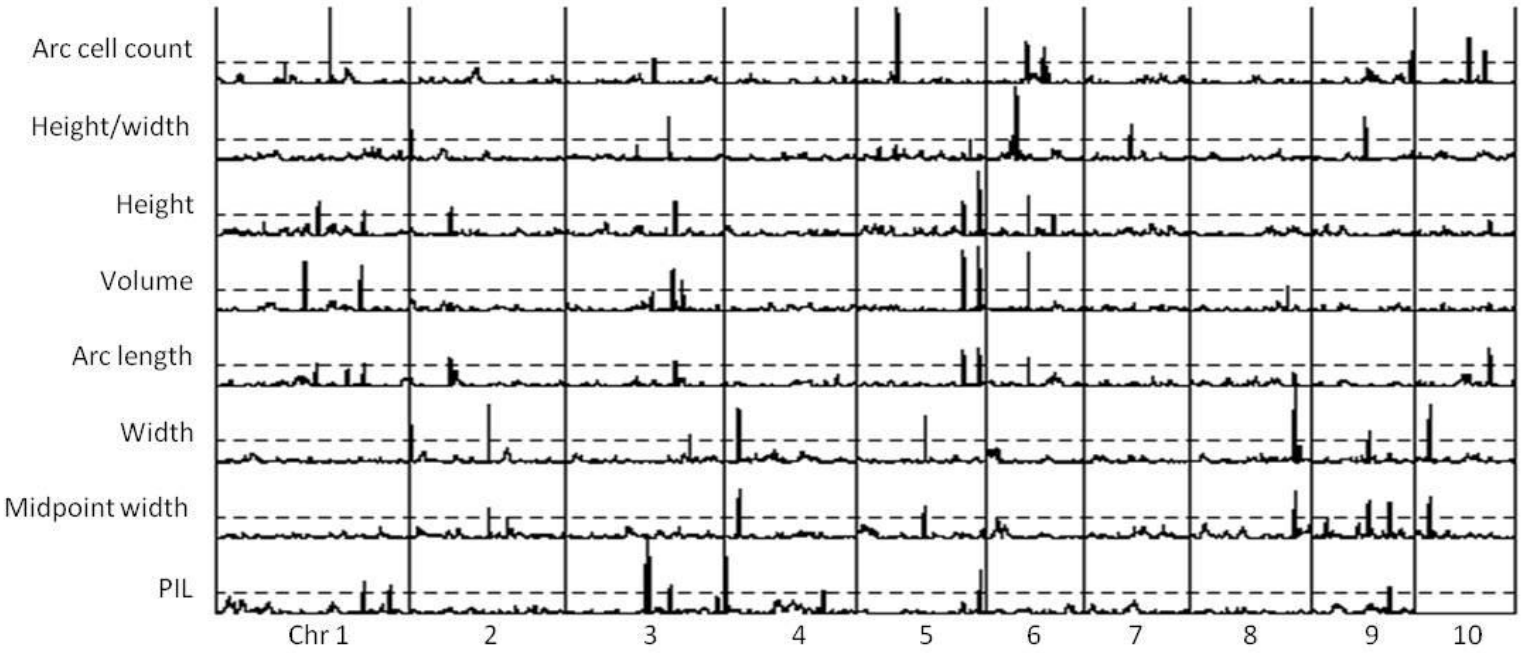
Arc cell count
Height/width
Height
Volume
Arc length
Width
Midpoint width
PIL
Chr 1
2
3
4
5
6
7
8
9
10

Figure 4. Validation of a QTL on chromosome 5 for SAM height. A: Genome-wide view of NIL introgressions present in the measured near-isogenic lines, and **B:** a close-up of chromosome 5 for the same lines, indicating the location of the QTL. **C:** NILs containing the QTL region introgression show differences in SAM height approximately equal to the expected parental deviations based on estimated QTL effects for B73-like NILs, though slightly less than predicted for Mo17-like NILs. **D:** All NILs were significantly different than their recurrent parent: * = $p<0.05$, *** = $p<0.001$ based on Student's t-test.

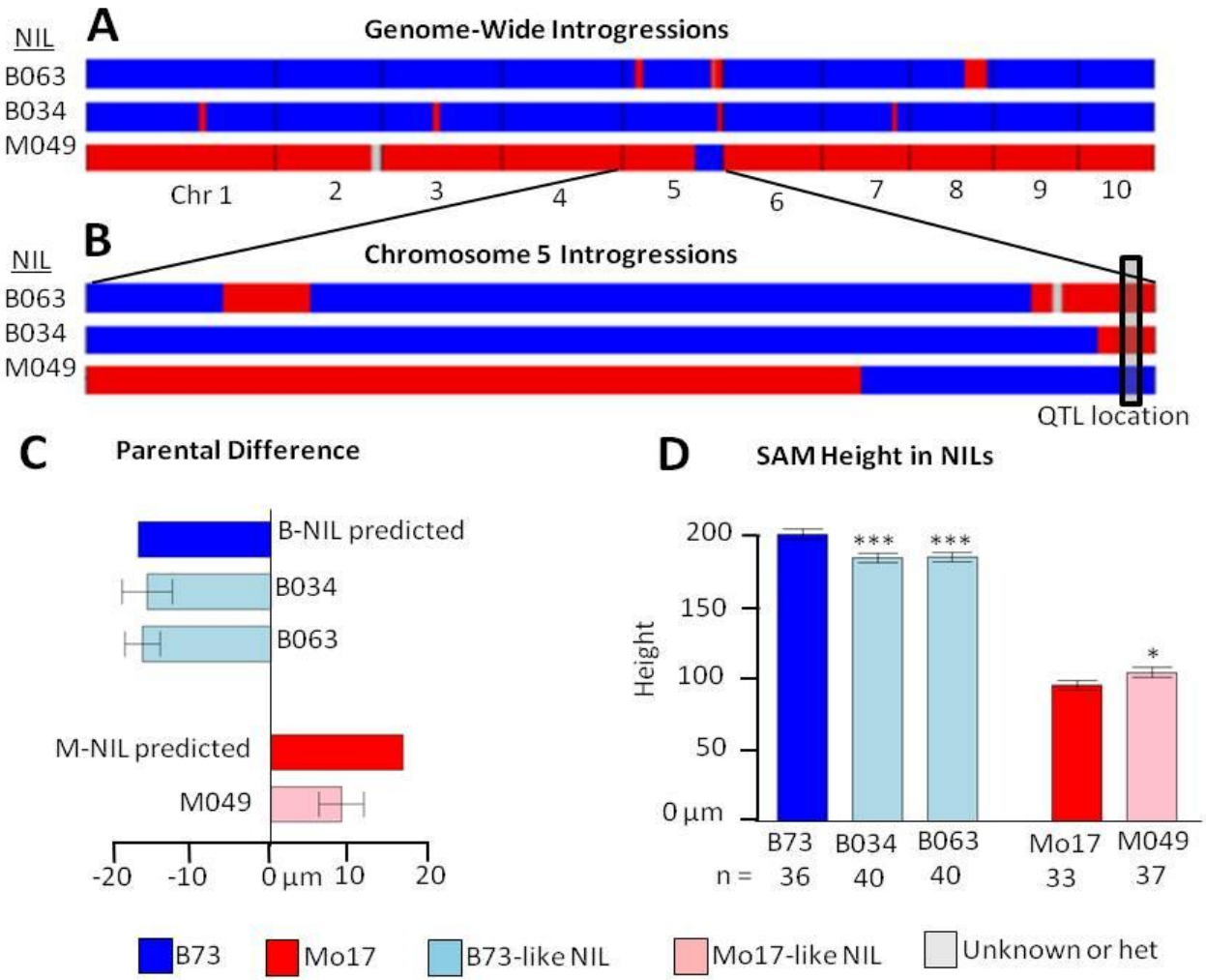
A
Genome-Wide Introgressions
NIL
B063
B034
M049
Chr 1
2
3
4
5
6
7
8
9
10
B
Chromosome 5 Introgressions
NIL
B063
B034
M049
QTL location
C
Parental Difference
B-NIL predicted
B034
B063
M-NIL predicted
M049
-20
-10
0 µm
10
20
D
SAM Height in NILs
Height
200
150
100
50
0 µm
***
***
*
B73
B034
B063
Mo17
M049
n =
36
40
40
33
37
B73
Mo17
B73-like NIL
Mo17-like NIL
Unknown or het

Figure 5. Identifying candidate genes based on expression. Numbers of genes expressed in the B73 SAM and IBMRIL apices located within the identified QTL intervals for each trait with expression significantly correlated (comparison-wise threshold $p<0.05$) with SAM architecture for SAM height (**A**), width (**B**), and plastochron difference (**C**).

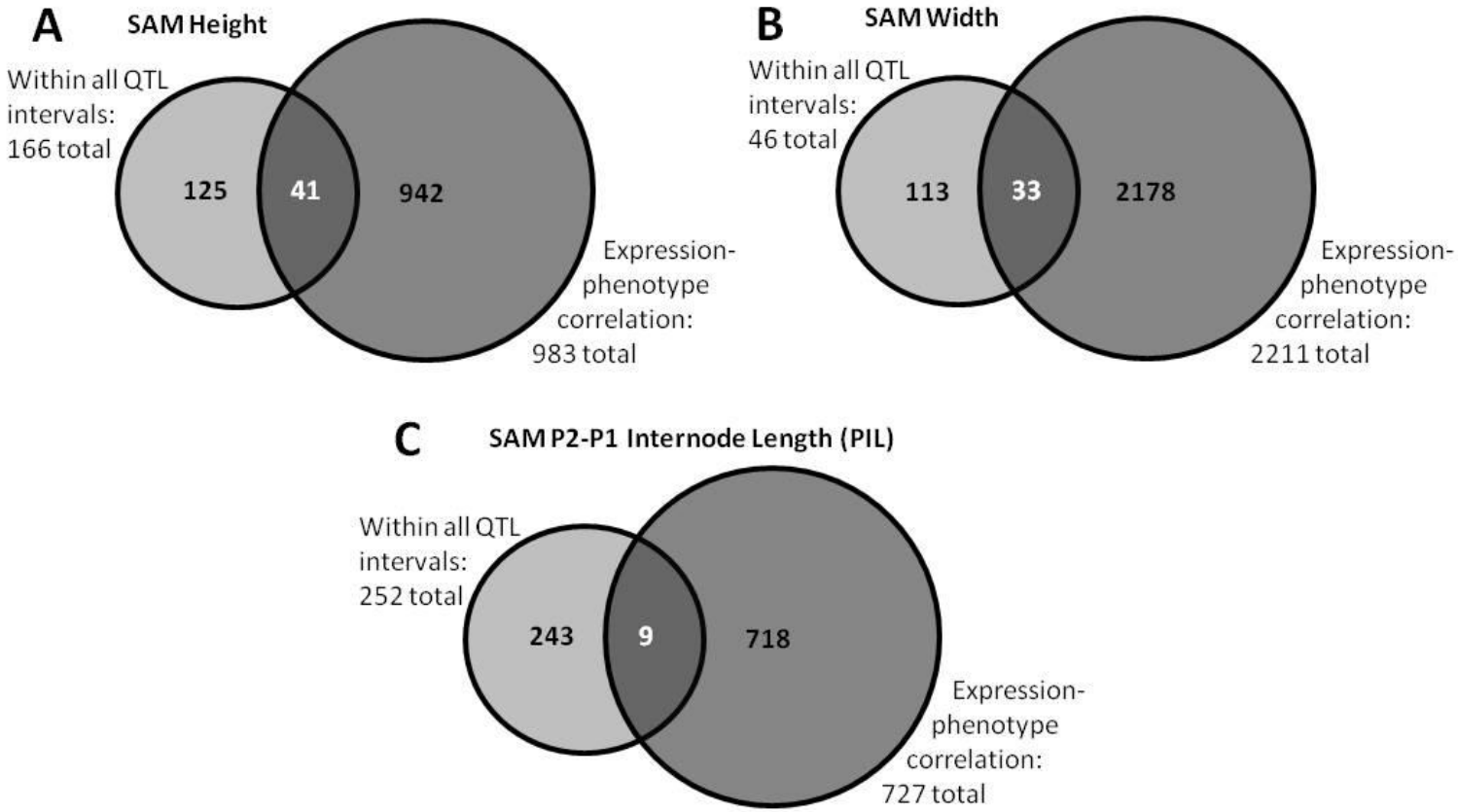
A
SAM Height
Within all QTL intervals: 166 total
125
41
942
Expression-phenotype correlation: 983 total
B
SAM Width
Within all QTL intervals: 46 total
113
33
2178
Expression-phenotype correlation: 2211 total
C
SAM P2-P1 Internode Length (PIL)
Within all QTL intervals: 252 total
243
9
718
Expression-phenotype correlation: 727 total

Supplemental Figure S1. Density distributions of remaining SAM traits in the IBMRIL population. B73 and Mo17 are indicated as B and M, respectively.

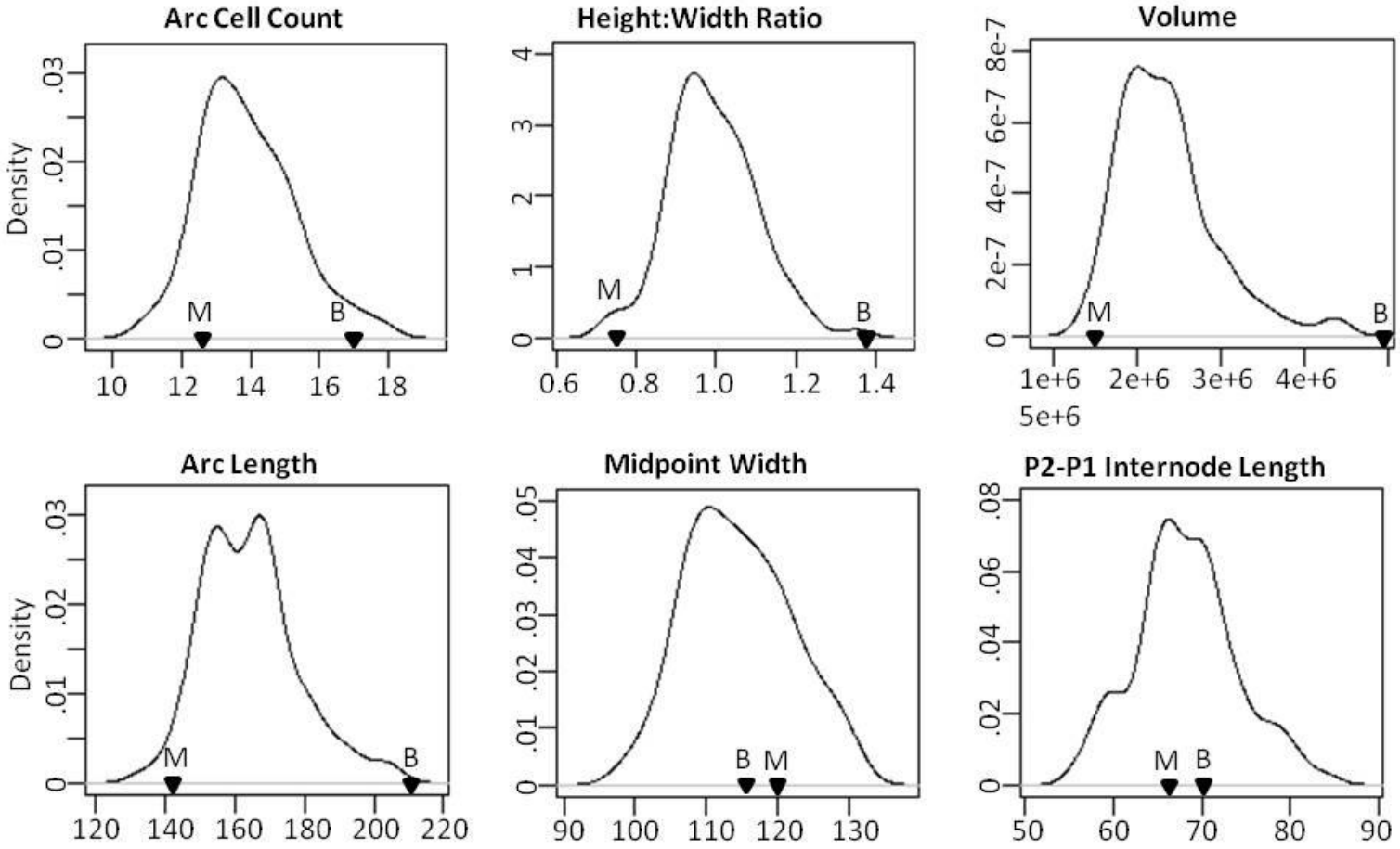
Arc Cell Count
Density
0
.01
.02
.03
M
B
10
12
14
16
18
Height:Width Ratio
0
1
2
3
4
M
B
0.6
0.8
1.0
1.2
1.4
Volume
0
2e-7
4e-7
6e-7
8e-7
M
B
1e+6
2e+6
3e+6
4e+6
5e+6
Arc Length
Density
0
.01
.02
.03
M
B
120
140
160
180
200
220
Midpoint Width
0
.01
.02
.03
.04
.05
B
M
90
100
110
120
130
P2-P1 Internode Length
0
.02
.04
.06
.08
M
B
50
60
70
80
90

Supplemental Figure S2. Patterns of expression in candidate genes. Gene expression across SAM ontogeny for genes expressed in the B73 SAM and IBMRIL apices located under QTL with expression significantly correlated with SAM architecture (see Figure 5) for SAM height (**A**), width (**B**), and PIL (**C**). PS=Proembryo stage SAM, TS=Transition stage SAM, CS=Coleoptile stage SAM, L1=L1 SAM of 14-day seedling, SAM=SAM of 14-day seedling, LM=Lateral Meristem of 14-day seedling. Annotations, locations, and RPM values of genes are listed in Table S4.

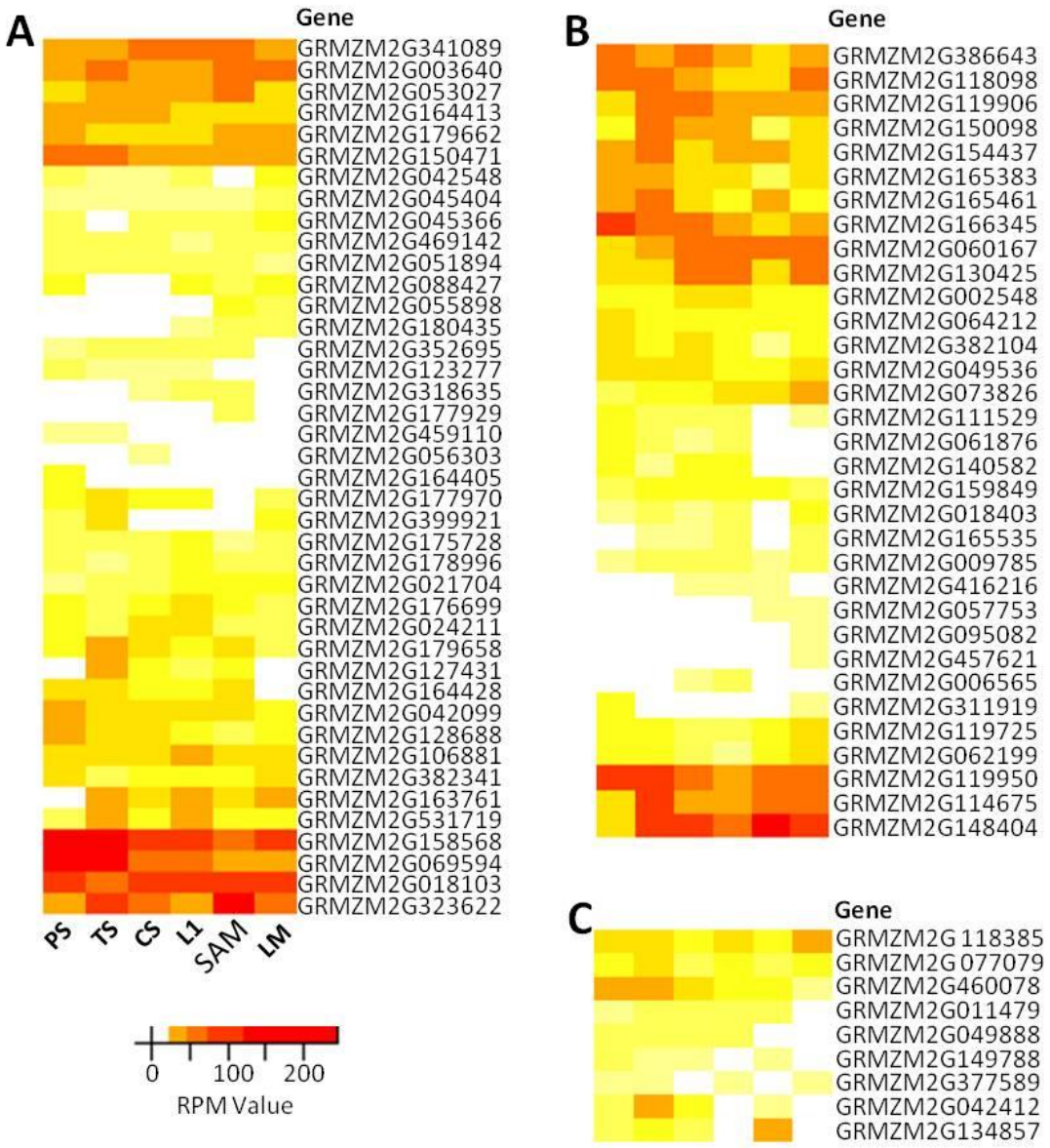
A
Gene
GRMZM2G341089
GRMZM2G003640
GRMZM2G053027
GRMZM2G164413
GRMZM2G179662
GRMZM2G150471
GRMZM2G042548
GRMZM2G045404
GRMZM2G045366
GRMZM2G469142
GRMZM2G051894
GRMZM2G088427
GRMZM2G055898
GRMZM2G180435
GRMZM2G352695
GRMZM2G123277
GRMZM2G318635
GRMZM2G177929
GRMZM2G459110
GRMZM2G056303
GRMZM2G164405
GRMZM2G177970
GRMZM2G399921
GRMZM2G175728
GRMZM2G178996
GRMZM2G021704
GRMZM2G176699
GRMZM2G024211
GRMZM2G179658
GRMZM2G127431
GRMZM2G164428
GRMZM2G042099
GRMZM2G128688
GRMZM2G106881
GRMZM2G382341
GRMZM2G163761
GRMZM2G531719
GRMZM2G158568
GRMZM2G069594
GRMZM2G018103
GRMZM2G323622
PS
TS
CS
L1
SAM
LM
0
100
200
RPM Value
B
Gene
GRMZM2G386643
GRMZM2G118098
GRMZM2G119906
GRMZM2G150098
GRMZM2G154437
GRMZM2G165383
GRMZM2G165461
GRMZM2G166345
GRMZM2G060167
GRMZM2G130425
GRMZM2G002548
GRMZM2G064212
GRMZM2G382104
GRMZM2G049536
GRMZM2G073826
GRMZM2G111529
GRMZM2G061876
GRMZM2G140582
GRMZM2G159849
GRMZM2G018403
GRMZM2G165535
GRMZM2G009785
GRMZM2G416216
GRMZM2G057753
GRMZM2G095082
GRMZM2G457621
GRMZM2G006565
GRMZM2G311919
GRMZM2G119725
GRMZM2G062199
GRMZM2G119950
GRMZM2G114675
GRMZM2G148404
C
Gene
GRMZM2G 118385
GRMZM2G 077079
GRMZM2G460078
GRMZM2G011479
GRMZM2G049888
GRMZM2G149788
GRMZM2G377589
GRMZM2G042412
GRMZM2G134857

Chapter 3

Diversity of maize shoot apical meristem architecture and its relationship to plant morphology

Abstract

The shoot apical meristem contains a pool of undifferentiated stem cells and is in charge of initiating all aerial plant organs. In maize (*Zea mays*), leaves and floral meristems are formed throughout vegetative development; upon transition to floral development, the shoot meristem forms the tassel. Due to the regulated balance between stem cell maintenance and organogenesis, the structure and morphology of the shoot meristem remain relatively constant during vegetative development. Previous work identified loci contributing to meristem architecture in a set of recombinant inbreds. This study expanded upon these initial results by investigating shoot apical meristem morphology across a diverse set of inbred lines. Parental values and their F1 progeny were examined, and genetic architecture was mapped in two divergent populations. The genetic control of meristem architecture was found to be mainly population-specific, and can sometimes overlap with known genes affecting the meristem. In addition, we described heterosis for meristem architecture traits in crosses among diverse inbreds, and identified some inbreds that seemed to act in a dominant fashion. Finally, we characterized correlations of meristem morphology with adult plant traits, revealing links between the control of architecture for undifferentiated and differentiated plant organs.

Introduction

Many of the advances in breeding for high-yielding crop varieties particularly in maize have been brought on by changes in plant morphology. Research efforts have focused on determining the genetic control of plant architecture and subsequent applications via mutant analyses and mapping experiments. One approach to identify factors contributing to differences in plant architecture is via quantitative trait loci (QTL) mapping. Previous studies of maize morphology have identified QTL for shoot architecture (Lauter *et al.* 2008), leaf shape (Tian *et al.* 2011), root architecture (Hochholdinger and Tuberosa 2009), inflorescence architecture (Upadyayula *et al.* 2006, Brown *et al.* 2011), and flowering time (Buckler *et al.* 2009), among many other fully developed plant organ characteristics. There have been far fewer investigations, however, into the architecture of undifferentiated plant structures such as the embryo (Moore *et al.* 2013, Yang *et al.* 2012) and meristem (Thompson *et al.* 2014). Describing the relationship of the architecture and genetic control of undifferentiated structures and those of differentiated plant parts, such as leaf morphology, plant height, flowering time, and inflorescence architecture, may lead to important insights into plant development and the regulators of differentiated plant morphology.

An important caveat in describing the genetic architecture of a trait using QTL mapping, particularly in a biparental population, is that only genes segregating within a given cross can be identified in the analysis. Mapping performed in different populations commonly show different results. In addition, non-genetic effects - contribution of

environment, population size leading to the Beavis Effect, etc. - may limit or change the QTL considered significant in each experiment (Beavis 1998).

The shoot apical meristem (SAM) produces all of the plant's above-ground organs. It performs the dual functions of organogenesis and stem cell maintenance via a pool of undifferentiated stem cells. Throughout vegetative development the SAM continues to grow and expand, though the rate is not constant; three phases take place between germination and floral transition, with a stage of slower growth between two periods of more rapid growth (Thompson *et al.* 2014). A balance of stem cell maintenance and organogenesis is maintained to prevent stem cell pool depletion or over-proliferation, which lead to developmental arrest or a failure to initiate leaves, respectively (Barton 2010). In maize, 100-200 founder cells act as leaf initials (Poethig 1984), and organogenesis takes place in the peripheral zone of the SAM. Between fertilization and seed maturation/quiescence, about five leaves are formed in the maize embryo. Leaf initiation and growth resume at regular intervals (plastochrons or P; Sharman 1942; Sylvester *et al.* 1990) after germination. Studies of SAM function have revealed many regulatory processes affecting growth and development; these investigations have been primarily analysis of developmental mutants, some of which alter whole plant and/or SAM morphology.

The CLAVATA (CLV) / *WUSHEL (WUS)* negative feedback loop regulating stem cell number in Arabidopsis has been extensively characterized and is known to impact SAM size (Schoof *et al.* 2000, Wang and Li 2008). Larger SAMs result from mutations in CLV signaling (Leyser and Furner 1992; Clark *et al.* 1993, 1995; Kayes and

Clark 1998), while meristem maintenance is impaired when *WUS* is defective (Laux *et al.* 1996). The maize mutants *faciated ear2 (fea2)* (Taguchi-Shiobara *et al.* 2001) and *compact plant2 (ct2)* (Bommert *et al.* 2013) are both in this pathway and affect the size of the SAM.

Knotted-1-like homeobox (KNOX) genes also play a major role in SAM function and identity and have been shown to affect meristem size (Hake *et al.* 1995, Kerstetter *et al.* 1994, Jackson *et al.* 1994), as well as leaf morphology (Nishimura *et al.* 2000, Smith and Hake 2003, Rosin *et al.* 2003). Maize *Knotted-1* (*kn1*) mutants lack meristem maintenance (Kerstetter *et al.* 1997) and show a range of penetrance of SAM size phenotypes across different inbred backgrounds (Vollbrecht *et al.* 2000). Orthologs of *kn1* in Arabidopsis and rice are similarly unable to maintain the meristem (Long *et al.* 1996; Tsuda *et al.* 2011). Other *KNOX* gene mutations in maize, including *rough sheath1*, *gnarley1/KNOX4*, and *liguleless3* (*lg3*) and *lg4* (Schneeberger et al. 1995; Foster et al. 1999; Muehlbauer et al. 1999; Bauer et al. 2004), have not been shown to impact the size of the meristem (Hake *et al.* 2004; Bolduc *et al.* 2014).

One way that KNOX proteins serve to maintain stem cell identity is through the regulation of the ratio and patterning of plant hormones (Kyozuka 2007; reviewed in Hay *et al.* 2004 and Vanstraelen and Benková 2012), particularly auxin and cytokinin (CK). Auxin is responsible for promoting organogenesis (Pernisová *et al.* 2009), and loss of auxin transport leads to the inability to produce organs (Reinhardt 2000; reviews in Gallavotti 2013, Forestan and Varatto 2012). Conversely, cytokinin promotes cell division. Disruption in cytokinin biosynthesis leads to loss of the SAM (Yanai *et al.*

2005), while larger meristems form in plants harboring mutations in CK response regulators like the maize *aberrant phyllotaxy1* (*abph1)* mutant (Jackson and Hake 1999; Giulini *et al.* 2004).

In addition to the KNOX genes, other plant hormones such as gibberellins and brassinosteroids contribute to the regulation of the ratio of auxin and CK during plant development (Vanstraelen and Benková 2012). The CK response pathway also interacts with chromatin remodeling components (Efroni *et al.* 2013), another process involved in stem cell maintenance (Shen and Xu 2009; for review of chromatin structure and remodeling regulators see Wagner 2003; Kwon and Wagner 2007; Sang *et al.* 2009).

Small RNAs are another important source of regulation in the establishment and function of the SAM (Zhang *et al.* 2006; microRNA review in Axtell 2013). In *Arabidopsis*, movement of microRNA394 (miR394) to the cell layers underlying the protoderm helps define stem cell location during the formation of the SAM (Knauer *et al.* 2013). The meristem is affected when regulators of miRNA biogenesis or function such as *ago1* (Vaucheret *et al.* 2004), *ago10* (Liu *et al.* 2009), and *dcl1* (Schauer *et al.* 2002) are disrupted. Meristem function is also regulated via components of trans-acting small interfering RNA biogenesis, as maize mutants *leafbladeless* and *ragged seedling2* show altered auxin response and misexpression of miR166 and HD-ZIPIII transcription factors (Nogueira *et al.* 2007; Douglas *et al.* 2010). SAM shape varies coordinately with altered phyllotaxy and plastochron time in rice *sho* mutants that affect the miRNA pathway (Itoh *et al.* 2000; Nagasaki *et al.* 2007), indicating a link between the morphologies of undifferentiated and differentiated plant structures.

The broad categories of gene expression regulatory mechanisms described above are complemented by several downstream factors contributing to SAM function; for instance, changes in cell wall properties and metabolic processes (Kierskowski *et al.* 2012; Peaucelle *et al.* 2011). A specific example of this is the maize thiamine auxotroph *bladekiller1-R* (*blk1-R),* which shows a SAM size that decreases progressively due to impaired meristem maintenance and organogenesis (Woodward *et al.* 2010).

A previous investigation suggested that much of the control of the natural variation present in SAM architecture takes place in the less well-characterized downstream processes rather than in major transcription factors with the potential to impact dozens of genes (Thompson *et al.* 2014). This study focused on one population (IBMRIL) and did not encompass a wide diversity of maize genotypes. Larger-effect genes contributing to meristem morphology may not be segregating in this particular population, and the range of diversity present for SAM architecture across a wider variety of maize backgrounds is unknown. Furthermore, the time line of SAM growth across vegetative development may vary in more highly divergent inbred lines. Two other unexplored areas of maize meristem architecture are the extent of heterosis present for SAM traits, and the relationship of these traits to adult plant morphology.

The objectives of this study were to: i) survey maize SAM architecture in a panel of diverse inbred lines; ii) test for the presence and extent of heterosis in crosses made among diverse lines; iii) map QTL for SAM morphology in two additional populations created from highly divergent parents; and iv) characterize correlations between

undifferentiated and differentiated plant structures, or connecting maize SAM architecture to adult plant morphology.

Materials and Methods

Plant materials

This study utilized the 27 nested association mapping (NAM) founder inbreds (includes Mo17 and B73), as well as individuals from two RIL sub-populations (CML277 and P39) of the NAM (Table S1; Yu *et al.* 2008). The intermated B73 x Mo17 recombinant inbred line (IBM RIL) population was also used (Lee *et al.* 2002), as well as F1 offspring of eight inbreds (B97, Hp301, IL14H, Ms71, NC358, Oh43, Oh7B, and P39) crossed to B73 and Mo17.

Plant growth and experimental design

The NAM founders, the two NAM RIL sub-populations and the NAM x B73 F1 crosses were all planted in 10x20 racks of tubes one inch wide and eight inches deep. Every third row of ten in each rack was left empty to allow for even air flow and light intensity and reduce edge effects. The soil used was a 1:1 mixture of black soil and SunGro potting soil, blended with 2 teaspoons per square foot of Osmocote Plus fertilizer. Plants were grown in growth chambers for 14 days at 25C during 16 hour days, and 20C nights.

The 27 NAM parental lines (Table S1; Yu *et al.* 2008) were grown in three replications of 10 plants per line, with lines randomly distributed throughout the growth chamber. All healthy plants were sampled for histology, and 10 to 27 images were measured per line.

For the NAM sub-populations CML277 x B73 (Z005) and P39 x B73 (Z024), 140 and 137 lines respectively were examined (Table S1). These lines were grown in five replications of one plant per line, all in one chamber, with lines randomly distributed. In addition to the 140 and 137 RILs, all parental lines (B73, Mo17, P39, CML277) as well as 10 representative inbred lines (Table S1) from the IBM RIL population (selected to encompass the ranges of observed SAM height and SNP diversity) were included in each set for data standardization. All healthy plants were sampled for histology, and 1 to 5 images (average 3.8) were measured per line for RILs, 6 to 10 (average 8.3) for each of the IBM controls, and 14 to 19 (average 16) per parental line.

Sixteen NAM founder x B73 F1 crosses (Table S1) and 10 parental inbreds were grown in 20 replications of one plant per rep, scattered randomly throughout each replication. All healthy plants were sampled, and 14 to 18 images were measured per line, with the exception of Hp301 and its crosses; these lines had very poor germination, and only 9, 3, and 1 plants were measured for Hp301, Hp301 x B73, and Hp301 x Mo17, respectively.

Histology

All samples were dissected and fixed in FAA, then processed according to one of the two methods described in Thompson *et al.* 2014: paraffin embedding / microtome sectioning, or methyl salicylate tissue-clearing. The 27 NAM founders were embedded in paraffin and sectioned. All other experiments utilized the methyl salicylate tissue-clearing protocol.

SAM architecture measurements

SAM images were measured using ImageJ software (http://rsbweb.nih.gov/ij/) according to Thompson *et al.* 2014. Briefly, SAM width, height, arc length, midpoint width, and plastochron internode length were measured relative to the P1 cleft (Figure 1A). The derived traits of height:width ratio and volume as a dome were also calculated for each sample. For the NAM founders, cells in the L1 layer along the arc length were counted and the derived trait of average cell size (arc length divided by arc cell number) was calculated; these two traits were not examined in the other datasets due to an inability to reliably see cell wall boundaries in images from cleared tissue.

Data analysis

Raw phenotypic data analysis and visualization, linear models to standardize datasets, ANOVAs, and Pearson's correlations were all conducted in R (http://www.r-project.org/). Heritability was calculated according to Bernardo 2010 (p. 153-156) as additive genetic variance of the RIL (Va_RIL) divided by total phenotypic variance (Vp).

QTL mapping was performed in QTLCartographer (http://statgen.ncsu.edu/qtlcart/) with genetic maps via Panzea (http://www.panzea.org), using composite interval mapping with 10 background markers and a window size of 5cM. Significance thresholds were determined via 1000 permutations at α=0.05 on each trait, and confidence intervals were calculated using a 1-LOD drop.

Correlations of SAM architecture with adult plant traits were conducted using Pearson's correlation coefficient. Adult plant trait measurements for the NAM sub-populations were obtained from Panzea (http://www.panzea.org). Trait values were averaged across environments, and correlations with SAM phenotypes were required to be significant ($p<0.05$) in at least half of the environments as well as the overall average in order to be reported.

To determine significant overlap of SAM genes, a list of 226 candidate SAM genes determined by expression patterns across ontogeny of the meristem in Takacs et al. 2012 was compared to genes located under QTL for each trait. Numbers of genes contained in both datasets were compared to the overlap of the candidate list with 1000 randomly located subsets of simulated random QTL containing the same gene number for each trait and each population.

Results

Natural diversity in maize SAM architecture

To examine the extent of natural variation for SAM architecture, we examined 27 diverse inbred maize lines used as parents in the maize NAM population (Yu *et al.* 2008). The NAM parents (Table S1) were selected to represent both allelic and phenotypic diversity in maize. At least five plants were measured from at least three replicates of each genotype. Measurements of nine traits were used to characterize SAM architecture: height, arc length, width, and midpoint width from the P1 cleft; cell number in the L1 layer along the arc length; plastochron internode difference; and the derived traits of cell size, height:width ratio, and volume (Figure 1A). The measurements of SAM traits in the NAM parents were used to estimate the phenotypic variation in maize (Table 1).

Distribution of the traits across NAM founder lines was approximately normal with the exception of SAM height:width ratio, and one to three high outliers for most traits (Figures 2 and S1, NAM founder histogram). For SAM height, arc length, and volume, the inbred lines P39, B73, and Mo18W were atypically large, whereas IL14H was the outlier for SAM width. The ratio of SAM height to width showed a bimodal distribution, with approximately half of the lines centered around a mean of 0.75, half centered around 1, and a high outlier of 1.25 for B73. Average arc cell size and plastochron internode difference showed lower heritabilities and were likely more influenced by the environment than the other traits (Table 1).

Heterosis for SAM architecture

B73 and Mo17 were crossed to eight diverse inbreds (Table S1), and the resulting F1 progeny were examined for SAM architecture traits alongside the parental inbreds. Heterosis, defined here as trait values significantly outside the range of the parents, was observed in many crosses made to Mo17 (Figure 3). Crosses exhibiting heterosis tended to be significant or near-significant across SAM traits (Figure S2). Some lines, including P39 and Oh7B, appeared dominant to Mo17, as SAM height, arc length, and height:width ratio in the Mo17-cross F1 were significantly different from Mo17 but equivalent to trait values for the other parental inbred. For B73, only crosses made to P39 showed values outside of parental ranges; SAM architecture of all remaining crosses to B73 appeared very near to mid-parent values. Inbred background type was not a predictor of presence or strength of heterosis, as the non-stiff stalk lines B97 and Oh43 showed some of the highest levels of heterosis with Mo17 (also a non-stiff stalk) but seemed additive with B73 (stiff stalk). P39 and Il14H, although both sweet corn lines, exhibited very different responses when combined with B73 and Mo17; P39 was heterotic for SAM traits with B73 while Il14H was not significantly outside any parental ranges.

QTL mapping in sub-populations derived from extreme founders

Inbreds at the extremes of the NAM parent distributions for both height and width were chosen to further investigate SAM diversity (Figure 1B-C). NAM RIL sub-populations derived from crosses of B73 to CML277 (the shortest and narrowest SAM) and P39 (the tallest and widest SAM) were examined for seven SAM traits; cell counts

and the derived trait of cell size were not included due to restrictions in the images produced by the protocol (see materials and methods). As expected, the combined resulting trait distributions encompassed the diversity present in the NAM founders (Figures 2 and S1). Interestingly, though previous work suggested that B73 represents the maximum height, volume, and height:width ratio for the maize SAM (Figure 2, IBM RIL distribution shown in dashed green/lighter line), RILs in the P39 x B73 population showed extensive transgressive segregation for these traits (Figure 2, blue/dark solid distribution line). However, in the RILs derived from CML277 x B73 (Figure 2, red/light solid distribution line), B73 was the highest value for these three traits, though transgressive segregation on the low end was observed.

For each of the seven SAM traits, one to five QTL were mapped per population. Estimated parental variance explained ranged from 6% to as high as 28% with an average of 12% (Table 2). The 34 total QTL were distributed across nine chromosomes (all but chromosome 7). QTL regions for SAM architecture traits within a population frequently overlapped, even among low-correlated traits, for example SAM height and width (Figure 4). Considering this co-localization of the 34 QTL, a total of 15 unique loci were identified, only one of which was identified in both of the populations (Table S2).

Overlap of QTL with known SAM genes

QTL identified in this study, particularly for SAM height-related traits in the CML277 x B73 population, frequently co-localized with genes implicated to function in the SAM or affect meristem or plant architecture (Table S3), as evidenced by overlap

with the list of 226 candidate SAM genes identified in Takacs et al. 2012. Some of these were known SAM-related genes in maize (Table 3). The candidates included genes involved in the CLAVATA/WUSCHEL pathway, knotted1-like homeobox genes, various members involved in hormone response and transport, and genes implicated in stem cell maintenance, SAM identity or organization or initiation, organ boundaries, cell differentiation and organogenesis.

Correlation of SAM architecture with adult plant traits

To investigate the relationship of SAM architecture with adult characteristics, public phenotype data from the NAM RILs (http://www.panzea.org) was leveraged to examine correlations with SAM architecture; these correlations among and between SAM and adult plant traits and their clustering can be visualized in Figure 5. The adult plant traits included several measures of flowering time, as well as germination rate, tassel morphologies, plant and ear height, leaf length and width, leaf number and angle, cob diameter and weight, ear diameter and length, and several measures of yield. Pearson's correlations were used to identify traits significantly robustly associated with SAM architecture (see Methods). Briefly, correlations were required to be present in at least half of the field environments measured as well as for the overall trait mean across grow-outs to avoid false positives. Correlations observed were weak to moderate ($r \approx 0.2$ - 0.4), but significant (see Table S4). Associations with flowering time, leaf angle, leaf length and width, ear height, and cob diameter and weight were all negative; in other words, larger SAM size generally led to faster flowering, shorter and more narrow and

upright leaves, lower ears, and smaller cobs: generally smaller plant stature characters. However, correlations with yield traits (ear diameter and length, seed set length, ear row and rank number, kernel volume, ear weight) were all positive, meaning that taller or wider meristems led to higher yield characteristics. Correlations with flowering time traits were present in both populations.

Discussion

Extreme SAM architecture can exhibit transgressive segregation and heterosis

Previously reported data for the IBM RIL population (Thompson *et al.* 2014) indicated that the height, arc length, and volume of the maize SAM did not exceed that of B73. Even in the diverse NAM founder inbreds, B73 was one of the three tallest outliers for SAM height (Table 1, Figure 2). However, SAM measurements of a RIL population derived from B73 x P39 (another tall outlier) revealed transgressive segregation occurring, leading to even larger SAM size (Table 1, Figure 2, Figure S2). Similarly, the RIL population derived from B73 x CML277 (the shortest of the NAM founders) exhibited a range of SAM sizes that included RILs shorter (or taller) than either of the two parents (Table 1, Figure 2). This indicates that the genes contributing to meristem size in these inbreds may be distinct, such that the additive effect of the new combinations of loci lead to the observation of exceptional phenotypes.

Crosses of several NAM founders to B73 and Mo17 were also examined for SAM architecture to determine the presence of heterosis. Many inbreds exhibited heterosis across several traits when crossed to Mo17, indicating that even very different SAM traits, for example height and width, are not inherently different in their potential or observed levels of heterosis (Figure 3). However, inbreds did show differences in their tendency to exhibit heterosis when crossed: although Mo17 crosses were frequently larger than their parents, only one cross to B73 was significantly larger than either parent. This cross was the F1 between B73 and P39, the early flowering sweet corn line with a

very tall and wide SAM. The remainder of the crosses to B73 showed F1 measures at or near midparent values.

P39 showed a number of unexpected results. In addition to exhibiting heterosis when crossed to B73, P39 seemed to have a dominant effect when crossed to Mo17, as P39 x Mo17 F1 values for SAM height, arc length, and height:width ratio were all significantly different from Mo17 but similar to P39 (Figure S2). This occurs in Oh7B x Mo17 F1 as well, with Oh7B alleles appearing to be dominant for the same three traits. Interestingly, heterosis did not seem to be predictable by inbred type.

Major loci affecting SAM architecture differ by genetic background

Only one of the 15 loci mapped for SAM traits overlapped between the two NAM RIL subpopulations (Figure 4, Table S2), and this locus did not confer a major effect. In the CML277 x B73 population (Z005), the chromosome 1 QTL was responsible for 7.3 - 12% of the parental variation in SAM height, arc, volume, width, and midpoint width; it was also associated with height:width ratio in the P39 x B73 population (Z024), explaining only 6.5%. A single gene may be causing the association in both populations, but given that the significant traits differ in each set of RILs this is less likely. Similarly, previous SAM architecture QTL mapping results from the IBM RIL population (Thompson *et al.* 2014) showed only one QTL overlap for the same significant trait with these 15 loci (Figure 4, Table S2). This locus, also on chromosome 1, was significant for ratio, volume, and height in the CML277 x B73 population, and for volume, arc length,

and height in the IBM RIL. Again, it was a low-effect QTL, explaining 6.9 - 11.8% of the parental variation.

Given the lack of significant overlap in QTL among populations, SAM architecture appears to be mainly controlled by different genes in different genetic backgrounds. This corroborates the observations of transgressive segregation and heterosis in RIL populations, with distinct sets of genes contributing to SAM size. Large-effect genes are particularly cross-dependent, as neither of the major loci (effect contribution above 20%) detected here were present in any other population. It could be that the smaller-effect loci shared between populations represent downstream genes in the same or related pathways that serve to fine-tune control of SAM size and function.

Known SAM genes co-localize with SAM architecture QTL

In contrast with the lack of such coincidence found in the IBM RIL (Thompson *et al.* 2014), one outcome of this work is the overlap of QTL with major known SAM-related genes. Candidate genes were identified via overlap with a list of 226 genes implicated to function in the SAM (Takacs et al. 2012). Candidate genes with known maize phenotypes are listed in Table 3, including *Knotted1* (Vollbrecht *et al.* 1991). This important marker for meristematic cell identity has been shown to affect SAM size in a background-dependent fashion (Vollbrecht *et al.* 2000). The full list of overlaps (Table S3) includes knotted1 and knotted1-like homeobox genes, members of the CLAVATA/WUSCHEL pathway, hormone response and transport genes, and genes

involved in meristem maintenance, SAM initiation/identity/organization, and cell differentiation and organogenesis.

The overlap of the 226 candidates with genes located under QTL was statistically significant for the CML277 (very short SAM) x B73 (very tall SAM) population, particularly for SAM height and related traits. This means that overlap between the two gene sets occurred more frequently for this population than expected via random chance in simulated QTLs of the same gene number. Though nowhere near conclusive, the overlap of known SAM genes with QTL supports the hypothesis that genes causing abnormal phenotypes when mutated also have the potential to contribute to observed natural variation of the same phenotypes across diverse backgrounds, particularly when the parental phenotypes are extremely different.

SAM size coincides with flowering time and other plant traits

A correlation analysis across the two NAM RIL subpopulations revealed several instances where diversity in SAM architecture coincided with differences in whole-plant morphology. These whole-plant traits included four measures of flowering time: days to silk or tassel, and growing degree days to silk or tassel. All four of these traits showed significant correlation with one or more SAM traits in both of the RIL populations (Figure 5, Table S4). Several leaf morphology and yield-related measurements also showed correlation in a population-specific manner. A connection between the growth pattern and form of the meristem and whole-plant architectures such as branching pattern has been previously discussed (see Sussex and Kirk 2001 for review), but this study is the

first to directly connect the architecture of undifferentiated cell structure to that of differentiated organs in the adult plant.

Literature cited

Axtell, M. J., 2013 Classification and comparison of small RNAs from plants. Ann. Rev. Plant Biol. 64: 137-159.

Barton, M. K., 2010 Twenty years on: The inner workings of the shoot apical meristem, a developmental dynamo. Dev. Biol. 341: 95-113.

Bauer, P., M. Lubkowitz, R. Tyers, K. Nemoto, R. B. Meeley *et al.,* 2004 Regulation and a conserved intron sequence of liguleless3/4 Knox Class-I homeobox genes in grasses. Planta 219: 359-368.

Beavis, W. D., 1998 QTL Analyses: Power, Precision, and Accuracy, pp. 145-161 in *Molecular dissection of complex traits*, edited by A. H. Paterson. CRC Press, Boca Raton, FL.

Bernardo, R., 2010 *Breeding for quantitative traits in plants*. Stemma Press, Woodbury, MN.

Bolduc, N., R. G. Tyers, M. Freeling, and S. Hake. 2014 Unequal redundancy in maize knotted1 homeobox genes. Plant Physiol. 164: 229-238.

Bommert, P., B. I. Je, A. Goldschmidt, and D. Jackson, 2013 The maize Ga gene *COMPACT PLANT2* functions in CLAVATA signaling to control shoot meristem size. Nature 502: 555-558.

Brown, P. J., N. Upadyayula, G. S. Mahone, F. Tian, P. J. Bradbury *et al.,* 2011 Distinct genetic architectures for male and female inflorescence traits of maize. PLOS Genetics 7: e1002383.

Buckler, E. S., J. B. Holland, P. J. Bradbury, C. B. Acharya, P. J. Brown *et al.,* 2009 The genetic architecture of maize flowering time. Science 325: 714-718.

Clark, S. E., M. P. Running, and E. M. Meyerowitz, 1993 *CLAVATA1*, a regulator of meristem and flower development in *Arabidopsis.* Development 119: 397-418.

Clark, S. E., M. P. Running, and E. M. Meyerowitz, 1995 *CLAVATA3* is a specific regulator of shoot and floral meristem development affecting the same processes as *CLAVATA1*. Development 121: 2057-2067.

Douglas, R. N., D. Wiley, A. Sarkar, N. Springer, M. C. P. Timmermans *et al.,* 2010 *ragged seedling2* encodes an ARGONAUTE7-Like protein required for mediolateral expansion, but not dorsiventrality, of maize leaves. The Plant Cell 22: 1441-1451.

Efroni, I., S. K. Han, H. J. Kim, M. F. Wu, E. Steiner et al., 2013 Regulation of leaf maturation by chromatin-mediated modulation of cytokinin responses. Dev. Cell 24: 438-445.

Forestan, C., and S. Varotto, 2012 The role of PIN auxin efflux carriers in polar auxin transport and accumulation and their effect on shaping maize development. Molecular Plant 5: 787-798.

Foster, T., J. Yamaguchi, B. C. Wong, B. Veit, and S. Hake, 1999 *Gnarley1* is a dominant mutation in the *knox4* homeobox gene affecting cell shape and identity. The Plant Cell 11: 1239-1252.

Gallavotti, A., 2013 The role of auxin in shaping shoot architecture. J. Exp. Bot. 64: 2593-2608.

Giulini, A., J. Wang, and D. Jackson, 2004 Control of phyllotaxy by the cytokinin-inducible response regulator homologue *ABPHYL1*. Nature 430: 1031-1034.

Hake, S., B. R. Char, G. Chuck, T. Foster, J. Long *et al.*, 1995 Homeobox genes in the functioning of plant meristems. Phil. Trans. R. Soc. Lond. B 350: 45-51.

Hake, S., H. M. S. Smith, H. Holtan, E. Magnani, G. Mele *et al.*, 2004 The role of Knox genes in plant development. Ann. Rev. Cell Dev. Biol. 20: 125-151.

Hay, A., J. Craft, and M. Tsiantis, 2004 Plant hormones and homeoboxes: Bridging the gap? BioEssays 26: 395-404.

Hochholdinger, F. and R. Tuberosa, 2009 Genetic and genomic dissection of maize root development and architecture. Curr. Opin. Plant Biol. 12: 172-177.

ImageJ (http://rsbweb.nih.gov/ij/)

Itoh, J. I., H. Kitano, M. Matsuoka, and Y. Nagato, 2000 Shoot organization genes regulate shoot apical meristem organization and the pattern of leaf primordium initiation in rice. The Plant Cell 12: 2161-2174.

Jackson, D., B. Veit and S. Hake, 1994 Expression of maize *KNOTTED1* related homeobox genes in the shoot apical meristem predicts patterns of morphogenesis in the vegetative shoot. Development 120: 405-413.

Jackson, D. and S. Hake, 1999 Control of phyllotaxy in maize by the *abphyl1* gene. Development 126: 315-323.

Kayes, J. M. and S.E. Clark, 1998 *CLAVATA2*, a regulator of meristem and organ development in Arabidopsis. Development 125: 1253-1260.

Kerstetter, R. A., D. Laudencia-Chingcuanco, L. G. Smith, and S. Hake, 1997 Loss-of-function mutations in the maize homeobox gene, *knotted1*, are defective in shoot meristem maintenance. Development 124: 3045-3054.

Kerstetter, R. A., E. Vollbrecht, B. Lowe, B. Veit, J. Yamaguchi *et al.*, 1994 Sequence analysis and expression patterns divide the Maize *knotted1*-like homeobox genes into two classes. The Plant Cell 6: 1877-1887.

Kierskowski, D., N. Nakayama, A. L. Routier-Kierzkowska, A. Weber, E. Bayer *et al.*, 2012 Elastic domains regulate growth and organogenesis in the plant shoot apical meristem. Science 335: 1096-1099.

Knauer, S., A. L. Holt, I. Rubio-Somoza, E. J. Tucker, A. Hinze *et al.*, 2013 A protodermal miR394 signal defines a region of stem cell competence in the Arabidopsis shoot meristem. Devel. Cell 24: 125-132.

Kwon, C. S. and D. Wagner, 2007 Unwinding chromatin for development and growth: A few genes at a time. Trends Genet. 23: 403-412.

Kyozuka, J., 2007 Control of shoot and root meristem function by cytokinin. Curr. Opin. Plant Biol. 10: 442-446.

Lauter, N., M.J. Moscou, J. Habiger, and S.P. Moose, 2008 Quantitative genetic dissection of shoot architecture traits in maize: towards a functional genomics approach. The Plant Genome 1: 99-110.

Laux, T., K.F.X. Mayer, J. Berger, and G. Jürgens, 1996 The *WUSCHEL* gene is required for shoot and floral meristem integrity in *Arabidopsis*. Development 122: 87-96.

Lee, M., N. Sharopova, W. D. Beavis, D. Grant, M. Katt *et al.*, 2002. Expanding the genetic map of maize with the intermated B73 × Mo17 (IBM) population. Plant Mol. Biol. 48: 453-461.

Leyser, H. M. O. and I. J. Furner, 1992 Characterisation of three shoot apical meristem mutants of *Arabidopsis thaliana.* Development 116: 397-403.

Liu, Q., X. Yao, L. Pi, H. Wang, X. Cui *et al.*, 2009 The ARGONAUTE10 gene modulates shoot apical meristem maintenance and establishment of leaf polarity by repressing miR165/166 in Arabidopsis. Plant J. 58: 27-40.

Long, J. A., E. I. Moan, J. I. Medford, and M. K. Barton, 1996 A member of the KNOTTED class of homeodomain proteins encoded by the STM gene of Arabidopsis. Nature 379: 66-69.

Moore, C. R., D.S. Gronwall, N.D. Miller, and E.P. Spalding, 2013 Mapping quantitative trait loci affecting *Arabidopsis thaliana* seed morphology features extracted computationally from images. G3 3: 109-118.

Muehlbauer, G. J., J. E. Fowler, and M. Freeling, 1999 Sectors expressing the homeobox gene liguleless3 implicate a time-dependent mechanism for cell fate acquisition along the proximal-distal axis of the maize leaf. Development 124: 5097-5106.

Nagasaki, H., J. Itoh, K. Hayashi, K. Hibara, N. Satoh-Nagasawa *et al.,* 2007 The Small interfering RNA production pathway is required for shoot meristem initiation in rice. Proc. Natl. Acad. Sci. USA 104: 14867-14871.

Nishimura, A., M. Tamaoki, T. Sakamoto, and M. Matsuoka, 2000 Over-expression of tobacco *knotted1*-type class1 homeobox genes alters various leaf morphology. Plant Cell Physiol. 41: 583-590.

Nogueira, F. T. S., S. Madi, D. H. Chitwood, M. T. Juarez, and M. C. P. Timmermans, 2007 Two small regulatory RNAs establish opposing fates of a developmental axis. Genes & Dev. 21: 750-755.

Panzea (http://www.panzea.org)

Peaucelle, A., S. A. Braybrook, L. Le Guillou, E. Bron, C. Kuhlemeier *et al.* 2011 Pectin-induced changes in cell wall mechanics underlie organ initiation in Arabidopsis. Curr. Biol. 21: 1720-1726.

Pernisová, M., P. Klíma, J. Horák, M. Válková, J. Malbeck *et al.,* 2009 Cytokinins modulate auxin-induced organogenesis in plants via regulation of the auxin efflux. Proc. Natl. Acad. Sci. USA 106: 3609-3614.

Poethig, R. S., 1984 Cellular parameters of leaf morphogenesis in maize and tobacco, pp. 235-238 in *Contemporary Problems in Plant Anatomy*, edited by R. A. White and W. C. Dickinson. Academic Press, New York.

QTL Cartographer (http://statgen.ncsu.edu/qtlcart/)

R (http://www.r-project.org/)

Reinhardt, D., T. Mandel, and C. Kuhlemeier, 2000 Auxin Regulates the initiation and radial position of plant lateral organs. The Plant Cell 12: 507-518.

Rosin, F. M., J. K. Hart, H. T. Horner, P. J. Davies, and D. J. Hannapel, 2003 Overexpression of a *Knotted*-like homeobox gene of potato alters vegetative development by decreasing gibberellin accumulation. Plant Physiol. 132: 106-117.

Sang, Y., M.Wu, and D. Wagner, 2009 The Stem cell—Chromatin Connection. Seminars in Cell & Developmental Biology 20(9): 1143-1148.

Schauer, S. E., S. E. Jacobsen, D. W. Meinke, and A. Ray, 2002 DICER-LIKE1: Blind men and elephants in Arabidopsis development. Trends Plant Sci. 7: 487-491.

Schneeberger, R. G., P. W. Becraft, S. Hake, and M. Freeling, 1995 Ectopic expression of the Knox homeo box gene *Rough sheath1* alters cell fate in the maize leaf. Genes Dev. 9: 2292-2304.

Schoof, H., M. Lenhard, A. Haecker, K. F.X. Mayer, G. Jurgens *et al.*, 2000 The stem cell population of *Arabidopsis* shoot meristems is maintained by a regulatory loop between the *CLAVATA* and *WUSCHEL* genes. Cell 100: 635-644.

Sharman, B. C., 1942 Developmental anatomy of the shoot of *Zea mays.* Ann. Bot. 6: 245-283.

Shen, W., and L. Xu, 2009 Chromatin remodeling in stem cell maintenance in Arabidopsis thaliana. Molecular Plant 2: 600-609.

Smith, H. M. S. and S. Hake, 2003 The interaction of two homeobox genes, *BREVIPEDICELLUS* and *PENNYWISE*, regulates internode patterning in the Arabidopsis inflorescence. The Plant Cell 15: 1717-1727.

Sylvester, A. W., W. Z. Cande, and M. Freeling, 1990 Division and differentiation during normal and liguleless-1 maize leaf development. Development 110: 985-1000.

Taguchi-Shiobara, F., Z. Yuan, S. Hake, and D. Jackson, 2001 The *fasciated ear2* gene encodes a leucine-rich repeat receptor-like protein that regulates shoot meristem proliferation in maize. Genes Dev. 15: 2755-2766.

Takacs, E. M., J. Li, C. Du, L. Ponnala, D. Janick-Buckner *et al.*, 2012 Ontogeny of the maize shoot apical meristem. The Plant Cell 24: 3219-3234.

Thompson, A. M., J. Crants, P. S. Schnable, J. Yu, M. C. P. Timmermans et al., 2014 Genetic control of maize shoot apical meristem architecture. G3 (doi: 10.1534/g3.114.011940)

Tian, F., P. J. Bradbury, P. J. Brown, H. Hung, Q. Sun *et al.,* 2011 Genome-wide association study of leaf architecture in the maize nested association mapping population. Nature Genetics 43: 159-162.

Tsuda, K., Y. Ito, Y. Sato, and N. Kurata, 2011 Positive autoregulation of a KNOX gene is essential for shoot apical meristem maintenance in rice. The Plant Cell 23: 4368-4381.

Upadyayula, N., H. S. da Silva, M. O. Bohn, and T. R. Rocheford, 2006 Genetic and QTL analysis of maize tassel and ear inflorescence architecture. Theor. Appl. Genet. 112: 592-606.

Vanstraelen, M., and E. Benková, 2012 Hormonal interactions in the regulation of plant development. Ann. Rev. Cell Dev. Biol. 28: 463-487.

Vaucheret, H., F. Vazquez, P. Crété, and D. P. Bartel, 2004 The action of ARGONAUTE1 in the miRNA pathway and its regulation by the miRNA pathway are crucial for plant development. Genes Dev. 18: 1187-1197.

Vollbrecht, E., B. Veit, N. Sinha, and S. Hake, 1991 The developmental gene *Knotted-1* is a member of a maize homeobox gene family. Nature 350: 241-243.

Vollbrecht, E., L. Reiser, and S. Hake, 2000 Shoot meristem size is dependent on inbred background and presence of the maize homeobox gene, knotted1. Development 127: 3161-3172.

Wagner, Doris, 2003 Chromatin regulation of plant development. Curr. Opin. Plant Biol. 6: 20-28.

Wang, Y. and J. Li, 2008 Molecular basis of plant architecture. Ann. Rev. Plant Biol. 59: 253-279.

Woodward, J. B., N. D. Abeydeera, D. Paul, K. Phillips, M. Rapala-Kozik et al., 2010 A maize thiamine auxotroph is defective in shoot meristem maintenance. The Plant Cell 22: 3305-3317.

Yanai, O., E. Shani, K. Dolezal, P. Tarkowski, R. Sablowski *et al.,* 2005 Arabidopsis KNOXI proteins activate cytokinin biosynthesis. Curr. Biol. 15: 1566-1571.

Yang, X., H. Ma, P. Zhang, J. Yan, Y. Guo *et al.,* 2012 Characterization of QTL for oil content in maize kernel. Theor. Appl. Genet. 125: 1169-1179.

Yu, X., H. Wang, W. Zhong, J. Bai, P. Liu *et al.,* 2013 QTL mapping of leafy heads by genome resequencing in the RIL population of *Brassica rapa.* PLOS ONE 8(10): e76059.

Zhang, B. H., X. P. Pan, S. B. Cox, G. P. Cobb, and T. A. Anderson, 2006 Evidence that miRNAs are different from other RNAs. Cellular and Molecular Life Sciences 63: 246-254.

Table 1. SAM architecture trait summaries in NAM founders and two RIL subpopulations

NAM FOUNDERS (AND INDEPENDENT MEASURES OF B73 AND Mo17)

	B73/Mo17		NAM FOUNDERS			
MERISTEM TRAIT	B73	Mo17	MEAN	RANGE	P-VALUE[a]	HERITABILITY
HEIGHT (μm)	178	114	122	90 - 179	<0.001	0.84
ARC LENGTH (μm)	208	152	155	119 - 217	<0.001	0.82
WIDTH (μm)	142	158	140	116 - 169	<0.001	0.82
MIDPOINT WIDTH (μm)	117	131	116	99 - 138	<0.001	0.76
VOLUME (million μm^3)	4.55	1.99	2.13	0.94 - 4.96	<0.001	0.83
HEIGHT:WIDTH RATIO	1.25	0.72	0.87	0.70 - 1.25	<0.001	0.89
PLASTOCHRON INTERNODE (μm)	77	73	63	47 - 79	0.0019	0.35
CELL COUNT IN ARC	21.9	15.7	16.9	13.3 - 23.7	<0.001	0.55
ARC CELL SIZE (μm)	9.4	9.4	9.2	8.2 - 10.4	0.022	0.24

Z005 (CML277 x B73) POPULATION AND PARENTS

	PARENTS		RILs			
MERISTEM TRAIT	B73	CML277	MEAN	RANGE	P-VALUE[a]	HERITABILITY
HEIGHT (μm)	182	90	113	66 - 170	<0.0001	0.38
ARC LENGTH (μm)	212	120	144	97 - 206	<0.0001	0.35
WIDTH (μm)	147	126	134	103 - 169	<0.0001	0.32
MIDPOINT WIDTH (μm)	122	107	113	90 - 150	<0.0001	0.37
VOLUME (million μm^3)	5	10	2	5 - 4.3	<0.0001	0.33
HEIGHT:WIDTH RATIO	1.26	0.71	0.84	0.55 - 1.17	<0.0001	0.51
PLASTOCHRON INTERNODE (μm)	67	55	65	43 - 93	0.0156	0.07

Z024 (P39 x B73) POPULATION AND PARENTS

	PARENTS		RILs			
MERISTEM TRAIT	B73	P39	MEAN	RANGE	P-VALUE[a]	HERITABILITY
HEIGHT (μm)	182	173	164	93 - 225	<0.0001	0.44
ARC LENGTH (μm)	212	211	200	122 - 265	<0.0001	0.44
WIDTH (μm)	147	165	156	124 - 192	<0.0001	0.42
MIDPOINT WIDTH (μm)	122	145	132	103 - 169	<0.0001	0.53
VOLUME (million μm^3)	5.01	4.68	4.24	1.1 - 8.6	<0.0001	0.39
HEIGHT:WIDTH RATIO	1.26	1.04	1.05	0.67 - 1.53	<0.0001	0.56
PLASTOCHRON INTERNODE (μm)	67	76	73	50 - 73	0.0246	0.06

[a]significance of the effect of genotype within the RIL population.

Table 2. Summary of SAM trait QTL.

	# OF QTL (+)[a]		RANGE OF PVE[b]		EFFECT RANGE[c]		MODEL PVE	
MERISTEM TRAIT	Z005	Z024	Z005	Z024	Z005	Z024	Z005	Z024
HEIGHT (µm)	3 (3)	2 (1)	8-14%	8-25%	5.5 - 7.2	7.9 - 14.3	0.43	0.25
ARC LENGTH (µm)	2 (2)	1 (0)	7-13%	28%	5.4 - 7.1	15.9	0.28	0.28
WIDTH (µm)	3 (3)	3 (0)	8-11%	8-13%	3.2 - 3.8	3.6 - 4.8	0.26	0.46
MIDPOINT WIDTH (µm)	3 (3)	5 (0)	8-12%	7-13%	2.8 - 3.5	3.3 - 4.8	0.34	0.56
VOLUME (million μm^3)	3 (3)	1 (0)	7-12%	23%	1.7 - 2.3	7.9	0.37	0.27
HEIGHT:WIDTH RATIO	2 (2)	4 (3)	12-25%	6-26%	.044 - .065	.043 - .086	0.39	0.39
P2P1 INTERNODE DIFF	1(1)	1(0)	14%	6%	3.5	2.6	0.18	0.07

[a]Numbers in parenthesis indicate QTL with positive effect in B73.

[b]Phenotypic Variation Explained

[c]Effect ranges shown are absolute values.

Table 3. Cloned SAM-related candidate genes located under QTL in the two RIL subpopulations.

Z005 (CML277 x B73) POPULATION	
SAM TRAIT QTL	SAM-RELATED GENES
height_2, arc_1, volume_2	knotted1, tb1, d8
midwidth_1	knotted1, dwarf8, knox8
height_1	rough sheath2
Z024 (P39 x B73) POPULATION	
midwidth_1	knox1
width_1	knox1, dwarf8
ratio_1	knox8
ratio_2	narrow sheath1

Table S1. Lines used in experiments

27 NAM FOUNDERS	CML277 RILs	P39 RILs	REPRESENTATIVE IBMRIL	F1 CROSSES AND INBREDS	TIME COURSE
B73	Z005E0001	Z024E0001	MO007	B97 x B73	CML277
B97	Z005E0005	Z024E0002	MO032	B97 x Mo17	Ms71
CML103	Z005E0007	Z024E0005	MO262	B97	B97
CML228	Z005E0008	Z024E0008	MO272	Hp301 x B73	Hp301
CML247	Z005E0010	Z024E0009	MO275	Hp301 x Mo17	NC358
CML277	Z005E0012	Z024E0010	MO311	Hp301	Oh43
CML322	Z005E0013	Z024E0011	MO322	IL14H x B73	IL14H
CML333	Z005E0015	Z024E0013	MO325	IL14H x Mo17	Oh7B
CML52	Z005E0016	Z024E0014	MO357	IL14H	CML61
CML69	Z005E0019	Z024E0015	MO369	Ms71 x B73	Ki14
Hp301	Z005E0020	Z024E0016		Ms71 x Mo17	CO255
IL14H	Z005E0021	Z024E0019		Ms71	CS405
Ki11	Z005E0022	Z024E0020		NC358 x B73	NC296
Ki3	Z005E0025	Z024E0021		NC358 x Mo17	P39
Ky21	Z005E0027	Z024E0022		NC358	Mo18W
M162W	Z005E0028	Z024E0023		Oh43 x B73	B73
M37W	Z005E0029	Z024E0024		Oh43 x Mo17	Mo17
Mo17	Z005E0032	Z024E0025		Oh43	
Mo18W	Z005E0033	Z024E0027		Oh7B x B73	
Ms71	Z005E0035	Z024E0028		Oh7B x Mo17	
NC350	Z005E0037	Z024E0029		Oh7B	
NC358	Z005E0039	Z024E0030		P39 x B73	
Oh43	Z005E0042	Z024E0033		P39 x Mo17	
Oh7B	Z005E0043	Z024E0034		P39	
P39	Z005E0044	Z024E0035		B73	
Tx303	Z005E0045	Z024E0036		Mo17	
Tzi8	Z005E0046	Z024E0037			
	Z005E0047	Z024E0038			
	Z005E0048	Z024E0040			
	Z005E0049	Z024E0041			
	Z005E0051	Z024E0042			
	Z005E0055	Z024E0043			
	Z005E0056	Z024E0044			
	Z005E0057	Z024E0045			
	Z005E0058	Z024E0046			
	Z005E0060	Z024E0047			
	Z005E0061	Z024E0048			
	Z005E0062	Z024E0049			

Z005E0063	Z024E0050
Z005E0066	Z024E0051
Z005E0068	Z024E0053
Z005E0069	Z024E0056
Z005E0074	Z024E0057
Z005E0075	Z024E0058
Z005E0079	Z024E0059
Z005E0080	Z024E0060
Z005E0081	Z024E0061
Z005E0082	Z024E0062
Z005E0083	Z024E0063
Z005E0084	Z024E0068
Z005E0085	Z024E0069
Z005E0087	Z024E0071
Z005E0088	Z024E0072
Z005E0090	Z024E0073
Z005E0091	Z024E0074
Z005E0092	Z024E0075
Z005E0093	Z024E0076
Z005E0094	Z024E0077
Z005E0095	Z024E0078
Z005E0096	Z024E0079
Z005E0097	Z024E0080
Z005E0099	Z024E0081
Z005E0100	Z024E0082
Z005E0102	Z024E0084
Z005E0104	Z024E0085
Z005E0105	Z024E0086
Z005E0106	Z024E0088
Z005E0107	Z024E0089
Z005E0108	Z024E0090
Z005E0109	Z024E0091
Z005E0110	Z024E0092
Z005E0111	Z024E0093
Z005E0112	Z024E0094
Z005E0113	Z024E0095
Z005E0114	Z024E0096
Z005E0115	Z024E0097
Z005E0116	Z024E0098
Z005E0117	Z024E0099
Z005E0118	Z024E0100

Z005E0119	Z024E0101
Z005E0121	Z024E0102
Z005E0122	Z024E0103
Z005E0123	Z024E0107
Z005E0124	Z024E0108
Z005E0126	Z024E0110
Z005E0127	Z024E0111
Z005E0128	Z024E0112
Z005E0129	Z024E0113
Z005E0130	Z024E0115
Z005E0131	Z024E0116
Z005E0133	Z024E0117
Z005E0134	Z024E0118
Z005E0135	Z024E0119
Z005E0136	Z024E0120
Z005E0137	Z024E0121
Z005E0138	Z024E0122
Z005E0139	Z024E0123
Z005E0141	Z024E0124
Z005E0142	Z024E0126
Z005E0144	Z024E0127
Z005E0145	Z024E0128
Z005E0146	Z024E0129
Z005E0147	Z024E0130
Z005E0148	Z024E0131
Z005E0149	Z024E0132
Z005E0150	Z024E0133
Z005E0151	Z024E0135
Z005E0154	Z024E0136
Z005E0155	Z024E0137
Z005E0156	Z024E0141
Z005E0158	Z024E0142
Z005E0159	Z024E0144
Z005E0160	Z024E0145
Z005E0162	Z024E0147
Z005E0163	Z024E0152
Z005E0164	Z024E0157
Z005E0166	Z024E0159
Z005E0168	Z024E0163
Z005E0169	Z024E0164
Z005E0170	Z024E0165

Z005E0171	Z024E0166
Z005E0172	Z024E0167
Z005E0173	Z024E0168
Z005E0174	Z024E0170
Z005E0175	Z024E0172
Z005E0176	Z024E0180
Z005E0179	Z024E0182
Z005E0181	Z024E0183
Z005E0183	Z024E0186
Z005E0184	Z024E0188
Z005E0185	Z024E0189
Z005E0186	Z024E0191
Z005E0190	Z024E0192
Z005E0192	Z024E0193
Z005E0193	Z024E0195
Z005E0195	Z024E0196
Z005E0196	Z024E0199
Z005E0197	
Z005E0198	
Z005E0199	

Table S2. QTLs across populations.

QTL	CHR	LOD	PVE[a]	EFFECT[b]	bp RANGE[c]	bp DISTANCE	# TOTAL GENES	# EXPRESSED GENES	COINCIDENT QTLs IN POP	COINCIDENT CROSS-POP
Z005_height_2	1	3.7	7.9	5.5	263603731 - 276209661	12605930	315	162	volume, arc, midwidth, width	Z024:ratio
Z005_arc_1	1	3.3	7.3	5.4	263603731 - 279682238	16078507	423	216	volume, height, midwidth, width	Z024:ratio
Z005_volume_2	1	3.4	7.7	1.87e5	263603731 - 279682238	16078507	423	216	height, arc, midwidth, width	Z024:ratio
Z005_midwidth_1	1	5.5	12.0	3.5	263603731 - 285650152	22046421	589	287	volume, height, arc, width	Z024:ratio
Z005_width_1	1	4.6	10.9	3.8	273305618 - 281206812	7901194	243	123	volume, height, arc, midwidth	Z024:ratio
Z005_ratio_1	1	5.3	11.8	0.044	64239480 - 107187523	42948043	662	266	height, volume	
Z005_volume_1	1	3.1	6.9	1.71e5	88998955 - 148458078	59459123	540	176	ratio, height	
Z005_height_1	1	3.7	8.7	5.6	88998955 - 195557990	106559035	1321	472	ratio, volume	
Z005_ratio_2	3	10.6	25.1	0.065	12132193 - 21368486	9236293	233	78	volume, arc, height	

Z005_p2p1diff_1	3	6.7	14.2	3.5	1298537 - 6739219	5673605	199	108		
Z005_width_2	3	3.3	7.6	3.2	216417210 - 223179497	6762287	231	105		
Z005_arc_2	3	5.1	13.2	7.1	8300032 - 21368486	13068454	331	124	volume, height, ratio	
Z005_height_3	3	5.9	14.2	7.2	8300032 - 21368486	13068454	331	124	volume, arc, ratio	
Z005_volume_3	3	4.6	12.3	2.30e5	8300032 - 21368486	13068454	331	124	arc, height, ratio	
Z005_midwidth_2	6	5.6	12.2	3.4	143696195 - 148634319	4938124	129	64	width	
Z005_width_3	6	3.9	8.7	3.3	143696195 - 154345567	10649372	324	151	midwidth	
Z005_midwidth_3	9	3.5	8.0	2.8	114072155 - 129011584	14939429	330	130		
Z024_midwidth_1	1	5.6	10.2	-4.2	238343143 - 259375688	21032545	470	215	width	
Z024_width_1	1	5.5	12.8	-4.8	253029622 - 269324476	16294854	416	205	midwidth	
Z024_ratio_1	1	3.2	6.5	0.043	281206812 - 289547937	8341125	236	117		Z005:vol,ht, arc,mw,wd; IBM:arc,ht
Z024_height_1	2	3.8	8.1	7.9	47158891 - 93130728	45971837	514	179	ratio	

Z024_ratio_2	2	5.7	11.6	0.056	48109181 - 189447059	141337878	1797	615	height
Z024_arc_1	4	11.2	27.9	-15.9	178580488 - 188385744	9805256	269	136	volume, height, midwidth, ratio
Z024_volume_1	4	9.4	23.2	-7.95e5	178580488 - 188385744	9805256	269	136	arc, height, midwidth, ratio
Z024_midwidth_2	4	6.6	13.0	-4.8	178889832 - 184547096	5657264	137	73	arc, volume, height, ratio
Z024_p2p1diff_1	4	2.9	6.2	-2.6	178889832 - 184547096	5657264	137	73	arc, volume, height, midwidth, ratio
Z024_height_2	4	10.4	25.3	-14.3	178889832 - 188385744	9495912	255	129	arc, volume, midwidth, ratio
Z024_ratio_4	4	10.3	25.8	-0.086	187355764 - 230190074	42834310	800	329	arc, volume, height, midwidth
Z024_ratio_3	4	3.1	6.1	0.045	66909481 - 144840177	77930696	721	257	
Z024_midwidth_3	5	5.7	13.1	-4.6	205308574 - 209682546	4373972	166	73	width
Z024_width_2	5	3.4	9.3	-4.0	205308574 - 209682546	4373972	166	73	midwidth
Z024_midwidth_4	8	3.5	6.5	-3.3	115134656 - 119831079	4696423	108	47	

Z024_width_3	10	3.5	7.5	-3.6	139978756 - 144469845	4491089	170	100	midwidth
Z024_midwidth_5	10	3.7	7.2	-3.4	139978756 - 146999603	7020847	170	100	width
								AVERAGE: 175	
								TOTAL: 3323	

[a]Phenotypic Variation Explained, as percent

[b]Effect is substitution of CML277 (Z005) or P39 (Z024) allele with B73.

[c]QTL intervals calculated by 1-LOD drop.

Table S3. Candidate SAM genes overlapping with QTL locations

GENE	RICE ANNOTATION	ARABIDOPSIS ANNOTATION	MAIZE (KNOWN GENES)
GRMZM2G003509	START domain	Homeobox-leucine zipper/lipid-binding START domain	NA
GRMZM2G004696	OsIAA1-Auxin-responsive Aux/IAA gene	AUX/IAA transcriptional regulator	NA
GRMZM2G014154	histidine-containing phosphotransfer	histidine-containing phosphotransfer factor 5	NA
GRMZM2G017087	Homeobox domain	KNOTTED-like from Arabidopsis thaliana	knotted1
GRMZM2G028151	AP2-like ethylene-responsive TF AINTEGUMENTA	Integrase-type DNA-binding superfamily	NA
GRMZM2G044902	DUF260 domain	LOB domain-containing 37	NA
GRMZM2G045678	dof zinc finger domain	cycling DOF factor 2	NA
GRMZM2G055204	ethylene-responsive transcription factor	related to AP2 4	NA
GRMZM2G058158	ZOS9-03-C2H2 zinc finger	VEFS-Box of polycomb	NA
GRMZM2G059392	uncharacterized PA4923	Putative lysine decarboxylase	NA
GRMZM2G069028	homeobox domain	Homeodomain-like superfamily	narrow sheath1
GRMZM2G071025	SNF2 N-terminal domain	chromatin remodeling 1	NA
GRMZM2G074267	auxin efflux carrier component	Auxin efflux carrier	NA
GRMZM2G075117	cyclin	CYCLIN D4	NA
GRMZM2G079957	OsIAA31-Auxin-responsive Aux/IAA gene	AUX/IAA transcriptional regulator	NA
GRMZM2G084462	IPP transferase	isopentenyltransferase 5	NA
GRMZM2G086869	haloacid dehalogenase-like hydrolase	Haloacid dehalogenase-like hydrolase (HAD) superfamily	NA
GRMZM2G090217	WD domain; G-beta repeat domain	Transducin/WD40 repeat-like superfamily	NA
GRMZM2G096171	OsRR2 type-A response regulator	response regulator 3	NA
GRMZM2G108865	dof zinc finger domain	DOF zinc finger 1	NA

GRMZM2G117940	GASR1-Gibberellin-regulated GASA/GAST/Snakin	Gibberellin-regulated	NA
GRMZM2G125976	homeodomain	POX (plant homeobox)	NA
GRMZM2G129147	growth-regulating factor	growth-regulating factor 5	NA
GRMZM2G135447	Homeobox domain	KNOTTED-like from Arabidopsis thaliana	knox8
GRMZM2G141955	YABBY domain	plant-specific transcription factor YABBY	NA
GRMZM2G142179	AP2 domain	cytokinin response factor 4	NA
GRMZM2G144744	GRAS transcription factor domain	GRAS transcription factor	dwarf8
GRMZM2G151223	histidine kinase	CHASE domain histidine kinase	NA
GRMZM2G159285	OsIAA13-Auxin-responsive Aux/IAA gene	indoleacetic acid-induced 16	NA
GRMZM2G163761	homeobox domain	BEL1-like homeodomain 11	kn-interacting1
GRMZM2G171702	auxin efflux carrier component	Auxin efflux carrier	NA
GRMZM2G171822	AGC PVPK like kin82y.20	Protein kinase superfamily	barren inf2
GRMZM2G403620	MYB transcription factor	myb-like HTH transcriptional regulator	rough sheath2
GRMZM2G412524	AGC PVPK like kin82y.19	KCBP-interacting kinase	NA
GRMZM2G423337	START domain	Homeobox-leucine zipper/lipid-binding START domain	NA
GRMZM2G430522	CUP-SHAPED COTYLEDON3	NAC (No Apical Meristem) domain transcriptional regulator	NA
GRMZM2G457370	retrotransposon; unclassified	Stabilizer of iron transporter SufD/Polynucleotidyl transferase	NA

Table S4. Correlation values for SAM traits with adult plant traits

Z005: CML277 x B73	HEIGHT	ARC LENGTH	WIDTH	MIDPOINT WIDTH	VOLUME	HEIGHT:WIDTH RATIO	P2-P1 DIFFERENCE
DAYS TO SILK	**-0.22**	-0.13	-0.15	**-0.17**	-0.11	-0.13	-0.03
DAYS TO TASSEL	**-0.22**	-0.12	-0.14	-0.16	-0.08	-0.14	-0.02
GDD TO SILK	**-0.19**	**-0.17**	**-0.18**	-0.13	-0.12	**-0.18**	-0.09
GDD TO TASSEL	**-0.19**	-0.12	-0.13	-0.13	-0.07	-0.13	-0.04
UPPER LEAF ANGLE	**0.18**	**-0.17**	-0.12	**0.17**	0.09	-0.11	-0.31
MIDDLE LEAF ANGLE	0.08	**-0.21**	**-0.19**	0.01	-0.13	**-0.17**	**-0.29**
COB DIAMETER	**0.25**	-0.05	0.00	**0.18**	0.07	0.05	**-0.21**
EAR DIAMETER	**0.27**	0.04	0.08	0.16	0.07	0.12	**-0.11**
EAR LENGTH	0.16	**0.21**	**0.22**	0.15	0.12	**0.25**	0.14
SEED SET LENGTH	0.14	0.12	0.14	0.12	0.13	**0.17**	0.05
EAR ROW NUMBER	**0.31**	0.08	0.12	**0.23**	0.14	0.15	-0.08
TOTAL KERNEL VOLUME	**0.27**	0.16	**0.19**	**0.23**	0.01	**0.22**	0.02
EAR WEIGHT	**0.27**	0.10	0.13	**0.18**	0.11	**0.18**	-0.04
EAR RANK NUMBER	0.06	**0.21**	**0.20**	0.05	0.05	**0.19**	**0.19**
Z024: P39 x B73							
DAYS TO SILK	**-0.37**	**-0.17**	**-0.20**	**-0.35**	-0.16	**-0.18**	0.02
DAYS TO TASSEL	**-0.36**	**-0.20**	**-0.22**	**-0.32**	-0.08	**-0.21**	-0.01
GDD TO SILK	**-0.38**	**-0.19**	**-0.22**	**-0.36**	**-0.17**	**-0.19**	0.00
GDD TO TASSEL	**-0.38**	**-0.25**	**-0.28**	**-0.35**	-0.13	**-0.26**	-0.07
EAR HEIGHT	**-0.26**	-0.10	-0.13	**-0.23**	-0.07	-0.13	0.04
LEAF LENGTH	**-0.24**	**-0.27**	**-0.27**	**-0.17**	0.04	**-0.25**	**-0.17**
LEAF WIDTH	-0.09	**-0.39**	**-0.38**	-0.12	-0.13	**-0.36**	**-0.38**
COB WEIGHT	-0.15	**-0.22**	**-0.23**	-0.16	-0.03	**-0.19**	**-0.17**

Values are the correlation coefficient r

To be considered significant (bold values), correlations had to be significant (at $p<0.05$) for at least half of the replications as well as for the overall mean (shown here).

Figure 1. SAM phenotypes examined. A-C: Median longitudinal sections of the SAM in inbred lines B73 (**A**), CML277 (**B**), and P39 (**C**), indicating measurements taken (**A**). Compared to B73, P39 is similar in height but wider, with a height:width ratio close to 1 (versus 1.26 in B73). CML277 is dramatically shorter than B73 and only slightly less wide, resulting in meristems typically shorter than their width (average ratio 0.71). Scale bar = 100μm.

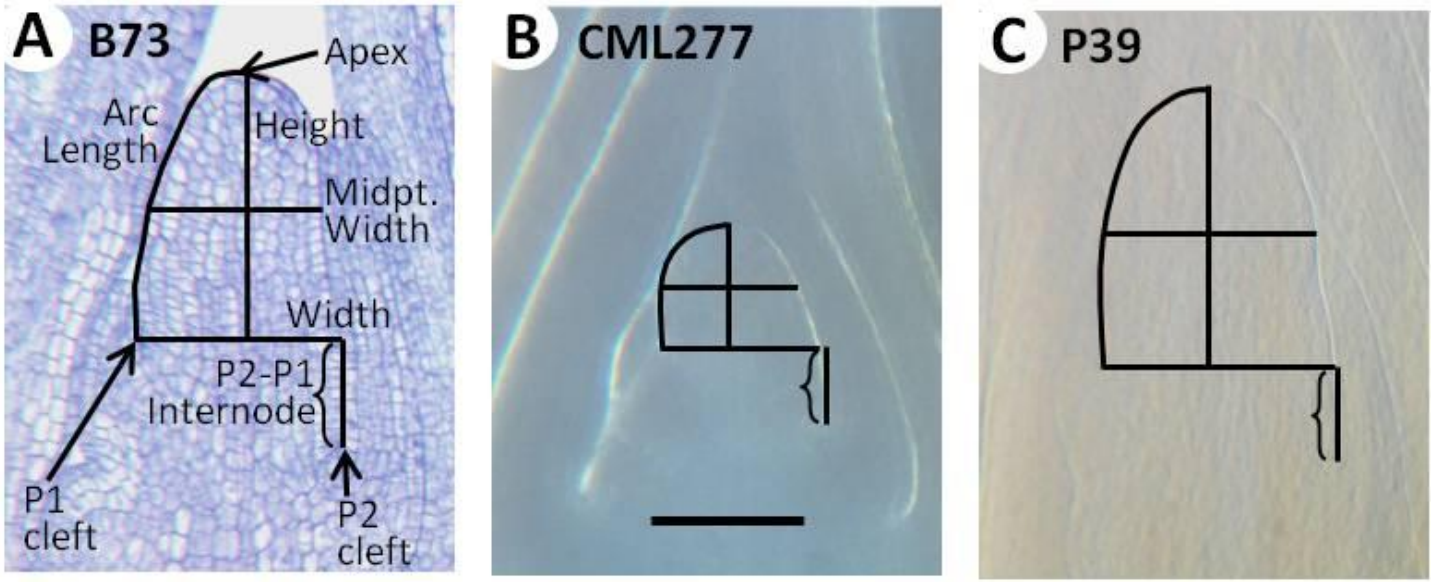
A
B73
Apex
Arc
Length
Height
Midpt.
Width
Width
P2-P1
Internode
P1
cleft
P2
cleft
B
CML277
C
P39

Figure 2. Distribution of main SAM traits across populations. Four inbred parental lines and distributions for line means of their populations are shown for three traits. Though B73 and P39 are both very tall, P39 is much wider, leading to distinct ratios of SAM height:width. Despite their extreme values for SAM height and width relative to the other NAM founders, populations created from P39 and CML277 still showed transgressive segregation for all traits when crossed to B73.

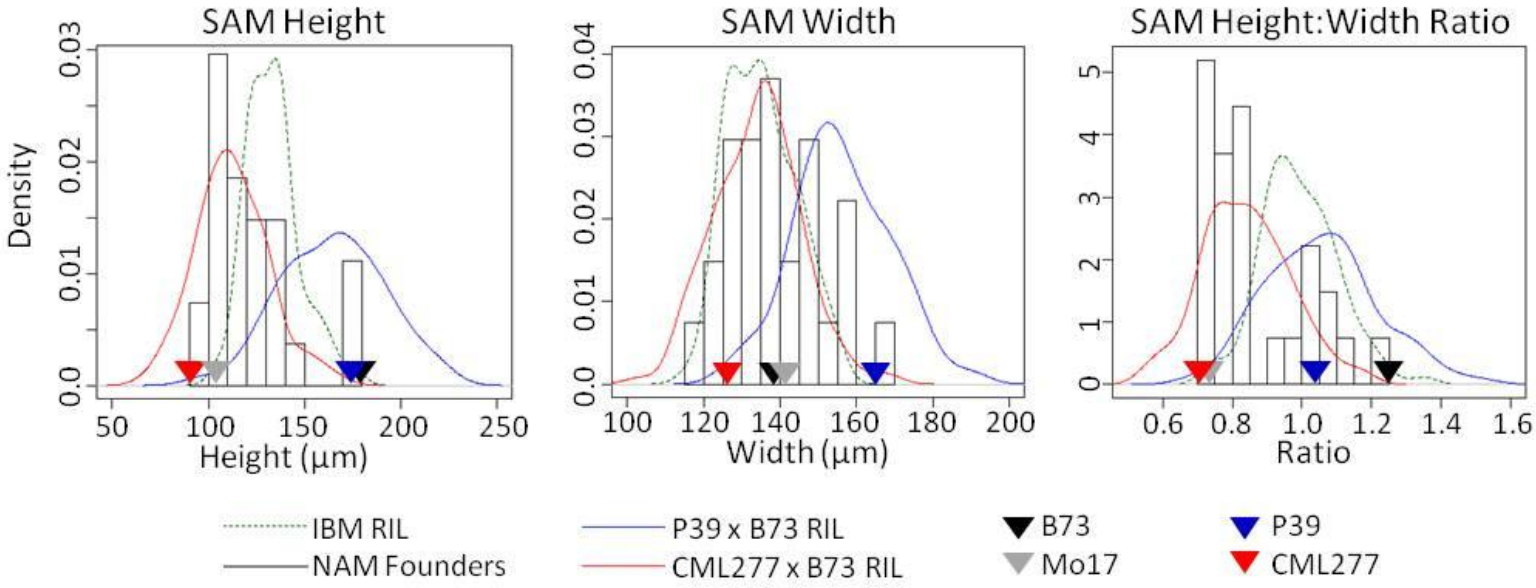
SAM Height
Density
0.0
0.01
0.02
0.03
50
100
150
200
250
Height (µm)
SAM Width
0.0
0.01
0.02
0.03
0.04
100
120
140
160
180
200
Width (µm)
SAM Height:Width Ratio
0
1
2
3
4
5
0.6
0.8
1.0
1.2
1.4
1.6
Ratio
IBM RIL
NAM Founders
P39 x B73 RIL
CML277 x B73 RIL
B73
Mo17
P39
CML277

Figure 3. Presence of heterosis in NAM founder x B73/Mo17 crosses. Each of eight inbred NAM founder lines were crossed to B73 and Mo17 and examined for outside-parent heterosis. Significant cases are shown starred and highlighted. Many lines showed heterosis when crossed to Mo17, for most traits. Only P39 exhibited heterosis when crossed to B73, indicating they contain unique alleles contributing to their large SAM size. Most inbred x B73 crosses showed near-midparent values.

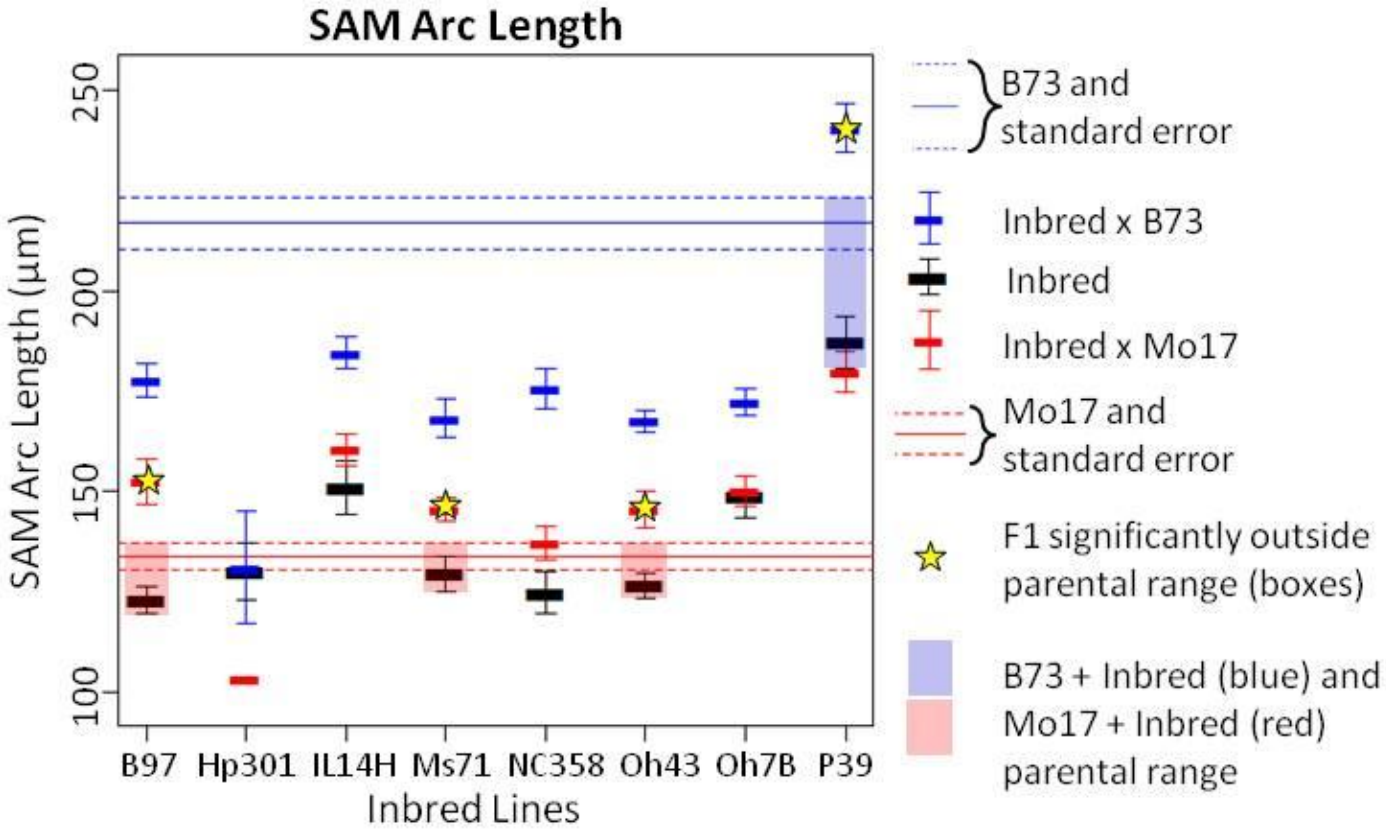
SAM Arc Length
SAM Arc Length (µm)
250
200
150
100
B97
Hp301
IL14H
Ms71
NC358
Oh43
Oh7B
P39
Inbred Lines
B73 and standard error
Inbred x B73
Inbred
Inbred x Mo17
Mo17 and standard error
F1 significantly outside parental range (boxes)
B73 + Inbred (blue) and Mo17 + Inbred (red) parental range

Figure 4. SAM QTL. QTL across 10 chromosomes in two populations as well as previously mapped IBMRIL for six traits. Height, arc length, and volume are shown in blue/darker; width and midpoint width are red/lighter; ratio is black. QTL are not coincident across populations. In contrast to previous studies, some QTL are significant for both height and width traits.

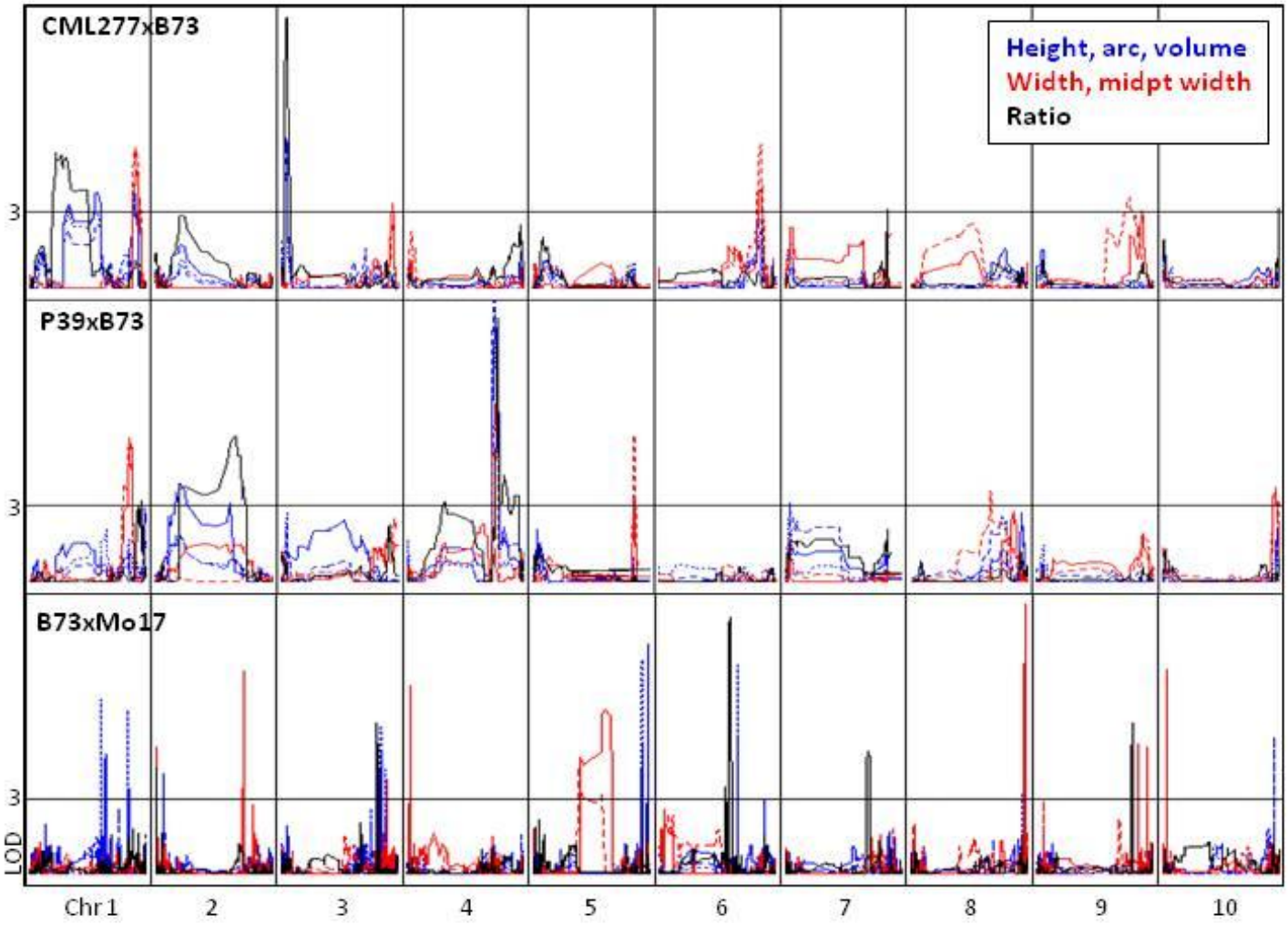
CML277xB73
P39xB73
B73xMo17
Height, arc, volume
Width, midpt width
Ratio
3
3
3
LOD
Chr 1
2
3
4
5
6
7
8
9
10

Figure 5. Correlations among SAM and adult plant traits. Adult plant traits significantly correlated with one or more of seven SAM traits in the CML277 (**A**) and P39 (**B**) populations. SAM width was related to flowering time and some yield measures, while SAM height was more related to leaf traits. All correlation values were moderate to weak (R^2 around 0.3), but robust, as correlations were required to be significant for the adult plant trait mean score as well as at least half of the individual replication:environment combinations.

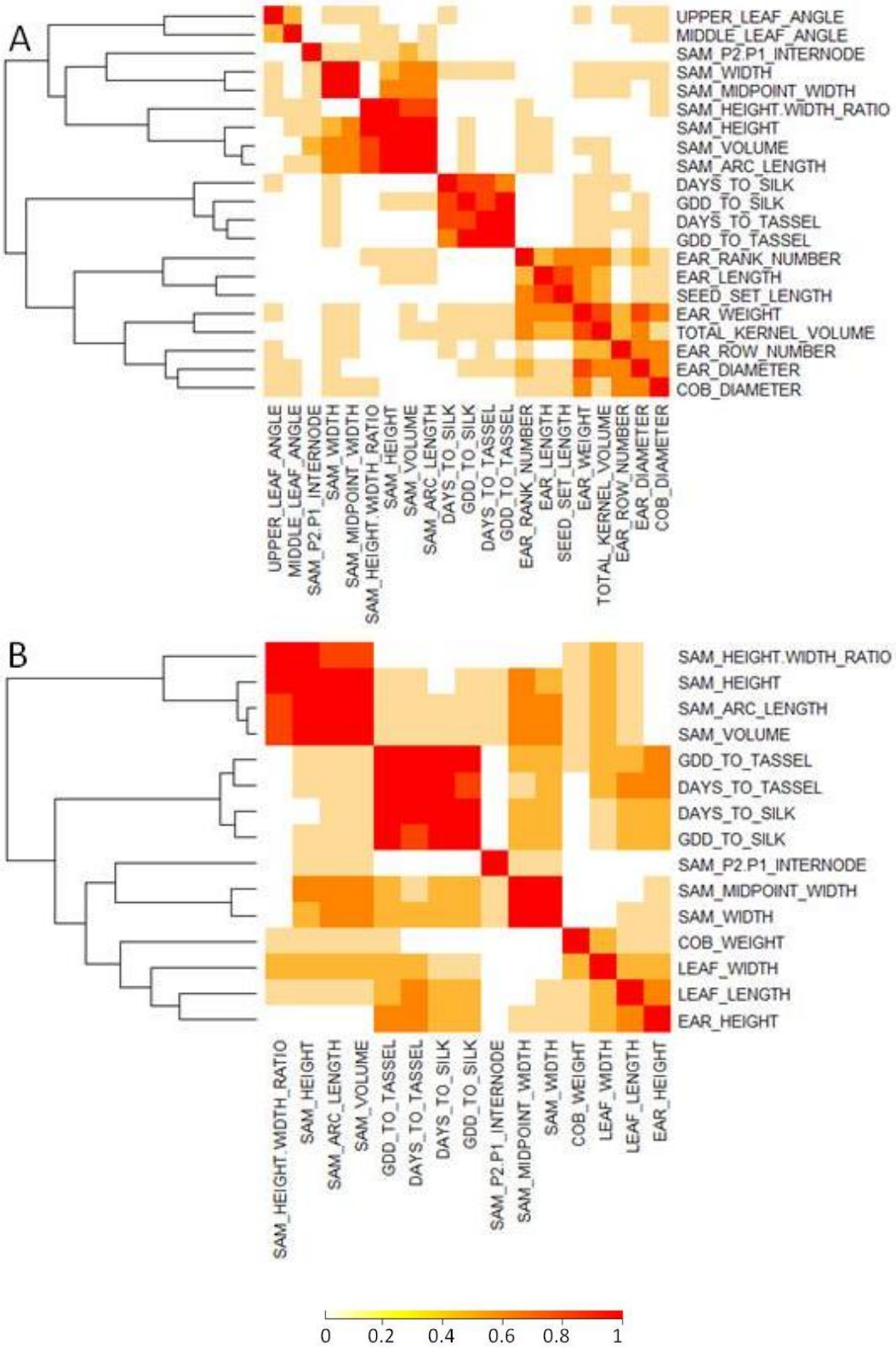
A
UPPER_LEAF_ANGLE
MIDDLE_LEAF_ANGLE
SAM_P2.P1_INTERNODE
SAM_WIDTH
SAM_MIDPOINT_WIDTH
SAM_HEIGHT.WIDTH_RATIO
SAM_HEIGHT
SAM_VOLUME
SAM_ARC_LENGTH
DAYS_TO_SILK
GDD_TO_SILK
DAYS_TO_TASSEL
GDD_TO_TASSEL
EAR_RANK_NUMBER
EAR_LENGTH
SEED_SET_LENGTH
EAR_WEIGHT
TOTAL_KERNEL_VOLUME
EAR_ROW_NUMBER
EAR_DIAMETER
COB_DIAMETER
B
SAM_HEIGHT.WIDTH_RATIO
SAM_HEIGHT
SAM_ARC_LENGTH
SAM_VOLUME
GDD_TO_TASSEL
DAYS_TO_TASSEL
DAYS_TO_SILK
GDD_TO_SILK
SAM_P2.P1_INTERNODE
SAM_MIDPOINT_WIDTH
SAM_WIDTH
COB_WEIGHT
LEAF_WIDTH
LEAF_LENGTH
EAR_HEIGHT
0
0.2
0.4
0.6
0.8
1

Figure S1. SAM phenotype distributions. Four inbred parental lines and distributions for line means of their populations for remaining traits. SAM height, arc length, and volume show similar distributions; SAM width and midpoint width are highly similar as well. P2-P1 internode is most similar to SAM widths, while SAM heigh:width ratio captures largely unique information that is slightly related to SAM volume. These similarities reflect correlations observed among the traits. SAM width-related traits have very normal distributions, while height-related traits seem to be nearly bi-modal due to a small number of higher values.

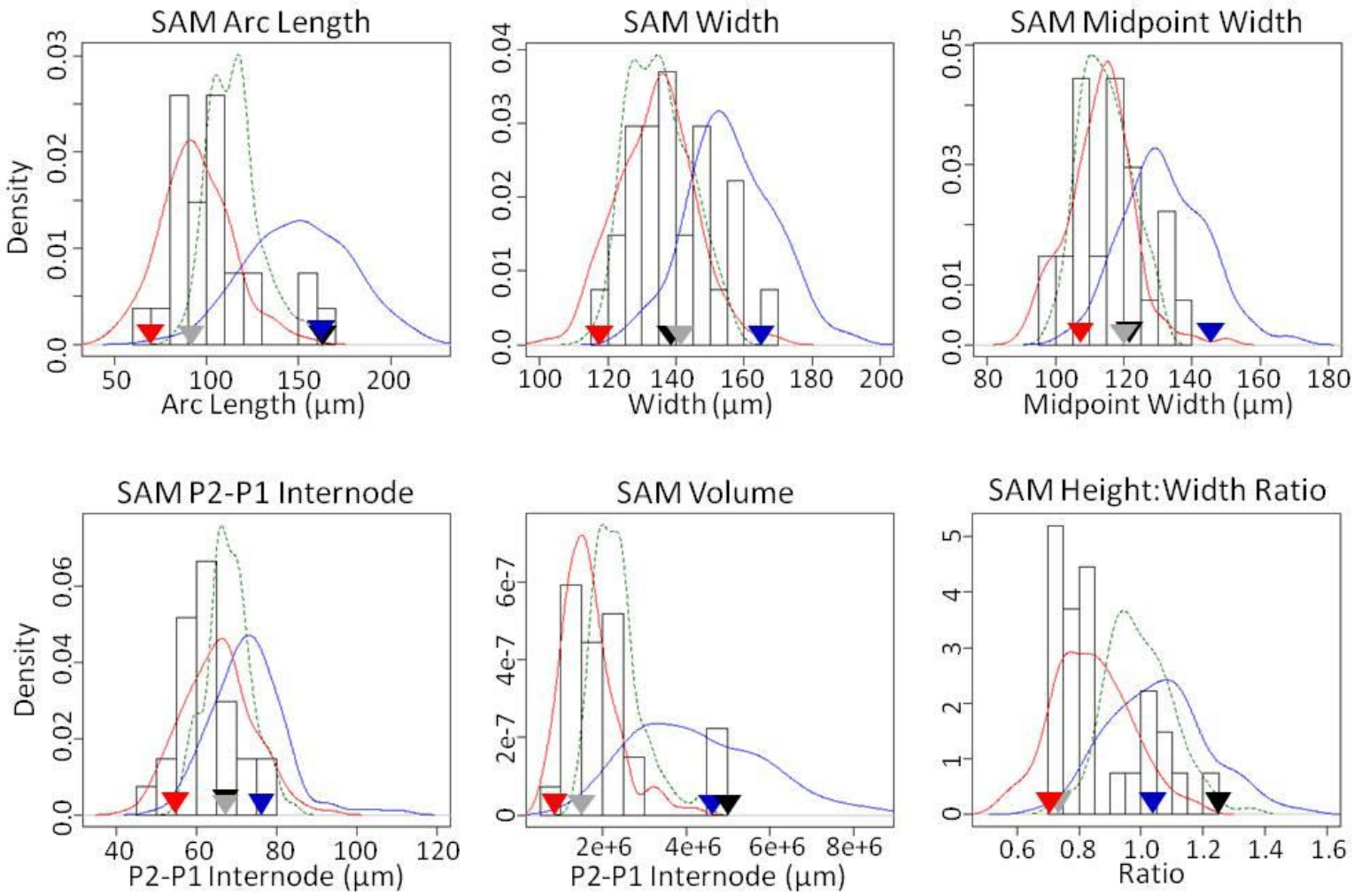
SAM Arc Length
Density
0.0
0.01
0.02
0.03
50
100
150
200
Arc Length (µm)
SAM Width
0.0
0.01
0.02
0.03
0.04
100
120
140
160
180
200
Width (µm)
SAM Midpoint Width
0.0
0.01
0.03
0.05
80
100
120
140
160
180
Midpoint Width (µm)
SAM P2-P1 Internode
Density
0.0
0.02
0.04
0.06
40
60
80
100
120
P2-P1 Internode (µm)
SAM Volume
0
2e-7
4e-7
6e-7
2e+6
4e+6
6e+6
8e+6
P2-P1 Internode (µm)
SAM Height:Width Ratio
0
1
2
3
4
5
0.6
0.8
1.0
1.2
1.4
1.6
Ratio

Figure S2. F1 SAM size. Each of eight inbred NAM founder lines were crossed to B73 and Mo17 and examined for outside-parent heterosis. Significant cases are shown starred and highlighted. Many lines showed heterosis when crossed to Mo17, for most traits. Only P39 exhibited heterosis when crossed to B73, indicating they contain unique alleles contributing to their large SAM size. Most inbred x B73 crosses showed near-midparent values.

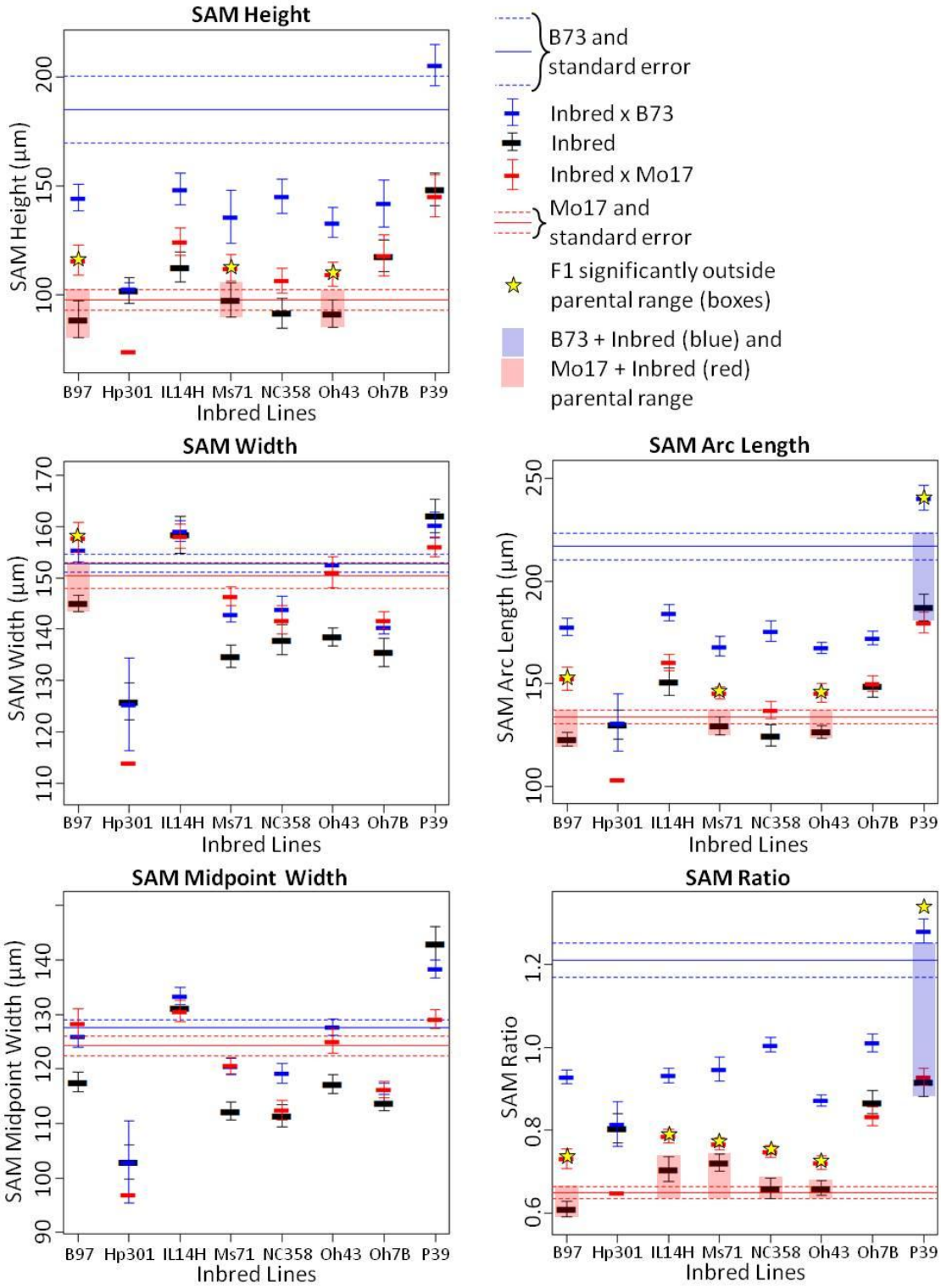
SAM Height
SAM Height (µm)
100
150
200
B97 Hp301 IL14H Ms71 NC358 Oh43 Oh7B P39
Inbred Lines
B73 and standard error
Inbred x B73
Inbred
Inbred x Mo17
Mo17 and standard error
F1 significantly outside parental range (boxes)
B73 + Inbred (blue) and Mo17 + Inbred (red) parental range
SAM Width
SAM Width (µm)
110
120
130
140
150
160
170
B97 Hp301 IL14H Ms71 NC358 Oh43 Oh7B P39
Inbred Lines
SAM Arc Length
SAM Arc Length (µm)
100
150
200
250
B97 Hp301 IL14H Ms71 NC358 Oh43 Oh7B P39
Inbred Lines
SAM Midpoint Width
SAM Midpoint Width (µm)
90
100
110
120
130
140
B97 Hp301 IL14H Ms71 NC358 Oh43 Oh7B P39
Inbred Lines
SAM Ratio
SAM Ratio
0.6
0.8
1.0
1.2
B97 Hp301 IL14H Ms71 NC358 Oh43 Oh7B P39
Inbred Lines

Comprehensive Bibliography

Axtell, M. J., 2013 Classification and comparison of small RNAs from plants. Ann. Rev. Plant Biol. 64: 137-159.

Balint-Kurti, P. J., J. C. Zwonitzer, R. J. Wisser, M. L. Carson, M. A. Oropeza-Rosas *et al.,* 2007 Precise mapping of quantitative trait loci for resistance to southern leaf blight, caused by *Cochliobolus heterostrophus* race O, and flowering time using advanced intercross maize lines. Genetics 176: 645-657.

Barton, M. K., 2010 Twenty years on: The inner workings of the shoot apical meristem, a developmental dynamo. Dev. Biol. 341: 95-113.

Bauer, P., M. Lubkowitz, R. Tyers, K. Nemoto, R. B. Meeley *et al.,* 2004 Regulation and a conserved intron sequence of liguleless3/4 Knox Class-I homeobox genes in grasses. Planta 219: 359-368.

Bauman, L. E., J. S. Sinsheimer, E. M. Sobel, and K. Lange 2008 Mixed effects models for quantitative trait loci mapping with inbred strains. Genetics 180: 1743-1761.

Baurle, I. and T. Laux, 2005 Regulation of *WUSCHEL* transcription in the stem cell niche of the *Arabidopsis* shoot meristem. The Plant Cell 17: 2271-2280.

Beavis, W. D., 1998 QTL Analyses: Power, Precision, and Accuracy, pp. 145-161 in *Molecular dissection of complex traits*, edited by A. H. Paterson. CRC Press, Boca Raton, FL.

Beavis, W. D., D. Grant, M. Albertsen, and R. Fincher, 1991 Quantitative trait loci for plant height in four maize populations and their associations with qualitative genetic loci. Theor Appl Genet 83: 141-145.

Belles-Boix, E., O. Hamant, S. M. Witiak, H. Morin, J. Traas *et al.,* 2006 *KNAT6:* An *Arabidopsis* homeobox gene involved in meristem activity and organ separation. The Plant Cell 18: 1900-1907.

Berke, T. G. and T. R. Rocheford, 1999 Quantitative trait loci for tassel traits in maize. Crop Sci 39: 1439-1443.

Bernardo, R., 2010 *Breeding for quantitative traits in plants*. Stemma Press, Woodbury, MN.

Bernier, G., 1997 Growth changes in the shoot apex of *Sinapis alba* during transition to flowering. J. Exp. Bot. 48: 1071-1077.

Bolduc, N., R. G. Tyers, M. Freeling, and S. Hake. 2014 Unequal redundancy in maize knotted1 homeobox genes. Plant Physiol. 164: 229-238.

Bommert, P., B. I. Je, A. Goldschmidt, and D. Jackson, 2013 The maize Ga gene *COMPACT PLANT2* functions in CLAVATA signaling to control shoot meristem size. Nature 502: 555-558.

Brown, P. J., N. Upadyayula, G. S. Mahone, F. Tian, P. J. Bradbury *et al.*, 2011 Distinct genetic architectures for male and female inflorescence traits of maize. PLOS Genetics 7: e1002383.

Buckler, E. S., J. B. Holland, P. J. Bradbury, C. B. Acharya, P. J. Brown *et al.*, 2009 The genetic architecture of maize flowering time. Science 325: 714-718.

Callos, J. D., M. DiRado, B. Xu, F. J. Behringer, B. M. Link et al., 1994 The *forever young* gene encodes an oxidoreductase required for proper development of the *Arabidopsis* vegetative shoot apex. Plant J. 6: 835-847.

Causse, M., P. Duffe, M.C. Buret, R. Damidaux, D. Zamir *et al.,* 2004 A genetic map of candidate genes and QTLs involved in tomato fruit size and composition. J. Exp. Bot. 55: 1671-1685.

Chitwood, D. H., R. Kumar, L. R. Headland, A. Ranjan, M. F. Covington *et al.*, 2013 A quantitative genetic basis for leaf morphology in a set of precisely defined tomato introgression lines. The Plant Cell 25: 2465-2481.

Chuck, G. and S. Hake, 2005 Regulation of developmental transitions. Curr. Opin.Plant Biol. 8: 67-70.

Clark, R. M., T. N. Wagler, P. Quijada, and J. Doebley, 2006 A distant upstream enhancer at the maize domestication gene *tb1* has pleiotropic effects on plant and inflorescent architecture. Nature Genetics 38: 594-597.

Clark, S. E., M. P. Running, and E. M. Meyerowitz, 1993 *CLAVATA1*, a regulator of meristem and flower development in *Arabidopsis.* Development 119: 397-418.

Clark, S. E., M. P. Running, and E. M. Meyerowitz, 1995 *CLAVATA3* is a specific regulator of shoot and floral meristem development affecting the same processes as *CLAVATA1*. Development 121: 2057-2067.

Clark, S. E., S. E. Jacobsen, J. Z. Levin, and E. M. Meyerowitz, 1996 The CLAVATA and SHOOT MERISTEMLESS loci competitively regulate meristem activity in *Arabidopsis*. Development 122: 1567-1575.

Coles, N. D., C. T. Zila, and J. B. Holland, 2011 Allelic effect variation at key photoperiod response quantitative trait loci in maize. Crop Science 51: 1036-1049.

Cook, J. P., M. D. McMullen, J. B. Holland, F. Tian, P. Bradbury *et al.*, 2012 Genetic architecture of maize kernel composition in the nested association mapping and inbred association panels. Plant Physiol 158: 824-834.

Courtois, B., N. Ahmadi, F. Khowaja, A. H. Price, J. F. Rami *et al.*, 2009 Rice root genetic architecture: meta-analysis from a drought QTL database. Rice 2: 115-128.

DeYoung, B. J., K. L. Bickle, K. J. Schrage, P. Muskett, K. Patel *et al.*, 2006 The CLAVATA1-related BAM1, BAM2 and BAM3 receptor kinase-like proteins are required for meristem function in Arabidopsis. Plant J. 45: 1-16.

Douglas, R. N., D. Wiley, A. Sarkar, N. Springer, M. C. P. Timmermans *et al.*, 2010 *ragged seedling2* encodes an ARGONAUTE7-Like protein required for mediolateral expansion, but not dorsiventrality, of maize leaves. The Plant Cell 22: 1441-1451.

Efroni, I., S. K. Han, H. J. Kim, M. F. Wu, E. Steiner et al., 2013 Regulation of leaf maturation by chromatin-mediated modulation of cytokinin responses. Dev. Cell 24: 438-445.

Eichten, S. R., J. M. Foerster, N. de Leon, Y. Kai, C. T. Yeh *et al.*, 2011 B73-Mo17 near-isogenic lines demonstrate dispersed structural variation in maize. Plant Physiol. 156: 1679-1690.

Flint-Garcia, S. A., A. L. Bodnar, and M. P. Scott, 2009 Wide variability in kernel coposition, seed characteristics, and zein profiles among diverse maize inbreds, landraces, and teosinte. Theor Appl Genet 100: 1129-1141.

Forestan, C., and S. Varotto, 2012 The role of PIN auxin efflux carriers in polar auxin transport and accumulation and their effect on shaping maize development. Molecular Plant 5: 787-798.

Foster, T., J. Yamaguchi, B. C. Wong, B. Veit, and S. Hake, 1999 *Gnarley1* is a dominant mutation in the *knox4* homeobox gene affecting cell shape and identity. The Plant Cell 11: 1239-1252.

Frary, A., T. C. Nesbitt, A. Frary, S. Grandillo, E. can der Knaap *et al.,* 2000 fw2.2: A quantitative trait locus key to the evolution of tomato fruit size. Science 289: 85-88.

Galinat, W. C., 1959 The phytomer in relation to floral homologies in the American *Maydeae*. Bot Mus Leafl 19: 1-32. Harvard Univ, Cambridge.

Gallavotti, A., 2013 The role of auxin in shaping shoot architecture. J. Exp. Bot. 64: 2593-2608.

Giulini, A., J. Wang, and D. Jackson, 2004 Control of phyllotaxy by the cytokinin-inducible response regulator homologue *ABPHYL1*. Nature 430: 1031-1034.

Grandillo, S., H.M. Ku, and S.D. Tanksley, 1999 Identifying the loci responsible for natural variation in fruit size and shape in tomato. Theor. Appl. Genet. 99: 978-987.

Hake, S., B. R. Char, G. Chuck, T. Foster, J. Long *et al.,* 1995 Homeobox genes in the functioning of plant meristems. Phil. Trans. R. Soc. Lond. B 350: 45-51.

Hake, S., E. Vollbrecht, and M. Freeling, 1989 Cloning *Knotted*, the dominant morphological mutant in maize using *Ds2* as a transposon tag. EMBO J. 8: 15-22.

Hake, S., H. M. S. Smith, H. Holtan, E. Magnani, G. Mele *et al.,* 2004 The role of Knox genes in plant development. Ann. Rev. Cell Dev. Biol. 20: 125-151.

Hay, A., H. Kaur, A. Phillips, P. Hedden, S. Hake *et al.,* 2002 The gibberelllin pathway mediates KNOTTED1-type homeobox function in plants with different body plans. Curr. Biol. 12: 1557-1565.

Hay, A., J. Craft, and M. Tsiantis, 2004 Plant hormones and homeoboxes: Bridging the gap? BioEssays 26: 395-404.

Hochholdinger, F. and R. Tuberosa, 2009 Genetic and genomic dissection of maize root development and architecture. Curr. Opin. Plant Biol. 12: 172-177.

ImageJ (http://rsbweb.nih.gov/ij/)

Itoh, J. I., H. Kitano, M. Matsuoka, and Y. Nagato, 2000 Shoot organization genes regulate shoot apical meristem organization and the pattern of leaf primordium initiation in rice. The Plant Cell 12: 2161-2174.

Jackson, D. and S. Hake, 1999 Control of phyllotaxy in maize by the *abphyl1* gene. Development 126: 315-323.

Jackson, D., B. Veit and S. Hake, 1994 Expression of maize *KNOTTED1* related homeobox genes in the shoot apical meristem predicts patterns of morphogenesis in the vegetative shoot. Development 120: 405-413.

Jiang, C., R. J. Wright, S. S. Woo, T. A. DelMonte, and A. H. Paterson, 2000 QTL analysis of leaf morphology in tetraploid *Gossypium* (cotton). Theor. Appl. Genet. 100: 409-418.

Johnson, W. C., L.E. Jackson, O. Ochoa, R. van Wijk, J. Peleman *et al.*, 2000 Lettuce, a shallow-rooted crop, and *Lactuca serriola*, its wild progenitor, differ at QTL determining root architecture and deep soil water exploration. Theor. Appl. Genet. 101: 1066-1073.

Juenger, T., M. Purugganan, and T. F. C. Mackay, 2000 Quantitative trait loci for floral morphology in *Arabidopsis thaliana*. Genetics 156: 1379-1392.

Jun, T. H., K. Freewalt, A. P. Michel, and R. Mian, 2013 Identification of novel QTL for leaf traits in soybean. Plant Breeding 133: 61-66.

Kayes, J. M. and S.E. Clark, 1998 *CLAVATA2*, a regulator of meristem and organ development in Arabidopsis. Development 125: 1253-1260.

Kerstetter, R. A., D. Laudencia-Chingcuanco, L. G. Smith, and S. Hake, 1997 Loss-of-function mutations in the maize homeobox gene, *knotted1*, are defective in shoot meristem maintenance. Development 124: 3045-3054.

Kerstetter, R. A., E. Vollbrecht, B. Lowe, B. Veit, J. Yamaguchi *et al.*, 1994 Sequence analysis and expression patterns divide the Maize *knotted1*-like homeobox genes into two classes. The Plant Cell 6: 1877-1887.

Kessler, S. and N. Sinha, 2004 Shaping up: the genetic control of leaf shape. Curr. Opin. Plant Biol. 7: 65-72.

Kessler, S., B. Townsley, and N. Sinha, 2006 L1 Division and differentiation patterns influence shoot apical meristem maintenance. Plant Physiol. 141: 1349-1362.

Kierskowski, D., N. Nakayama, A. L. Routier-Kierzkowska, A. Weber, E. Bayer *et al.*, 2012 Elastic domains regulate growth and organogenesis in the plant shoot apical meristem. Science 335: 1096-1099.

Knauer, S., A. L. Holt, I. Rubio-Somoza, E. J. Tucker, A. Hinze *et al.*, 2013 A protodermal miR394 signal defines a region of stem cell competence in the Arabidopsis shoot meristem. Devel. Cell 24: 125-132.

Krill, A. M., M. Kirst, L. V. Kochian, E. S. Buckler, and O. A. Hoekenga, 2010 Association and linkage analysis of aluminum tolerance genes in maize. PLoS ONE 5: e9958.

Kump, K. L., P. J. Bradbury, R. J. Wisser, E. S. Buckler, A. R. Belcher et al., 2011 Genome-wide association study of quantitative resistance to southern leaf blight in the maize nested association mapping population. Nature Genetics 43: 163-168.

Kwon, C. S. and D. Wagner, 2007 Unwinding chromatin for development and growth: A few genes at a time. Trends Genet. 23: 403-412.

Kyozuka, J., 2007 Control of shoot and root meristem function by cytokinin. Curr. Opin. Plant Biol. 10: 442-446.

Langlade, N. B., X. Feng, T. Dransfield, L. Copsey, A. I. Hanna *et al.,* 2005 Evolution through genetically controlled allometry space. Proc. Natl. Acad. Sci. USA 102: 10221-10226.

Lauter, N., M.J. Moscou, J. Habiger, and S.P. Moose, 2008 Quantitative genetic dissection of shoot architecture traits in maize: towards a functional genomics approach. The Plant Genome 1: 99-110.

Laux, T., K.F.X. Mayer, J. Berger, and G. Jürgens, 1996 The *WUSCHEL* gene is required for shoot and floral meristem integrity in *Arabidopsis*. Development 122: 87-96.

Lawrence, C. J., L. C. Harper, M. L. Schaeffer, T. Z. Sen, T. E. Siegfried *et al.,* 2008 MaizeGDB: The maize model organism database for basic, translational, and applied research. Intl. J. Plant Genomics. 2008:496957.

Lee, M., N. Sharopova, W. D. Beavis, D. Grant, M. Katt *et al.,* 2002. Expanding the genetic map of maize with the intermated B73 × Mo17 (IBM) population. Plant Mol. Biol. 48: 453-461.

Leyser, H. M. O. and I. J. Furner, 1992 Characterisation of three shoot apical meristem mutants of *Arabidopsis thaliana.* Development 116: 397-403.

Li, L., K. Petsch, R. Shimizu, S. Liu, W. W. Xu *et al.,* 2013 Mendelian and non-mendelian regulation of gene expression in maize. PLOS Genetics 9: e1003202.

Liu, Q., X. Yao, L. Pi, H. Wang, X. Cui *et al.,* 2009 The ARGONAUTE10 gene modulates shoot apical meristem maintenance and establishment of leaf polarity by repressing miR165/166 in Arabidopsis. Plant J. 58: 27-40.

Long, J. A., E. I. Moan, J. I. Medford, and M. K. Barton, 1996 A member of the KNOTTED class of homeodomain proteins encoded by the STM gene of Arabidopsis. Nature 379: 66-69.

Loudet, O., V. Gaudon, A. Trubuil, and F. Daniel-Vedele, 2005 Quantitative trait loci controlling root growth and architecture in *Arabidopsis thaliana* confirmed by heterogeneous inbred family. Theor. Appl. Genet. 110: 742-753.

Lunde C., S. Hake, 2009 The interaction of knotted1 and thick tassel dwarf1 in vegetative and reproductive meristems of maize. Genetics 181: 1693-1697.

Lyndon, R. F., and N. H. Battey, 1985 The growth of the shoot apical meristem during flower initiation. Biologia Plantarum (Praha) 27: 339-349.

Mayer, K. F. X., H. Schoof, A. Haecker, M. Lenhard, G. Jurgens *et al.,* 1998 Role of *WUSCHEL* in regulating stem cell fate in the *Arabidopsis* shoot meristem. Cell 95: 805-815.

McMullen, M. D., S. Kresovich, H. S. Villeda, P. Bradbury, H. Li *et al.,* 2009 Genetic properties of the maize nested association mapping population. Science 7: 737-740.

Moore, C. R., D.S. Gronwall, N.D. Miller, and E.P. Spalding, 2013 Mapping quantitative trait loci affecting *Arabidopsis thaliana* seed morphology features extracted computationally from images. G3 3: 109-118.

Moose, S. P. and P. H. Sisco, 1994 *Glossy15* controls the epidermal juvenile-to-adult phase transition in maize. The Plant Cell 6: 1343-1355.

Muehlbauer, G. J., J. E. Fowler, and M. Freeling, 1999 Sectors expressing the homeobox gene *liguleless3* implicate a time-dependent mechanism for cell fate acquisition along the proximal-distal axis of the maize leaf. Development 124: 5097-5106.

Nagasaki, H., J. Itoh, K. Hayashi, K. Hibara, N. Satoh-Nagasawa *et al.,* 2007 The small interfering RNA production pathway is required for shoot meristem initiation in rice. Proc. Natl. Acad. Sci. USA 104: 14867-14871.

Nishimura, A., M. Tamaoki, T. Sakamoto, and M. Matsuoka, 2000 Over-expression of tobacco *knotted1*-type class1 homeobox genes alters various leaf morphology. Plant Cell Physiol. 41: 583-590.

Nogueira, F. T. S., S. Madi, D. H. Chitwood, M. T. Juarez, and M. C. P. Timmermans, 2007 Two small regulatory RNAs establish opposing fates of a developmental axis. Genes Dev. 21: 750-755.

Omori, F. and Y. Mano, 2007. QTL mapping of root angle in F2 populations from maize 'B73' x teosinte *'Zea luxurians'*. Plant Root 1: 57-65.

Ormenese, S., A. Havelange, G. Bernier, C. van der Schoot, 2002 The shoot apical meristem of *Sinapis alba* L. expands it central symplasmic field during the floral transition. Planta 215: 67-78.

Panzea (http://www.panzea.org)

Peaucelle, A., S. A. Braybrook, L. Le Guillou, E. Bron, C. Kuhlemeier *et al.* 2011 Pectin-induced changes in cell wall mechanics underlie organ initiation in Arabidopsis. Curr. Biol. 21: 1720-1726.

Peiffer, J. A., M. C. Romay, M. A. Gore, S. A. Flint-Garcia, Z. Zhang *et al.* 2014 The genetic architecture of maize height. Genetics (doi: 10.1534/genetics.113.159152).

Peiffer, J. A., S. A. Flint-Garcia, N. De Leon, M. D. McMullen, S. M. Kaeppler *et al.*, 2013 Genetic architecture of maize stalk strength. PLoS ONE 8: e67066.

Pernisová, M., P. Klíma, J. Horák, M. Válková, J. Malbeck *et al.*, 2009 Cytokinins modulate auxin-induced organogenesis in plants via regulation of the auxin efflux. Proc. Natl. Acad. Sci. USA 106: 3609-3614.

Poethig, R. S. and E. J. Szymkowiak, 1995 Clonal analysis of leaf development in maize. Maydica 40: 67-76.

Poethig, R. S., 1984 Cellular parameters of leaf morphogenesis in maize and tobacco, pp. 235-238 in *Contemporary Problems in Plant Anatomy*, edited by R. A. White and W. C. Dickinson. Academic Press, New York.

Poethig, R. S., 1990 Phase change and the regulation of shoot morphogenesis in plants. Science 250: 923-930.

Poethig, R. S., E. H. Coe Jr., and M. M. Johri, 1986 Cell lineage patterns in maize embryogenesis: a clonal analysis. Dev Biol 117: 392-404.

Poland, J. A., P. J. Bradbury, E. S. Buckler, and R. J. Nelson, 2011. Genome-wide nested association mapping of quantitative resistance to northern leaf blight in maize. Proc. Natl. Acad. Sci. USA 108: 6893-6898.

Pressoir, G., P. J. Brown, W. Y. Zhu, N. Upadyayula, T. Rocheford *et al.*, 2009 Natural variation in maize architecture is mediated by allelic differences at the *PINOID* co-ortholog *barren inflorescence2*. Plant J. 58: 618-628.

QTL Cartographer (http://statgen.ncsu.edu/qtlcart/)

R (http://www.r-project.org/)

Reinhardt, D., T. Mandel, and C. Kuhlemeier, 2000 Auxin Regulates the initiation and radial position of plant lateral organs. The Plant Cell 12: 507-518.

Rosin, F. M., J. K. Hart, H. T. Horner, P. J. Davies, and D. J. Hannapel, 2003 Overexpression of a *Knotted*-like homeobox gene of potato alters vegetative development by decreasing gibberellin accumulation. Plant Physiol. 132: 106-117.

Rupp, H. M., M. Frank, T. Werner, M. Strnad, and T. Schmulling, 2002 Increased steady state mRNA levels of the *STM* and *KNAT1* homeobox genes in cytokinin overproducing *Aravidopsis thaliana* indicate a role for cytokinins in the shoot apical meristem. Plant J. 18: 557-563.

Ruzin, S. E., 1999 *Plant microtechnique and microscopy*. Oxford University Press, Oxford, NY.

Salvi, S., G. Sponza, M. Morgante, D. Tomes, X. Niu *et al.*, 2007 Conserved noncoding genomic sequences associated with a flowering-time quantitative trait locus in maize. Proc. Natl. Acad. Sci. USA 104: 11376-11381.

Salvi, S., R. Tuberosa, E. Chiapparino, M. Maccaferri, S. Veillet *et al.*, 2002 Toward positional cloning of *Vgt1*, a QTL controlling the transition from the vegetative to the reproductive phase in maize. Plant Mol. Biol. 48: 601-613.

Sang, Y., M.Wu, and D. Wagner, 2009 The Stem cell—Chromatin Connection. Seminars in Cell & Developmental Biology 20: 1143-1148.

Scanlon, M. J., 2000 NARROW SHEATH1 functions from two meristematic foci during founder-cell recruitment in maize leaf development. Development 127: 4573-4585.

Scanlon, M. J., D.C. Henderson, and B. Bernstein, 2002 *SEMAPHORE1* functions during regulation of ancestrally duplicated knox genes and polar auxin transport in maize. Development 129: 2663-2673.

Scanlon, M. J., R. G. Schneeberger, and M. Freeling, 1996 The maize mutant narrow sheath fails to establish leaf margin identity in a meristematic domain. Development 122: 1683-1691.

Schauer, S. E., S. E. Jacobsen, D. W. Meinke, and A. Ray, 2002 DICER-LIKE1: Blind men and elephants in Arabidopsis development. Trends Plant Sci. 7: 487-491.

Schnable, J. C. and M. Freeling, 2011 Genes identified by visible mutant phenotypes show increased bias toward one of two subgenomes of maize. PLOS ONE 6: e17855.

Schnable, P. S., D. Ware, R. S. Fulton, J. C. Stein, F. Wei *et al.*, 2009 The B73 Maize Genome: Complexity, Diversity, and Dynamics. Science 326: 1112-1115.

Schneeberger, R. G., P. W. Becraft, S. Hake, and M. Freeling, 1995 Ectopic expression of the Knox homeo box gene *Rough sheath1* alters cell fate in the maize leaf. Genes Dev. 9: 2292-2304.

Schoof, H., M. Lenhard, A. Haecker, K. F. X. Mayer, G. Jurgens *et al.*, 2000 The stem cell population of *Arabidopsis* shoot meristems is maintained by a regulatory loop between the *CLAVATA* and *WUSCHEL* genes. Cell 100: 635-644.

Sharman, B. C., 1942a Onset of reproductive phase in grasses and cereals. Nature 150: 208.

Sharman, B. C., 1942b Developmental anatomy of the shoot of *Zea mays.* Ann. Bot. 6: 245-283.

Shen, W., and L. Xu, 2009 Chromatin remodeling in stem cell maintenance in Arabidopsis thaliana. Molecular Plant 2: 600-609.

Sinha, N., 1999 Leaf development in angiosperms. Ann. Rev. Plant Physiol. Plant Mol. Biol. 50: 419-446.

Smith, H. M. S. and S. Hake, 2003 The interaction of two homeobox genes, *BREVIPEDICELLUS* and *PENNYWISE*, regulates internode patterning in the Arabidopsis inflorescence. The Plant Cell 15: 1717-1727.

Smith, L. G., B. Greene, B. Veit, and S. Hake, 1992 A dominant mutation in the maize homeobox gene, Knotted-1, causes its ectopic expression in leaf cells with altered fates. Development 116: 21-30.

Sylvester, A. W., W. Z. Cande, and M. Freeling, 1990 Division and differentiation during normal and liguleless-1 maize leaf development. Development 110: 985-1000.

Taguchi-Shiobara, F., Z. Yuan, S. Hake, and D. Jackson, 2001 The *fasciated ear2* gene encodes a leucine-rich repeat receptor-like protein that regulates shoot meristem proliferation in maize. Genes Dev. 15: 2755-2766.

Takacs, E. M., J. Li, C. Du, L. Ponnala, D. Janick-Buckner *et al.*, 2012 Ontogeny of the maize shoot apical meristem. The Plant Cell 24: 3219-3234.

Thompson, A. M., J. Crants, P. S. Schnable, J. Yu, M. C. P. Timmermans et al., 2014 Genetic control of maize shoot apical meristem architecture. G3 (doi: 10.1534/g3.114.011940)

Tian, F., P. J. Bradbury, P. J. Brown, H. Hung, Q. Sun *et al.*, 2011 Genome-wide association study of leaf architecture in the maize nested association mapping population. Nature Genetics 43: 159-162.

Timmermans, M. C. P., A. Hudson, P. W. Becraft, and T. Nelson, 1999 ROUGH SHEATH2: a myb protein that represses *knox* homeobox genes in maize lateral organ primordia. Science 284: 151-153.

Tsiantis, M., R. Schneeberger, J. F. Golz, M. Freeling, and J. A. Langdale, 1999 The maize *rough sheath2* gene and leaf development programs in monocot and dicot plants. Science 284: 154-156.

Tsuda, K., Y. Ito, Y. Sato, and N. Kurata, 2011 Positive autoregulation of a KNOX gene is essential for shoot apical meristem maintenance in rice. The Plant Cell 23: 4368-4381.

Uchida, N., B. Townsley, K. Chung, and N. Sinha, 2007 Regulation of *SHOOT MERISTEMLESS* genes via an upstream-conserved noncoding sequence coordinates leaf development. Proc. Natl. Acad. Sci. USA 104: 15953-15958.

Upadyayula, N., H. S. da Silva, M. O. Bohn, and T. R. Rocheford, 2006 Genetic and QTL analysis of maize tassel and ear inflorescence architecture. Theor. Appl. Genet. 112: 592-606.

Vanstraelen, M., and E. Benková, 2012 Hormonal interactions in the regulation of plant development. Ann. Rev. Cell Dev. Biol. 28: 463-487.

Vaucheret, H., F. Vazquez, P. Crété, and D. P. Bartel, 2004 The action of ARGONAUTE1 in the miRNA pathway and its regulation by the miRNA pathway are crucial for plant development. Genes Dev. 18: 1187-1197.

Vladutu, C., J. McLaughlin, and R. L. Phillips, 1999 Fine mapping and characterization of linked quantitative trait loci involved in the transition of the maize apical meristem from vegetative to generative structures. Genetics 153: 993-1007.

Vollbrecht, E., B. Veit, N. Sinha, and S. Hake, 1991 The developmental gene *Knotted-1* is a member of a maize homeobox gene family. Nature 350: 241-243.

Vollbrecht, E., L. Reiser, and S. Hake, 2000 Shoot meristem size is dependent on inbred background and presence of the maize homeobox gene, knotted1. Development 127: 3161-3172.

Wagner, Doris, 2003 Chromatin regulation of plant development. Curr. Opin. Plant Biol. 6: 20-28.

Wang, Y. and J. Li, 2008 Molecular basis of plant architecture. Ann. Rev. Plant Biol. 59: 253-279.

Woodward, J. B., N. D. Abeydeera, D. Paul, K. Phillips, M. Rapala-Kozik et al., 2010 A maize thiamine auxotroph is defective in shoot meristem maintenance. The Plant Cell 22: 3305-3317.

Yanai, O., E. Shani, K. Dolezal, P. Tarkowski, R. Sablowski *et al.*, 2005 Arabidopsis KNOXI proteins activate cytokinin biosynthesis. Curr. Biol. 15: 1566-1571.

Yang, X., H. Ma, P. Zhang, J. Yan, Y. Guo *et al.*, 2012 Characterization of QTL for oil content in maize kernel. Theor. Appl. Genet. 125: 1169-1179.

Yu, X., H. Wang, W. Zhong, J. Bai, P. Liu *et al.*, 2013 QTL mapping of leafy heads by genome resequencing in the RIL population of *Brassica rapa.* PLOS ONE 8: e76059.

Zeng, Z. B., 1994 Precision mapping of quantitative trait loci. Genetics 136: 1457-1468.

Zhang, B. H., X. P. Pan, S. B. Cox, G. P. Cobb, and T. A. Anderson, 2006 Evidence that miRNAs are different from other RNAs. Cell. Mol. Life Sci. 63: 246-254.

Zhang, X., S. Madi, L. Borsuk, D. Nettleton, R. J. Elshire *et al.*, 2007 Laser microdissection of narrow sheath mutant maize uncovers novel gene expression in the shoot apical meristem. PLOS Genetics 3: e101.

Zhu, J., S. M. Kaeppler, and J. P. Lynch, 2005 Mapping of QTLs for lateral root branching and length in maize (*Zea mays* L.) under differential phosphorus supply. Theor. Appl. Genet. 111: 688-695.